MICROGLIAL BEHAVIOUR DURING PHOTORECEPTOR DEGENERATION

SUBMITTED TO THE UNIVERSITY OF LONDON FOR THE DEGREE OF MD

EDWARD H. HUGHES

ProQuest LLC
789 East Eisenhower Parkway
P.O. Box 1346
Ann Arbor, MI 48106-1346

ABSTRACT

Inherited photoreceptor dystrophies are a leading cause of blindness and have no effective treatment. Despite advances in our understanding of the genetic mechanisms underlying this diverse group of conditions, the sequence of events leading from genetic miscoding to photoreceptor death by apoptosis are still unknown, although influences from other cells within the retina have been implicated. Microglia, the macrophages of the central nervous system, have previously been shown to increase in number and migrate to the photoreceptor layer to phagocytose apoptotic cell debris. However increasing awareness of the cytotoxic potential of microglia, has led me to undertake this work with the primary remit of investigating the possible involvement of microglia in photoreceptor apoptosis using the *rds* mouse model of inherited photoreceptor degeneration.

Using immunohistochemical and immunofluorescent methods I have demonstrated increased microglial numbers in the degenerating *rds* retina, resulting from both *in situ* proliferation and recruitment from the blood, with migration to the outer retinal layers and sub-retinal space. However, by closely scrutinising the period of greatest disease activity we have demonstrated that the peak rate of photoreceptor apoptosis precedes the peak in microglial numbers by approximately five days, suggesting that microglia respond to, rather than cause photoreceptor death. In addition, evidence of oxidative damage (a major mechanism of microglial cytotoxicity) is absent and depletion of retinal microglia using macrophage-depleting clodronate liposomes did not lead to a reduction in the rate of photoreceptor death,

providing further evidence that microglia are not involved in causing photoreceptor apoptosis.

Additional studies with the neuroprotective tetracycline antibiotic, minocycline showed that this drug was able to delay the onset of photoreceptor apoptosis in the *rds* mouse, possibly through a direct inhibitory effect on apoptosis and the caspase cascade. Delayed apoptosis was associated with a corresponding delay in microglial migration to the outer retina.

TABLE OF CONTENTS

ACKNOWLEDGEMENTS

I would like to sincerely thank my supervisors Professor Andrew Dick and Professor Robin Ali for their enthusiasm, support and advice during this work and Dr Frank Schlichtenbrede for his assistance with the laboratory work at the Institute of Ophthalmology.

CHAPTER ONE

INTRODUCTION

PHOTORECEPTOR DYSTROPHIES

The eye is a common site for genetic disease. Inherited photoreceptor dystrophies constitute a large proportion of genetic eye disease and form a heterogeneous group of conditions differing in their mode of inheritance, pattern of visual loss and clinical appearance(Bird 1995). These photoreceptor dystrophies may affect predominantly the central retina (macular dystrophies) or, more commonly, the peripheral retina (typically presenting as Retinitis Pigmentosa (RP), *figure 1.1*), depending on the extent to which they affect the rod and cone photoreceptors.

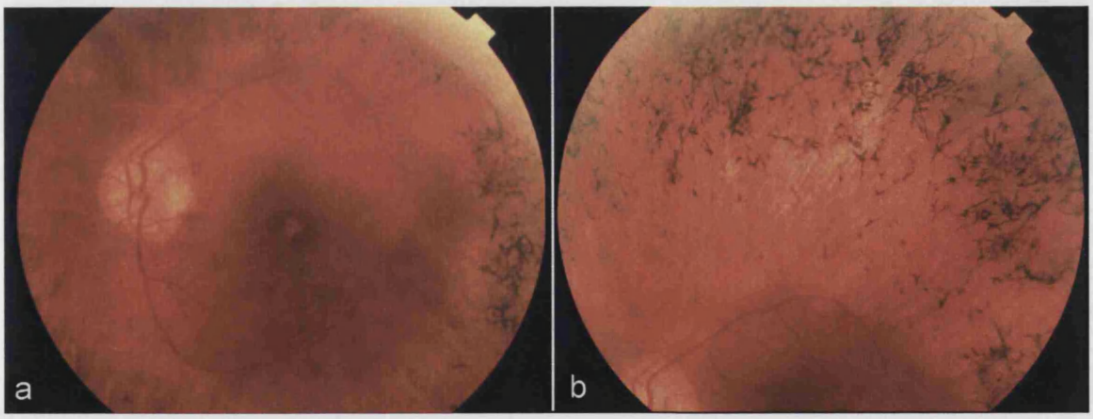

Figure 1.1 Colour retinal photographs illustrating the advanced degenerative changes in a patient with retinitis pigmentosa. Although the central retina may remain relatively spared until the later stages of the disease (a), vascular attenuation and optic disc pallor are an indication of the severity of the changes more peripherally (b). The classical black 'bone spicule' pigmentation corresponds with areas of profound atrophy of the neuroretina with migration of retinal pigment epithelium into the inner retinal layers.

The central, or macular, dystrophies affect central vision early, often leaving peripheral vision spared until later or even indefinitely. Conversely, RP presents with night blindness and progressive restriction of peripheral vision as the condition progresses to ultimately involve the macula, resulting in late central visual loss. As a group these conditions are a leading cause of blindness with RP affecting between 1/3000 and 1/5000 people in all ethnic groups (Bunker et al. 1984; Pagon 1988; Haim et al. 1992). There is no treatment for RP and other photoreceptor dystrophies and although age of onset varies depending on gene defect and inheritance mode, the onset of symptoms in RP is before the age of 20 years in 68% of cases(Niemeyer and Gurewitsch 1982) and by the age of 50 years over 50% have a visual acuity of 6/60 or worse(Marmor 1980) (legal blindness in UK); as such the conditions are costly in terms of lost work productivity, need for social support and individual suffering.

Although photoreceptor dystrophies may be part of a broader clinical syndrome with involvement of other tissues and organs, such as Usher's syndrome, Refsum's disease and abetalipoproteinaemia, they are more commonly found as an isolated condition inherited in autosomal dominant, autosomal recessive or X-linked fashion as single gene disorders. Molecular genetic studies have identified a large number of genes involved in photoreceptor dystrophies (http://www.sph.uth.tmc.edu/retnet/) and, with the help of animal models, much has been learnt about the structure and function of the proteins they encode.

These genes may be broadly divided into three classes, according to their pattern of expression (Pacione et al. 2003). The first group, which represents the great majority of genes involved in photoreceptor degenerations, consists of genes expressed predominantly or exclusively in the photoreceptors or underlying retinal pigment epithelium (RPE) and their mutations therefore manifest solely in the retina. This

group includes genes which encode proteins participating in the phototransduction cascade (i.e. the conversion of light to an electrical stimulus), proteins responsible for the structural integrity of photoreceptors and their outer segments which house the visual pigments and proteins involved in the cycling and regeneration of photoreceptor outer segments and visual pigments by the RPE. A detailed description of human and murine ocular anatomy is given in the appendix.

The second group of genes involved in photoreceptor degenerations are those which are ubiquitously or widely expressed and, as a result, retinal degeneration is associated with disease in other tissues (multi-organ phenotype, such as Bardet Biedl syndromes).

The third group is perhaps the least understood, since it consists of mutations in ubiquitously or widely expressed genes which nonetheless lead to disease exclusively in the photoreceptors. The reasons for this are not yet clear but the very high metabolic rate and protein turn-over in photoreceptors has been suggested to make these cells particularly vulnerable to such genetic insults (Pacione et al. 2003). This category includes genes involved in pre-mRNA splicing (*PRPF,* autosomal dominant RP), phagocytosis (*MERTK,* autosomal recessive RP and the *RCS* rat model), matrix metalloproteinase inhibition (*TIMP 3*, Sorsby macular dystrophy), as well as others such as *RP9* (autosomal dominant RP) whose product have as yet unknown function.

Since the first group of genes involved in photoreceptor degenerations (those expressed predominantly or exclusively in photoreceptors or the RPE) represent the great majority of cases, these mutations are discussed further below:

Huang et al. 1995), the rod cGMP-gated Cation Channel(Dryja et al. 1995) and arrestin(Nakazawa et al. 1998)have also been discovered in RP with recessive inheritance.

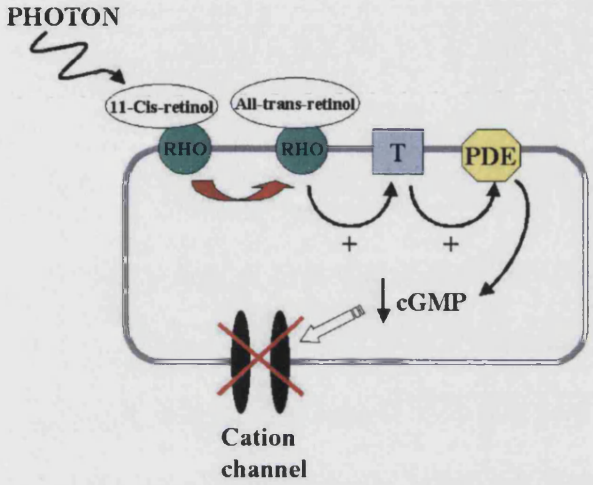

Figure 1.2 Schematic depiction of the phototransduction cascade. A photon of light induces a conformational change from 11-cis-retinol to all-trans-retinol within the transmembrane rhodopsin protein (RHO). This causes activation of a G protein transducin (T) which in turn activates cGMP phosphodiesterase (PDE) which hydrolyses cGMP The resulting reduction in intracellular levels of cGMP leads to closure of the cGMP-gated cation channel preventing the influx of sodium and calcium ions with hyperpolarisation of the cell.

Mutations affecting photoreceptor outer segment structural proteins

Peripherin/*rds* (retinal degeneration slow) is an integral membrane glycoprotein that, together with its non-glycosylated homologue ROM1, forms a multisubunit heterotetramer complex at the rim region of rod outer segment discs (Molday et al. 1987; Connell et al. 1991). Peripherin/*rds* appears to be essential for the formation and maintenance of normal photoreceptor outer segments, which contain the visual pigments necessary for photon capture. Mutations in peripherin/*rds* have been linked to a variety of progressive retinal degenerations, including autosomal dominant RP and macular dystrophies (Farrar et al. 1991; Wells et al. 1993). ROM1 is only

well as being responsible for cases of recessive RP and congenital stationary night blindness.

Mutations in genes encoding α and β subunits of photoreceptor cGMP phosphodiesterase (cGMP PDE) (McLaughlin et al. 1993; Danciger et al. 1995; Huang et al. 1995), the rod cGMP-gated Cation Channel(Dryja et al. 1995) and arrestin (Nakazawa et al. 1998) have also been discovered in RP with recessive inheritance.

Mutations affecting photoreceptor outer segment structural proteins

Peripherin/*rds* (retinal degeneration slow) is an integral membrane glycoprotein that, together with its non-glycosylated homologue ROM1, forms a multisubunit heterotetramer complex at the rim region of rod outer segment discs (Molday et al. 1987; Connell et al. 1991). Peripherin/*rds* appears to be essential for the formation and maintenance of normal photoreceptor outer segments, which contain the visual pigments necessary for photon capture. Mutations in peripherin/*rds* have been linked to a variety of progressive retinal degenerations, including autosomal dominant RP and macular dystrophies (Farrar et al. 1991; Wells et al. 1993). ROM1 is only expressed in rods, leaving peripherin/*rds* to form homotetramers in the discs of cone photoreceptors. Mutations in ROM1 are found in digenic forms of RP in which patients are heterozygous for mutations in peripherin/*rds* and ROM1, although isolated, targeted disruption of ROM1 in mice leads to retinal degeneration (Clarke et al. 2000).

Mutations affecting the metabolism of visual pigments

The series of biochemical steps that provide and recycle the chromophore of rhodopsin, 11-*cis* retinaldehyde involves the retinal pigment epithelium (RPE), which converts both dietary all-*trans* retinol (vitamin A) and the phototransduction product all-*trans* retinaldehyde, back to 11-*cis* retinaldehyde for reuse by the photoreceptors. This process involves isomerisation via a protein known as RPE 65, as well as other RPE proteins employed in the binding and transporting of the chromophores, such as cellular retinaldehyde binding protein, both of which are products of genes known to be mutated in RP(Maw et al. 1997; Morimura et al. 1998). The removal of photoisomerised chromophores from rod photoreceptors involves the ATP-binding cassette transporter of rods (ABCR), whose gene is also known to be involved in RP (Martinez-Mir et al. 1998).

The *rds* mouse model

The *rds* (retinal degeneration slow) or rd2 mouse (recently also termed $Prph2^{Rd2/Rd2}$) is a naturally occurring strain characterised by photoreceptor degeneration resulting from a null mutation in the Peripherin/*rds* gene. The mouse was so named after the prior discovery of the faster-degenerating *rd* or rd1 (retinal degeneration) mouse which has a *Tyr347stop* mutation in the gene encoding cGMP phosphodiesterase. The *rds* mutation which was first identified in 1978 by van Nie *et al.*(van Nie et al. 1978) and later localised to murine chromosome 17(Demant et al. 1979), is now known to be a 9.2 kb insertion into exon 2 of the peripherin/*rds* gene (Ma et al. 1995). Since the gene is expressed exclusively in photoreceptors, photoreceptor degeneration is the only phenotypic manifestation of the mutation. The normal gene product,

Peripherin2/*rds*, is an integral membrane glycoprotein found at the rim region of rod outer segment discs (Molday et al. 1987; Connell et al. 1991). It appears to be essential for the formation and maintenance of normal photoreceptor outer segments, with homozygous *rds*$^{-/-}$ mice failing to develop these structures, having only disorganised stumps (*figure 1.3*).

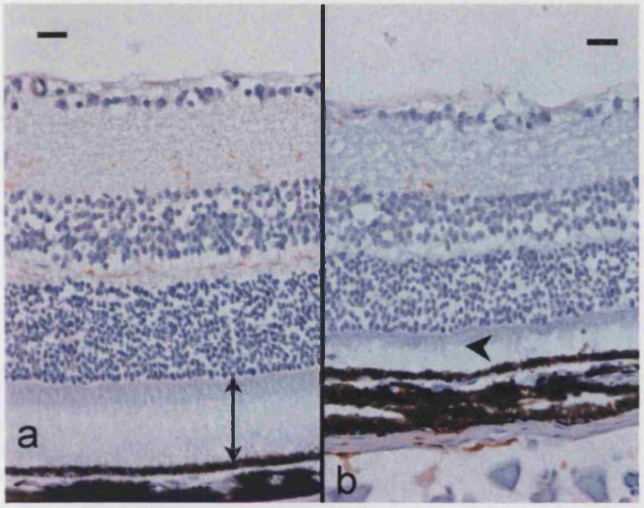

Figure 1.3 Sections of wild type retina at P30 with well developed photoreceptor outer segments (a, arrows) and *rds* retina at the same age possessing only vestigial stumps (b, arrowhead). Haematoxylin, scale bar: 20 μm. Microglia stained with F4/80 (brown)

The earliest detailed description of the retinal histology in *rds* mice was performed by Sanyal *et al.*(Sanyal et al. 1980). At birth the retina of *rds*$^{-/-}$ and wild type mice are morphologically indistinguishable, with a single thick nuclear layer that divides into the inner and outer nuclear layers at around the 4th postnatal day (P4). By P11 wild type mice have begun to develop a layer of photoreceptor outer segments, which is fully formed by P21. In contrast, *rds*$^{-/-}$ mice never exhibit this layer, with instead an accumulation of membrane bound vesicles in the sub-retinal space,(Jansen and Sanyal 1984) and recognisable thinning of the outer nuclear layer starts at P14 as the photoreceptors die. A surge of photoreceptor apoptosis occurring between P14 and P19 has been observed by several investigators, with an ongoing lower frequency of photoreceptor loss thereafter(Chang et al. 1993; Portera-Cailliau et al. 1994; Ali et al. 1998). The disease affects the peripheral retina more severely with complete loss of

photoreceptors by 9 months, whereas more centrally they persist until about one year. The inner retinal layers remain relatively spared(Sanyal et al. 1980). The electroretinogram (ERG), a method of recording retinal electrical responses to flashes of light and thus an indicator of retinal function and visual potential, is severely impaired in *rds*$^{-/-}$ mice from birth, and in keeping with the extent of photoreceptor loss, is completely undetectable by 1 year(Reuter and Sanyal 1984).

The human *rds* gene on chromosome 6 has 85% sequence homology with that of the mouse(Jordan et al. 1992). The peripherin/*rds* protein is found in the same location in human photoreceptors as in the mouse, and in humans mutations in peripherin also cause photoreceptor dystrophies such as autosomal dominant RP and macular dystrophies (Farrar et al. 1991; Wells et al. 1993). Pathological studies of retina from the *rds* mouse and patients with retinitis pigmentosa share many common features; selective loss of photoreceptors with peripheral predilection, relative sparing of inner retinal layers and an enhanced microglial/macrophage presence(Sanyal et al. 1980; Santos et al. 1997; Gupta et al. 2003). So, the *rds* mouse is a good model for human photoreceptor degenerations, having the advantages of both closely related aetiology and of common neuronal and non-neuronal retinal cell pathologic features. The rate of degeneration is, however much faster and more aggressive than most human photoreceptor dystrophies, and this offers both advantages and disadvantages in terms of experimental approach, and should be borne in mind when interpreting results.

Mechanisms of photoreceptor cell death

Although knowledge of the underlying genetic basis for photoreceptor dystrophies is ever increasing, the precise sequence of cellular events leading from genetic miscoding of a protein to the instigation of cell death are, in many instances, unclear.

Many of the genes implicated in RP are exclusively expressed in photoreceptors, and as such encode proteins that are non-essential to cells of other tissues. Why, therefore, such mutations should lead to photoreceptor death rather than simply loss of function is a fundamental question that remains to be answered. Theories abound about the causes of photoreceptor death with each mutation, some of which have sound scientific basis with supporting experimental evidence (from animal models), while others remain largely unsubstantiated. An example of the former is mutations in the gene encoding cGMP PDE, where loss of cGMP PDE enzyme activity would lead to continuously high concentrations of cGMP within the cell ('super-dark' state) with the consequently increased conductance through cGMP-gated cation channels resulting in massive influxes of Na^+ and Ca^{2+}. This proposed sequence of pathological events is corroborated by investigations in the *rd* mouse, which has a null mutation in the gene encoding the β subunit of cGMP PDE. Photoreceptors in the mouse have raised levels of cGMP prior to cell death(Farber and Lolley 1974; Lolley et al. 1977) and this and/or the associated rise in intracellular calcium levels is thought to lead to apoptosis(Ulshafer et al. 1980). Investigations using a cation channel blocking agent in the *rd* mouse have shown partial rescue of the photoreceptors(Frasson et al. 1999), although others have not been able to verify this(Pearce-Kelling et al. 2001; Pawlyk et al. 2002).

For many other mutations, explanations for photoreceptor death are less watertight but include the following theories.

a) *Constitutive activation of the phototransduction cascade*

Continuous exposure of experimental animals to light results in photoreceptor degeneration(Fain and Lisman 1993). Certain mutations in rhodopsin(Rim and Oprian 1995) and cGMP gated cation channel(Dryja et al. 1995), may produce a 'super-light' state in which constitutive activation of phototransduction may lead to cell damage.

b) *'Clogging' of golgi and endoplasmic reticulum*

While the product of some mutated rhodopsin genes will associate with 11-cis retinaldheyde and integrate with the plasma membrane, many other forms accumulate within the endoplasmic reticulum of cells(Sung et al. 1993), possibly leading to fundamental disturbance of basic cellular functions. This phenomenon probably results from abnormal folding of the mutant rhodopsin.

c) *Altered photoreceptor-RPE interface*

With the functions of the RPE and photoreceptors so intricately intertwined, it can be expected that RPE pathology might lead to damage to the overlying photoreceptors. Apart from the recycling of photopigments, the RPE has a major phagocytic role and is responsible for the clearance of the continually shed photoreceptor outer segment membrane discs. Failure of this process (as occurs in the Royal College of Surgeons rat) results in accumulation of debris in the sub-retinal space with death of the overlying photoreceptors, possibly due to failure of the diffusion of essential nutrients from the choroid.

d) *Outer segment shortening*

Shortening of the photoreceptor outer segment occurs in mutations affecting the structural proteins peripherin/*RDS* and ROM1, and also mutations involving rhodopsin, which constitutes around 85% of the total protein in photoreceptor outer segments. The *Prph2*$^{Rd2/Rd2}$ (*rds*, retinal degeneration slow) mouse has a null mutation in the peripherin gene, and consequently the hallmark of homozygous mice (*rds/rds*) is complete failure to develop photoreceptor outer segments(Sanyal et al. 1980) which results in death of the photoreceptors. A reduced oxygen demand and closer proximity to the highly vascular choroid in the absence of outer segments have been proposed to conspire to predispose to oxidative damage(Travis 1998), although there is no evidence supporting this hypothesis.

Regardless of the genetic defect and proposed mechanisms leading to photoreceptor death, the final, unifying process of cell demise in all animals models studied to date is through apoptosis (discussed further in chapter five). Included in this list are the *rd, rds* and rhodopsin mutant mice(Chang et al. 1993; Portera-Cailliau et al. 1994), RCS rat(Tso et al. 1994) and albino animals with light-induced photoreceptor damage(Abler et al. 1996; Hafezi et al. 1997). Whether this process is also responsible for photoreceptor death in human degenerations is unknown, owing to the paucity of tissue specimens and the inability to study *in vivo* processes. However the information available from post-mortem studies on human eyes with retinitis pigmentosa reveals selective loss of the photoreceptor layer in the early stages(Santos et al. 1997), correlating with the findings in animal models.

Evidence for extrinsic photoreceptor-toxic influences during retinal degeneration

The apoptotic death of photoreceptors is not restricted to those expressing the mutated gene as is evident with respect to loss of cones (containing functionally normal photopigments) in humans suffering RP due to rhodopsin mutations. For example, in an aggregation chimera produced from wild-type and transgenic mice carrying a mutated rhodopsin allele, uniform loss of both wild-type and transgenic photoreceptors is observed(Huang et al. 1993), a phenomenon also seen in a mosaic *Prph2*$^{Rd2/Rd2}$ (*rds*) mouse with random expression of wild-type and mutant *rds* genes(Kedzierski et al. 1998). Similarly, in the Irish Setter which has a null mutation in the β subunit of rod cGMP PDE, there is degeneration of both rod photoreceptors with absent PDE activity and their neighbouring cones which possess a normal complement of PDE(Suber et al. 1993).

Although apoptosis is classically described as a process involving individual cells, leaving neighbouring cells healthy, theories have been proposed that 'bystander' damage might result from release of a diffusible toxic factor by dying rods, or depletion of a protective/trophic effect normally provided by rods that is lost by their demise. Toxic factors might include intracellular substances (such as Ca^{2+} and ATP) spreading through gap junctions between photoreceptors(Ripps 2002) as has been demonstrated with calcium fluxes between apoptotic and healthy glia after ischaemia(Budd and Lipton 1998; Lin et al. 1998) or extracellular substances such as glutamate diffusing across the extracellular space.

Another possibility for such 'non-cell-autonomous' photoreceptor death is the involvement of other cells within the retina, and in particular the non-neuronal cell population, i.e. the glia.

THE GLIAL ELEMENTS OF THE MAMMALIAN RETINA

The mammalian retina possesses two main types of glia: a modified neuroglia known as Müller cells and a myeloid population of specialised tissue macrophage known as microglia. Whilst microglia are present throughout the central nervous system (CNS), the two predominant populations of neuroglia are the astrocytes and oligodendrocytes. In the mammalian retina astrocytes are present, but they are limited to the nerve fibre layer, and oligodendrocytes are completely absent.

Müller Cells

The close physical and functional relationship between Müller cells and the neuronal population has been extensively studied as summarised by Newman and Reichenbach (Newman and Reichenbach 1996). Müller cells, present in all vertebrate retinae, assume the roles of astrocytes, ependymal cells and oligodendrocytes. They span the retina and, through their intricate arrangement of processes, develop intimate contact with all neuronal cell types, allowing a constitutive functional relationship (*figure 1.4*).

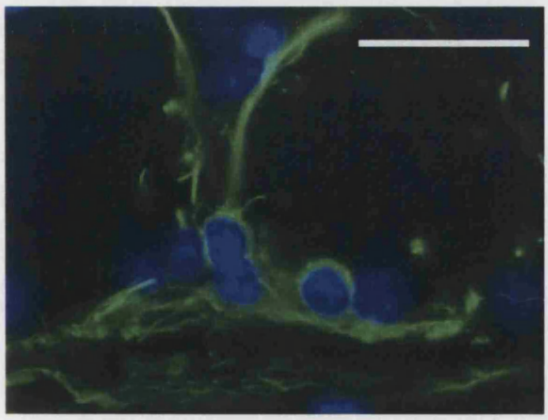

Figure 1.4 The intimate anatomical relationship between Muller cells and the retinal neurones allows for their close functional interplay. The figure shows human retinal Muller cells (green) stained for glial fibrillary acid protein (GFAP) surrounding retinal ganglion cells. Counterstain: DAPI, scale bar: 20 μm.

Müller cells are involved in neurotransmitter uptake and recycling, homeostasis of ionic components and pH of the extra-cellular space, and the provision of both metabolic and trophic support. The possibility that these glia are able to recognise and are modulated by retinal neuronal activity is given weight by their expression of receptors for a variety of neurotransmitters(Wakakura and Yamamoto 1994; Puro et al. 1996; Reichelt et al. 1996) and their sensitivity to extra-cellular K^+ (Reichenbach et al. 1997). These features give retinal Müller cells credible potential to respond to pathological alterations in neuronal behaviour by the withdrawl of metabolic or growth factor support, such as fibroblast growth factor(Harada et al. 2000), or the release of cytotoxic compounds such as nitric oxide(Goureau et al. 1999; Kobayashi et al. 2000).

However it is the other glial presence within the retina, the microglia, that have not only a far more established cytotoxic potential but also a more overt and robust response to photoreceptor degeneration, and would thus constitute a more likely culprit in a non-cell-autonomous model of photoreceptor death.

The Myeloid Presence Within the Central Nervous System and Retina

All organs outside the CNS possess a resident population of myeloid-derived, innate immune cells: macrophages and dendritic cells (DCs), which have essential roles in host defence through participation in non-specific immune responses and the initiation and regulation of adaptive immunity. Dendritic cells are the professional antigen presenting cells, whose ability to endocytose antigen, migrate to regional lymph nodes and present antigen to naïve CD4+ T cells in conjunction with Major

Histocompatibility Complex (MHC) class II molecules, allows them to initiate a primary adaptive immune response.

Macrophages have a broader role than dendritic cells. They have phagocytic capability and as such are responsible for removal of macromolecules and apoptotic / dying cells. They are also able to recognise common antigenic determinants and thereby clear invading pathogens through phagocytosis and the release of cytotoxic factors. In addition they, like DCs, are capable of MHC class II expression and antigen presentation to T cells, although their repertoire is limited to the initiation of secondary immune responses (the re-stimulation of mature T cells) and immune regulation.

The CNS has certain characteristics that distinguish it immunologically from other tissues: it resides behind the tight endothelial junctions of the blood-brain barrier and its parenchyma lacks dendritic cells(Hart and Fabre 1981) and conventional lymphatics(Perry 1998). The CNS does, however possess a resident myeloid population, namely the parenchymal microglia and perivascular macrophages, both of mononuclear phagocyte lineage(Perry et al. 1985; Hickey and Kimura 1988). In addition it is now widely accepted that immune surveillance of the CNS and cerebrospinal fluid compartment is performed by T cells that may readily cross the intact blood brain barrier(Wekerle 1986; Hickey et al. 1991) and by dendritic cells residing in the meninges and choroid plexus(McMenamin 1999).

The mouse CNS and retina is populated by blood-borne macrophages during ontogeny(Perry et al. 1985), particularly during the late embryonic stages and early post-natal period, when they are involved in the phagocytic clearance of redundant apoptotic cells generated by neuronal remodelling. In the developing mouse retina macrophages enter during in utero life from the vessels on the inner retinal surface,

their distribution and numbers paralleling the appearance of apoptotic ganglion cells and subsequently apoptotic inner nuclear layer neurons, which they phagocytose(Hume et al. 1983). Relative to the loss of inner retinal neurones during *in utero* and early postnatal life, murine photoreceptors are subject to minimal developmental apoptosis and as a result macrophages are not found in the outer nuclear (photoreceptor) layer(Hume et al. 1983). As the wave of neuronal remodelling abates, the number of parenchymal macrophages reduces, and they differentiate into a typically complex, ramified, process bearing microglial phenotype, forming a regular network in the inner retinal layers, as seen distributed throughout the adult CNS.

In the resting state microglia maintain low-level expression of many surface markers common to all macrophage populations, including the macrophage-restricted F4/80 marker and receptors for Fc and complement (CR-3/CD11b) in the mouse, and have a very low rate of turn over with the systemic myeloid pool(Hickey and Kimura 1988; Perry and Gordon 1991). The perivascular macrophages probably have a higher blood replacement rate and, since in the retina, they more readily express MHC molecules than their parenchymal counterparts(Provis et al. 1995), they may play a constitutive role in T cell dialogue and have antigen presentation capability(Dick 1999).

Although the function of microglia during physiological conditions is still largely unknown, their vigorous response to CNS pathology is well recognised and has been the subject of much research over the last 20 years.

MICROGLIA DURING CNS INJURY

There have been a large number of studies on the responses of microglia to a variety of types of CNS injury. Perhaps the simplest of these is the stab injury to the rodent brain which causes damage to neuronal and connective tissues, and disrupts the blood-brain barrier(Giulian et al. 1989). Reactive microgliosis and recruitment of blood borne macrophages are seen with this model where, like macrophages in other sites, they participate in tissue repair and the induction of astroglial proliferation and neovascularisation; effects that could be inhibited by administration of chloroquine or colchicine to attenuate macrophage involvement. Microglia and macrophages may mediate stimulation of astroglial proliferation through the release of IL1(Giulian et al. 1986; Giulian et al. 1988), which may also be involved in the regulation of brain development by microglia during ontogeny(Giulian et al. 1988).

More useful when considering microglial responses to neurodegeneration are the facial nerve transection and chemical injury models, which leave the blood-brain barrier intact and yet cause central neuronal degeneration within the facial nerve nucleus in the brain stem(Streit and Kreutzberg 1988; Streit et al. 1989). After peripheral neural injury, microglia proliferate(Graeber et al. 1988), adopt a more rounded (activated) morphology and migrate to the site of injury, where they up-regulate expression of several markers including CR-3 and MHC class I and II(Graeber et al. 1988; Streit et al. 1989). An interesting distinction can be drawn between microglial behaviour after facial nerve transection (so called sub-lethal injury) in which the central neurones survive and eventually regenerate, and the injection of a neurotoxin (ricin) into the nerve, which causes lethal injury and central motor neuronal death. In the former, microglial responses are restricted to activation and proliferation without phagocytosis. In the latter, with central neuronal death,

microglia rapidly develop phagocytic capability and remove the neuronal debris resulting from the lethal injury(Streit and Kreutzberg 1988). So it seems that microglia respond to both neuronal injury and neuronal death in a discretional manner, with capacity to adapt to the requirements of the pathology.

Since these seminal studies, *in vivo* and *in vitro* responses of microglia to various stimuli have been extensively examined and a more detailed picture of the remarkable functional repertoire of these cells is beginning to emerge.

Influence of the CNS environment on microglial activity

Microglial immune functions are regulated by intrinsic inhibitory factors within the CNS. Neurones are thought to constitutively release certain neurotrophins (e.g. brain derived neurotrophin, nerve growth factor and neurotrophin-3) that have inhibitory effects on microglial MHC class II expression(Neumann et al. 1998), and the recent discovery of interaction between neurones and myeloid cells via the CD200 and CD200 receptor (CD200-R) axis has introduced a new paradigm in neurone-mediated suppression of CNS myeloid activity(Wright et al. 2000). CD200 (also known as OX2) is expressed on neurones, endothelium and lymphoid cells and is the ligand for CD200-R, which is restricted to cells of myeloid lineage, delivering an inhibitory signal. When this signal is missing, as in the CD200 knockout mouse, microglia adopt an activated phenotype and a more aggressive response to CNS injury(Hoek et al. 2000; Broderick et al. 2002).

Involvement in immune responses

Microglia express receptors for a host of different pro- and anti-inflammatory cytokines, including the interferon-γ (IFN), tumour necrosis factor-α (TNF-α), interleukins (IL) 1, 4, 10, 12, 13, 15 and 18 (reviewed by Aloisi(Aloisi 2001) and Lee(Lee et al. 2002)) which may be released by T cells during CNS inflammation. The effects of some of these cytokines on microglia has been determined *in vitro*, but in view of the alteration of microglial phenotype when placed in culture(Becher and Antel 1996; Mertsch et al. 2001), the applicability of such studies to the *in vivo* setting is open to debate. Nevertheless, it is clear that the archetypal Th1 cytokine IFNγ is a potent stimulator of microglial activation, enhancing their antimicrobial, pro-inflammatory functions(Colton et al. 1992) although antigen presentation capability may be enhanced(Vass and Lassmann 1990; Seguin et al. 2003) or reduced(Broderick et al. 2000). TNFα and IL-1β also have stimulatory effects on phagocytosis and oxidative activity respectively(Smith et al. 1998), while Th2 cytokines such as IL-4, IL-10 and TGFβ tend to suppress Th1-mediated microglial activation(Frei et al. 1994).

As well as receptors for a large number of cytokines and chemokines, microglia are able to secrete a plethora of these molecules(Aloisi 2001). Although many of these cytokines are considered pro-inflammatory (e.g. IL-1 and TNFα), much interest has been focused recently on the immuno-regulatory function of microglia and their production of IL-1 receptor antagonist, IL-10 and transforming growth factor beta (TGFβ), which have suppressing effects on Th1 responses(Martin and Near 1995; Bettelli et al. 1998), and potential autocrine regulatory functions(Broderick et al. 2000).

Evidence also suggests that the regulatory effects of microglia may occur through antigen presentation to T cells. It is clear that microglia possess, *in vivo*, the

molecular repertoire to present antigen in conjunction with MHC class II and essential co-stimulatory molecules such as CD40, CD80 and CD86 since the expression of these are induced during various human CNS disease states and after stimulation *in vitro*(Penfold et al. 1993; De Simone et al. 1995; Gerritse et al. 1996; Togo et al. 2000). It is also likely that microglia are able to liaise with T cells in the perivascular space since they are a component of the perivascular glia limitans(Lassmann et al. 1991; Provis et al. 1995). However, although stimulated microglia may present antigen and induce T cell proliferation *in vitro*(Aloisi et al. 1998), they do not have the efficiency of dendritic cells in stimulating naïve T cells(Aloisi et al. 1999) and there is doubt about whether they induce full T cell stimulation *in vivo*. Ford *et al.* found that while CNS associated macrophages could produce proliferation and full effector function in encephalitic myelin basic protein-reactive T cells, CNS microglia could induce the T cells to release pro-inflammatory cytokines, but the T cells subsequently underwent apoptosis(Ford et al. 1996). This suggests either that microglia can not provide the necessary co-stimulatory signals or that inhibitory signals are delivered, and may represent a mechanism by which microglia down regulate CNS immune responses by auto-reactive T cell clones.

Recognition and phagocytosis of pathogens and apoptotic cells

Macrophages are a major component of the innate immune response, and as such have an important role in defence against many pathogens. Pathogens are identified through a series of pattern recognition receptors(Janeway and Medzhitov 2002) leading to the induction of antimicrobial genes and release of inflammatory cytokines. Among these, CD11b (complement receptor 3), mannose receptor and the lipopolysaccharide (LPS) receptor CD14 are expressed by microglia (Becher and

Antel 1996; Linehan et al. 1999), and bacterial LPS has been extensively used to activate microglia *in vitro* and *in vivo*. In concert with CD11b and the mannose receptor, microglia express other opsonic receptors such as Fc receptors and other complement receptors which instigate targeted phagocytosis (Mosley and Cuzner 1996).

The phagocytic capacity of macrophages is not restricted to pathogens and, as mentioned above, microglia are responsible for the clearance of dead and dying cells resulting from developmental remodelling and disease. Apoptotic cells attract phagocytes by presenting certain "eat me" signals, including phosphatidylserine and altered carbohydrates on their surface(Fadok et al. 2001). Macrophages possess receptors, such as the phosphatidylserine receptor(Hoffmann et al. 2001), the vitronectin receptor(Fadok et al. 1992) and the scavenger receptor class A(Platt et al. 1996) to enable them to respond to these signals and these have been shown in mice to be involved in the phagocytosis of apoptotic photoreceptors by microglia(Hisatomi et al. 2003).

It is unclear, however, which signalling pathways convey the message of cell injury to distant microglia, thereby initiating their migration to the site of pathology as is seen in photoreceptor degenerations. Neuronally derived chemoattractants, and in particular the chemokines fractalkine(Harrison et al. 1998), IL6(Streit et al. 2000) and monocyte chemoattractant protein 3(Zhang 2003) have been studied in rodents and may play a role in microglial recruitment. It is interesting to note that neuronal apoptosis is not a pre-requisite for microglial activation, and indeed in some animal models of neurodegeneration microglial activation is seen in response to subtle morphological alteration, well before neuronal death occurs(Boillee et al. 2001).

Microglial involvement in neurodegeneration and cytotoxicity

Of the many molecules produced by activated microglia, several have been shown to have neurotoxic properties. These include the cytokines TNFα and IL-1β(Chao et al. 1995; Jeohn et al. 1998; Takahashi et al. 2003), free radicals nitric oxide and superoxide(Boje and Arora 1992; Chao et al. 1995; Liberatore et al. 1999; Dehmer et al. 2000; Liversidge et al. 2002), prostaglandins(Araki et al. 2001) and excitatory amino acids(Piani et al. 1992; Giulian 1999) in both humans and rodent models. Furthermore, studies of mixed neuronal-glial cultures from rats (Bronstein et al. 1995) and mice ((Bronstein et al. 1995; Araki et al. 2001) show that stimulation of microglia by LPS leads to neuronal death, whereas LPS itself has no such effect on neuronal cultures alone.

The initial link between microglia and the pathogenesis of neurodegenerative conditions was made after analysis of brains from patients with Alzheimer's disease (AD) and Parkinson's disease (PD)(McGeer et al. 1987; McGeer et al. 1988; Rogers et al. 1988). In pathology samples from patients with Alzheimer's disease microglia may be found clustered around senile plaques, and when incubated *in vitro* the plaque material (β-Amyloid) is rapidly ingested by microglia and induces their activation and release of a neurotoxic factor that is probably an excitatory amino acid(Giulian et al. 1995; Giulian 1999). Nitric oxide has also been implicated in the pathogenesis of Alzheimer's(Law et al. 2001).

In Parkinson's disease, large numbers of activated microglia are found in the substantia nigra, a finding confirmed in the 1-methyl-4- phenyl-1,2,3,6-tetrahydropyridine mouse model of Parkinson disease(Kohutnicka et al. 1998). Inhibition of microglial activation and in particular their inducible nitric oxide synthase (iNOS) activity in this animal model leads to reduced loss of dopaminergic

neurones(Du et al. 2001; Wu et al. 2002), and furthermore, iNOS deficient mice are resistant to disease(Liberatore et al. 1999; Dehmer et al. 2000), although not all investigators have confirmed this(Itzhak et al. 1999).

Several other neuropathologies have since been added to the list of conditions with possible pathogenic microglial involvement, including cerebral ischaemia (stroke)(Danton and Dietrich 2003), neuronal ceroid lipofuscinoses(Nakanishi et al. 2001)(also known as Batten's disease) and prion disease(Brown 2001).

Microglial activity during retinal degeneration

Thus, there is an expanding body of evidence supporting the notion that microglia may respond to CNS injury in a damaging way, with secretion of cytotoxic factors that exacerbate neuronal loss. This concept is therefore of interest to those studying retinal disease, since microglial activation and migration to the injured layer of the retina has been recognised for many years, and was noted by Sanyal in his detailed descriptions of the retinal pathology in the *Prph2*$^{Rd2/Rd2}$ (*rds*) mouse (Sanyal et al. 1980). He described that photoreceptor degeneration was accompanied by 'altered macrophage activity' with a migration of large numbers of macrophages (microglia) from their normal location in the inner retinal layers, to the outer nuclear layer and sub-retinal space, where they had high histochemical activity of the lysosomal enzyme N-acetyl-β-glucosaminidase and appeared to be responsible for 'removing the debris of dying cells'. Similar observations have been made in other models of inherited photoreceptor degeneration such as the RCS rat(Essner and Gorrin 1979; Thanos 1992; Roque et al. 1996) and the *rd* mouse(Sanyal 1972), in light-induced photoreceptor death in albino mice(Ng and Streilein 2001), and also in a recent

histopathological study of retina from a patient with retinitis pigmentosa(Gupta et al. 2003).

It seems likely that in these instances microglia have a phagocytic role in assisting the over-burdened retinal pigment epithelium in the clearance of apoptotic cell debris. Indeed this has been confirmed by ingenious experiments by Thanos, who retrogradely stained retinal ganglion cells by application of a fluorescent dye to the cut end of the sectioned optic nerve in RCS rats. Microglia were found to phagocytose the flourescently labeled, damaged ganglion cells in the inner retina, before migrating to the outer retina to undertake phagocytosis of photoreceptor debris when these cells subsequently underwent apoptotic cell death(Thanos 1992). This sub-retinal phagocytic role has been confirmed by others(Ng and Streilein 2001; Hisatomi et al. 2003).

It is possible, however that microglial activation in retinal degenerations may be secondary to photoreceptor (or other neuronal) injury and that, once activated, microglia may participate in a local inflammatory cascade resulting in the release of cytotoxic mediators which exacerbate photoreceptor injury and death, as has been suggested in other neurodegenerative conditions discussed above. This concept, in the context of retinal microglia, has been applied by some to models of glaucoma with several authors suggesting a pathogenic role of microglia on ganglion cells in the optic nerve head(Neufeld 1999; Wang et al. 2000; Yuan and Neufeld 2001) through TNFα, nitric oxide (NO) and matrix metalloproteinase release. Thanos *et al.* attempted to inhibit the response of retinal microglia to transection of the optic nerve in the rat by intravitreal injection of macrophage inhibitory factor (MIF)(Thanos et al. 1993). They found significant retardation of axotomy-induced ganglion cell degradation in the retina of MIF treated eyes and noted morphological changes in the

microglia. In the same model, stimulation of microglia with intravitreal injection of a tetrapeptide macrophage stimulating factor led to increased microglial numbers and ganglion cell death was accordingly increased.

There has, however, been remarkably little investigation of the direct cytotoxic effects of microglia on photoreceptors during outer retinal degeneration, and the issue has probably only been purposefully addressed by two studies(Roque et al. 1999; Koike et al. 2003). The first was in a mouse model for neuronal ceroid lipofuscinosis (Batten's disease, lysosomal storage disorder), the Cathepsin $D^{-/-}$ mouse, in which there is rapid neonatal CNS degeneration with particularly prominent apoptotic loss of neurones in the thalamus and the photoreceptors(Nakanishi et al. 2001; Koike et al. 2003). Reactive, activated microglia are found in both areas where they express iNOS and have therefore been implicated as mediators of the neuronal and photoreceptor apoptosis (through NO production). However, although iNOS inhibitors reduce brain neuronal loss and prolong lifespan, they do not affect the rate of photoreceptor apoptosis.

The second study was conducted in vitro using retinal microglia isolated from the dystrophic RCS rat and a photoreceptor cell line(Roque et al. 1999). They found that the culture medium from microglia extracted and cultured for 48 hours, contained a heat stable factor that was toxic to the photoreceptors, with a four-fold increase in their apoptotic death as compared with basal medium or medium from cultured Müller cells. A couple of criticisms may be leveled at this study: firstly all microglia adopt a more activated phenotype when placed in culture, so it is difficult to know the relevance to the *in vivo* state. Secondly, because of the difficulty experienced in isolating a pure and stable culture of RCS rat photoreceptors, they used a transgenic photoreceptor cell line with proliferative capacity (661w), quite different from the

diseased photoreceptors that may have provoked reaction from the microglia *in situ*, and with possibly greater (or lesser) sensitivity to cytotoxic insults.

So, to summarise, although dramatic alterations in microglial behaviour have long been recognised as part of photoreceptor degeneration, and increasing evidence in other areas of the CNS demonstrates the cytotoxic behaviour of these cells during responses to neuropathology, their potential pathogenic role in photoreceptor degeneration has been inadequately studied and is unknown. In addition, the mechanisms underlying photoreceptor apoptosis in many of the genetic defects causing these diseases is also unexplained, although evidence suggests an indirect or 'non-cell autonomous' process. If microglia were involved in the initiation or exacerbation of retinal damage in these diseases, then a multitude of therapeutic approaches, targeting microglial behaviour, would be made available for a group of conditions that have, at present, no treatment.

AIMS OF THE WORK

The objective of this research is to characterise microglial behaviour during photoreceptor degeneration, using a naturally occurring mouse model. That microglia undertake phagocytic clearance of apoptotic cell debris is not in question and the project has not studied this aspect of their behaviour specifically. It is the potential cytotoxicity of retinal microglia during photoreceptor degeneration and their influence over the disease process that has been the primary area of interest. In investigating this concept, I aimed to learn more about microglial biology in general with potential applicability to other pathologies within the CNS.

CHAPTER TWO

MATERIALS AND METHODS

The Animals

Homozygous *rds*$^{-/-}$ mice used in this project were bred and housed in the Biological Services Unit at the Institute of Ophthalmology, University College London. They were bred on a CBA background. Wild-type CBA mice were bred and housed in the Animal Unit, School of Medical Sciences, Bristol University. All animals were treated in accordance with the Animal License Act (UK).

Animal Sacrifice and fixation of tissues

Mice were terminally anaesthetised with an intra-peritoneal injection of Pentobarbitone sodium (Sagatal, 60 mg/ml, Rhone Merieux, GA, USA) and intra-cardially perfused with PLP-fixative (2% paraformaldehyde and 0.05% glutaraldehyde, preparation described below). Cardiac perfusion was carried out, after carefully ensuring the absence of reflex pain responses, by opening of the thoracic cage, exposure of the heart, incision of the right atrium followed by needle puncture and perfusion of the left ventricle until clear fixative was seen issuing from the right atrial incision. Both eyes were enucleated using dissecting forceps and scissors, taking care to leave the globe intact with a length of optic nerve attached. The eyes were then immersed in PLP fixative (2% paraformaldehyde and 0.05% glutaraldehyde) for four to six hours, before incubation overnight in 20% sucrose at 4°

Celsius. Then, after drying with paper tissue the eyes were embedded in OCT (Optimal Cutting Temperature compound, Sakura, distributed by R. A. Lamb, Eastbourne, UK), snap frozen in liquid nitrogen and stored at -70^{o} Celsius. Occasionally the spleen and/or thymus were also taken and were fixed in an identical fashion to the eyes.

The method of fixation seemed critical to the preservation of retinal histology during sectioning and also of the morphological clarity of microglia during staining. One set of *rds* eyes taken at P24 without perfusion fixation, were snap frozen immediately and then fixed as the first step of the immuno-staining run. Retinal histological preservation was poor and microglial staining blurred and imprecise (*figure 2.1*)

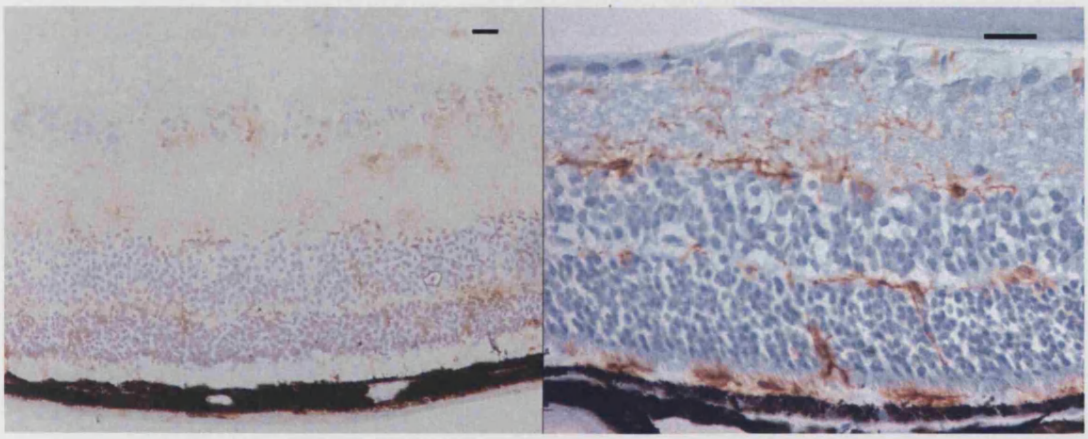

Figure 2.1 Fixation method was of utmost importance in obtaining clear immunohistochemical results. Two retinal sections are shown counterstained with haematoxylin and immunohistochemically stained for F4/80 for microglial detection. Snap freezing of the tissue without fixation and subsequent fixation in 1% paraformaldehyde prior to staining led to poor histological preservation and smudged cellular outlines on immunostaining for the cell surface marker (a). Perfusion fixation with PLP fixative followed by further ex-vivo fixation and sucrose cryoprotection gave excellent results (b). Scale bar 20 μm.

Periodate-Lysine-Paraformaldehyde (PLP) fixative preparation

To prepare 300 ml of PLP with 2% paraformaldehyde and 0.05% glutaraldehyde

1) Mix:

112 ml 0.2M L-lysine

75 ml 0.2M phosphate buffer pH 7.4

13 ml water

Adjust to pH 7.4

2) Prepare separately:

6g paraformaldehyde in 80 ml water

Add 100-150 µl 10M NaOH

Stir until dissolved

Add 5 ml 0.2M phosphate buffer pH 7.4

Check pH and adjust to 7.4

Adjust to 100 ml with water

Add 640 mg sodium periodate and stir to dissolve

3) Mix both solutions and add 300 µl 50% glutaraldehyde.

Cutting of Frozen Tissue Sections

Preparation of microscope slides

76 mm x 26 mm glass microscope slides were coated with Poly-L-Lysine (Sigma, Poole, UK) to ensure adhesion of tissue sections, and thus prevent deterioration and loss of sections during the immunohistochemical staining process. The manner of coating of the slides is critical to section adhesion, particularly with sections through an eye which consist of concentric layers of very thin tissue more prone to detachment than homogenous tissues such as spleen and thymus. The manufacturer's instructions on Poly-L-Lysine coating should be followed to the letter and this is described:

A solution of 0.01% Poly-L-Lysine was prepared by diluting 22 ml of 0.1% stock solution in 200 ml distilled water. Racks holding 25 slides were immersed in the solution for no less than 5 minutes and then dried in a 37° Celsius incubator overnight. With this method excellent section adhesion was obtained.

It was found to be critical, however that only 200 slides are used per 200 ml of diluted Poly-L-Lysine (0.01%) solution, since the coating efficacy reduces after this number. Inadvertent overuse of Poly-L-Lysine solutions (i.e. coating of over 200 slides) led to significant problems of section detachment during staining in the early part of the project. Furthermore, an alternative method of coating, commonly used for paraffin embedded section adhesion, which involves wiping of stock Poly-L-Lysine solution over the slides with a tissue was found to lead to inadequate section adhesion. This method may be adequate for paraffin embedded sections because they adhere more strongly to glass slides.

Frozen Sectioning

A Reichert-Jung (now Leica Microsystems Nussloch GmbH, Wetzlar, Germany) cryostat was used for the cutting of sections from the frozen tissue blocks. Blocks were retrieved from the –70°C freezer and allowed to warm to –20°C before mounting on a metal plate with further OCT. Sections were cut at –20°C, and after initially testing various thicknesses, 12 μm was used as this was found to provide the best morphology. Eyes were cut in the antero-posterior plane. Tissue sections were collected on the Poly-L-Lysine coated glass microscope slides and allowed to dry for 1 to 4 hours before staining or storage in sealed containers with silica gel at –70°C. Generally only the central portion of the retina (i.e. those sections passing close to or through the optic nerve head) was used for immuno-staining and therefore, as much as was possible, this was the region of the eye sectioned.

Early in the project, sections were collected sequentially on the slides, such that each slide would hold three adjacent sections. This led to redundancy of some sections when cell counting was carried out, since it was deemed inappropriate to count adjacent sections. Therefore the first and third on each slide could be counted, while the second (middle) section could not.

Later, most eyes were cut onto 16 slides with 4 sections per slide. The first section would be applied to slide 1, the second to slide 2 and so on until the 17th section was applied to slide 1 again. This sequence continued until 64 sections had been cut, with each slide having 4 widely distributed non-adjacent sections, giving a better representation of the whole tissue and allowing four sections to be counted per slide. Care was taken not to count adjacent numbered slides (e.g. slide numbers 3 and 4) for the same immunohistochemical stain.

Immunohistochemical and Immunofluorescent Staining

Reagents

Phosphate Buffered Saline (PBS)

Bovine Serum Albumin (BSA, 2% and 0.1% in PBS, Sigma, Poole, UK)

Triton X-100 (Sigma, Poole, UK)

Sodium citrate (BDH, Poole, UK)

Hydrogen peroxide 3% (Sigma, Poole, UK)

Methanol (BDH, Poole, UK)

Elgastat water

Avidin-biotin peroxidase complex (ABC kit, Vector, Burlingame CA, USA)

Diaminobenzidine peroxidase substrate (DAB, Vector, Burlingame CA, USA)

3-amino-9-ethylcarbazole peroxidase substrate (AEC, Vector, Burlingame CA, USA)

Levamisole (Sigma, Poole, UK)

NBT/BCIP (Nitroblue Tetrazolium Chloride / 5-Bromo 4-chloro 3-indolyl phosphate) tablets (Roche Diagnostics, Lewes, UK

Gill's Haematoxylin (number 2, Thermo Shandon, Pittsburg PA, USA)

Histoclear (National Diagnostics, Atlanta GA, USA)

Histomount (National Diagnostics, Atlanta GA, USA)

Vectashield mounting medium with DAPI (4',6 diamidino-2-phenylindole) (Vector, Burlingame CA, USA)

Normal Sera for Blocking Solutions

Unless otherwise stated, normal serum was obtained from Vector. Serum was used from the animal in which the secondary antibody was generated, to block unwanted binding prior to addition of the primary antibody.

Primary Antibodies

The primary antibodies used in this project are described in table 2.1 and 2.2.

Table 2.1: Mouse Myeloid Cell Surface Markers

Antigen	Host	Mono/polyclonal	Cat No/clone	Dilution	Source
F4/80	Rat	Monoclonal	MCAP497/Cl:A3-1.	1:50-200	Serotec, Oxford, UK
F4/80:Biotin	Rat	Monoclonal	MCA497B/Cl:A3-1.	1:5	Serotec, Oxford, UK
Sialoadhesin	Rat	Monoclonal	MCA884/3d6.112	1:250	Serotec, Oxford, UK
CD11b	Rat	Monoclonal	MCA74G/M1/70.	1:50	Serotec, Oxford, UK
CD11c	Hamster	Monoclonal	MCA1369Z/N418.	1:100	Serotec, Oxford, UK
CD205	Rat	Monoclonal	MCA949/NLDC-145.	1:10	Serotec, Oxford, UK
MHC class II	Rat	Monoclonal	556999/M5-114.15.2	1:200	Pharmingen, Oxford, UK

Table 2.2: Intracellular Markers

Antigen	Host	Mono/polyclonal	Cat No/Clone	Dilution	Source
iNOS	Rabbit	Polyclonal	AHP30 /	1:2000	Serotec, Oxford, UK
Nitrotyrosine	Rabbit	Polyclonal	06-284 /	1:200	Upstate Biotech, Lake Placid NY, USA
Proliferating Cell Nuclear Antigen (PCNA)	Mouse	Monoclonal	M0879/PC10	1:250	DAKO, Glostrup, Denmark
Cleaved Caspase 3	Rabbit	Polyclonal	Asp175 /	1:200	Cell Signalling Technology, Beverly MA, USA

Secondary antibodies

For immunohistochemistry, biotinylated secondaries were used and were acquired from Vector (Burlingame CA, USA). For immunofluorescence, fluorochrome (FITC and TRITC) conjugated secondary antibodies were used from Jackson Immunoresearch (West Grove PA, USA). Antibodies not already pre-absorbed for mouse, were absorbed by the addition of 20 µl of normal mouse serum per ml of diluted secondary antibody.

Protocols

During this project, a large number of variations of immunohistochemical and immunofluorescent staining were used, which will be described in each chapter in

turn. However, the basic techniques used for immunohistochemistry for cell surface markers and apoptosis detection by terminal deoxynucleotidyl transferase (TdT)-mediated dUTP nick end-labeling (TUNEL) are described here.

Immunohistochemical detection of cell surface markers using a peroxidase-based detection system

1) Slides out 30-60 minutes to dry
2) Encircling of sections with 'Immedge' hydrophobic pen
3) Wash 20 min in PBS
4) Block endogenous peroxidase activity with 0.3% hydrogen peroxide in methanol for 15 min
5) Wash 2x5 min in PBS
6) Blocking serum 1.5% in 2% BSA for 30 min
7) Tip off excess blocking serum and add Primary antibody diluted in 2% PBSA for 2 hours at room temperature or overnight at 4°C
8) Wash 2x5 min in PBS
9) Secondary biotinylated antibody diluted 1:200 in 0.1% BSA
10) Wash 2x5 min in PBS
11) Add ABC for 30 min
12) Wash 2x5 in PBS
13) Add DAB for 2-5 minutes (checking for development)
14) Rinse in PBS then into running water for 3 min
15) Counterstain with haematoxylin
16) Running water for 3 min
17) Dehydrate sections in alcohols: 75% Alcohol 2min, 100% Alcohol 2x2 min
18) Immerse in Histoclear 2x2 min.
19) Apply Histomount and cover with cover slips

Apoptosis detection by terminal deoxynucleotidyl transferase (TdT)-mediated dUTP nick end-labeling (TUNEL)

A: <u>Immunohistochemical detection</u> using In Situ Cell Death Detection Kit, TUNEL (Alkaline phosphatase method), Roche Diagnostics, Lewes, UK

1) Slides out 30-60 minutes to dry
2) Encircling of sections with 'Immedge' hydrophobic pen
3) Wash 30 min in PBS
4) Permeabilise cells by immersion of slides in 0.1%Triton X-100 in PBS containing 0.1% sodium citrate for 2 minutes
5) Wash 2x5 min in PBS
6) Add TUNEL mixture 60 min at 37°C
7) Wash 2x5 min in PBS
8) Add converter solution 30 min at 37°C
9) Wash 3x5 min in PBS
10) NBT/BICP (1tablet in 10ml of elgastat water containing 1mM Levamisole*) 10 min
11) PBS wash 5 min then running water 2 min
12) Counterstain with methyl green
13) Dehydrate sections in alcohols: 75% Alcohol 2 min, 100% Alcohol 2x2 min
14) Immerse in Histoclear 2x2 min.
15) Apply Histomount and cover with cover slips
16) Allow to dry overnight

* Levamisole, a blocker of endogenous alkaline phosphatase activity within the tissue being stained, was found to reduce unwanted background staining.

B: Immunofluorescent detection using In Situ Cell Death Detection Kit, TUNEL TMRred (Tetramethylrhodamine), Roche, Lewes, UK

1) Slides out 30-60 minutes to dry
2) Encircling of sections with 'Immedge' hydrophobic pen
3) Wash 30 min in PBS
4) Permeabilise cells by immersion of slides in 0.1% Triton X-100 in PBS containing 0.1% sodium citrate for 2 minutes
5) Wash 2x5 min in PBS
6) Add TUNEL mixture 60 min at 37°C in dark
7) Wash 3x5 min in PBS in dark
8) Mount with Vectashield mounting medium with DAPI and cover with coverslip. Stored in dark until viewed by fluorescence microscopy.

Controls

Appropriate negative and positive controls were used in all experiments. Negative controls included both slides treated with no primary antibody and also slides treated with isotype controls. Isotype controls and positive control tissues used for each antibody are detailed in *table 2.3* and illustrated in *figure 2.2*. As much as possible, slides stained for a particular marker and to be compared with each other, were immunohistochemically processed the same time to avoid variations in staining intensities between runs biasing results.

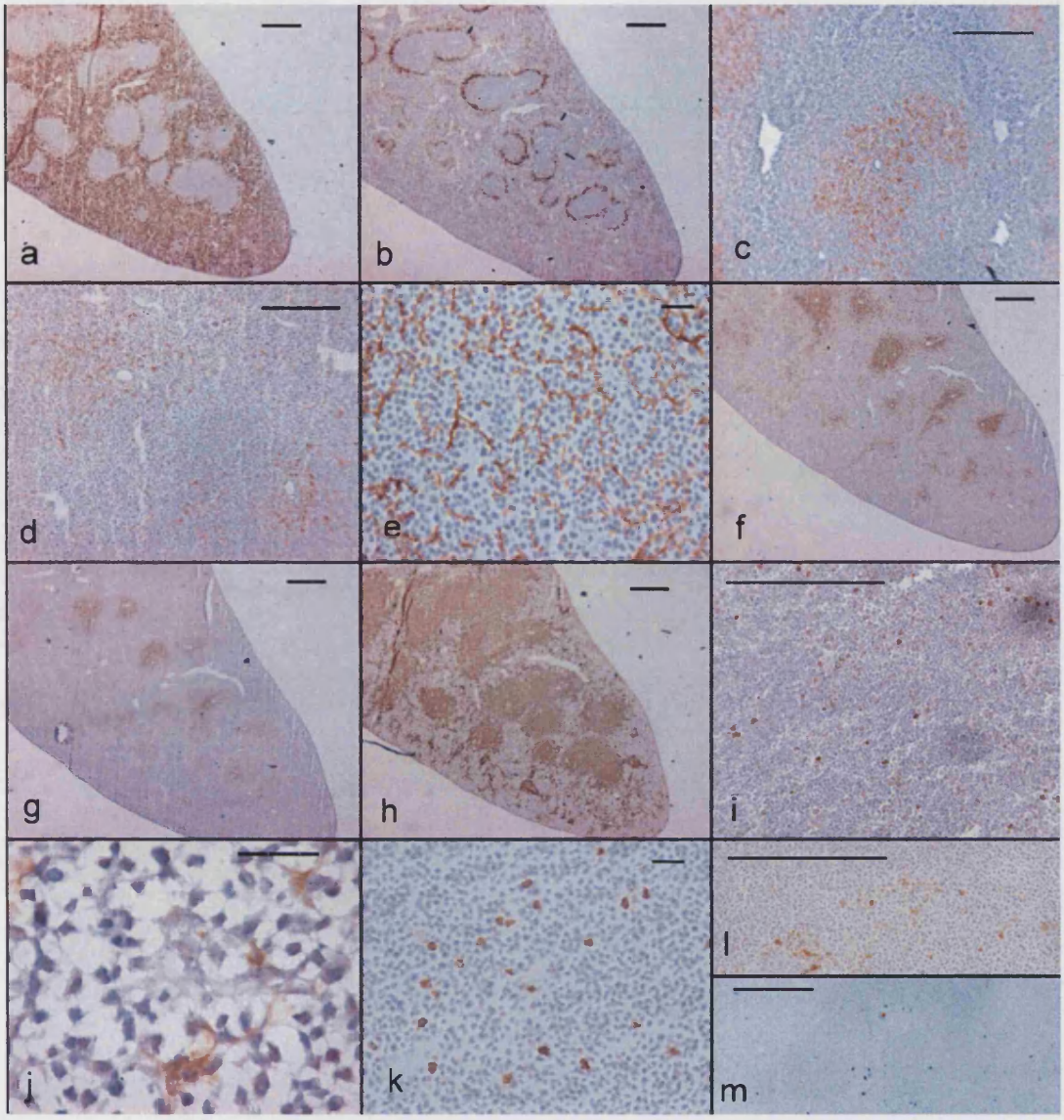

Figure 2.2 Positive controls. a, F4/80 on splenic macrophages (identical to CD11b); b, sialoadhesin on splenic macrophages; c, MHC class II on splenic leukocytes; d, CD11c on splenic dendritic cells; e, CD205 on thymic dendritic cells; f, CD4 on splenic T lymphocytes; g, CD8 on splenic T lymphocytes; h, B220 on splenic B lymphocytes; i, PCNA on thymocytes; j, iNOS on thymic dendritic cells; k, nitrotyrosine on thymocytes; l, activated caspase 3 on apoptotic thymocytes; m, TUNEL positive (apoptotic) thymocytes. Counterstain: haematoxylin, scale bar: 200μm (except on e, j and k: 20μm).

Table 2.3: Isotype and positive controls

Antibody	Positive Control Tissue / Cell	Isotype negative control
F4/80	Spleen / macrophages	Rat IgG2b, Serotec MCA1125
Sialoadhesin	Spleen / marginal zone macrophages	Rat IgG2a, Serotec MCA1212
CD11b	Spleen / macrophages	Rat IgG2b, Serotec MCA1125
CD11c	Spleen or thymus / dendritic cells (DCs)	Hamster IgG, Serotec MCA1367
CD205	Thymus / DCs	Rat IgG2a, Serotec MCA1212
MHC II	Spleen / B lymphocytes and DCs	Rat IgG2b, Serotec MCA1125
TUNEL	Neonatal thymus / apoptotic thymocytes	Supplied in TUNEL Kit, Roche
PCNA	Neonatal thymus / proliferating cells Eye / lens epithelial cells	Negative supplied with MOM kit
Nitrotyrosine	Neonatal thymus / thymocytes*	Rabbit Ig, Serotec, PRABP01
iNOS	Neonatal thymus / DCs*	Rabbit Ig, Serotec, PRABP01
Caspase 3	Neonatal thymus / apoptotic thymocytes	Rabbit Ig, DAKO, X0903

* Dendritic cells within the neonatal thymus effect clonal deletion of autoreactive thymocytes through NO(Tai et al. 1997; Aiello et al. 2000), and thus thymus from P14 mice was used as a positive control for iNOS and for nitrotyrosine (found in thymocytes undergoing NO-mediated apoptosis).

Microscopy and Quantification

All retinal sections that underwent immuno-staining were analysed by light or fluorescent microscopy. Data collected during this research was predominantly in the form of cell numbers counted in retinal sections. For this purpose, slides were coded so as to blind the observers to the type of the tissue and the antibody used. Three observers were used during the project: Professor Andrew Dick (supervisor), Dr Conor Murphy (research colleague) and Dr Edward Hughes. Distinct criteria and parameters were first defined for cell counting and are listed below. In retrospect the gold standard of quantification would have involved some estimation of intra- and inter-observer error, which should be less than 10%. This was not done but inter-observer error will not have been an issue in individual experiments since a single observer was assigned an entire experiment, and therefore counted all the slides for both treated and control animals.

Sections counted

Two to eight non-adjacent sections per antibody, per eye were counted depending on the experiment (this will be elaborated upon in each chapter). Only sections with adequate histological preservation were used.

Region counted

For the majority of markers, positively stained cells were counted in the most central 1.2 mm length of retina in the section (centred in the optic nerve head or posterior pole of the eye). This length of retina was measured using an eye-piece graticule measuring 300 μm, four lengths of which were used as the target region (*figure 2.3*).

This ensured that bias resulting from regional variations in cell density was minimised.

For two double immunofluorescent experiments, F4/80 / TUNEL and TUNEL / Proliferating Cell Nuclear Antigen (PCNA), the entire retinal section was counted and results expressed and cells per mm^2. The area of each retinal section was measured using an image analysis system (Quantimet; Leica Cambridge, Cambridge, UK).

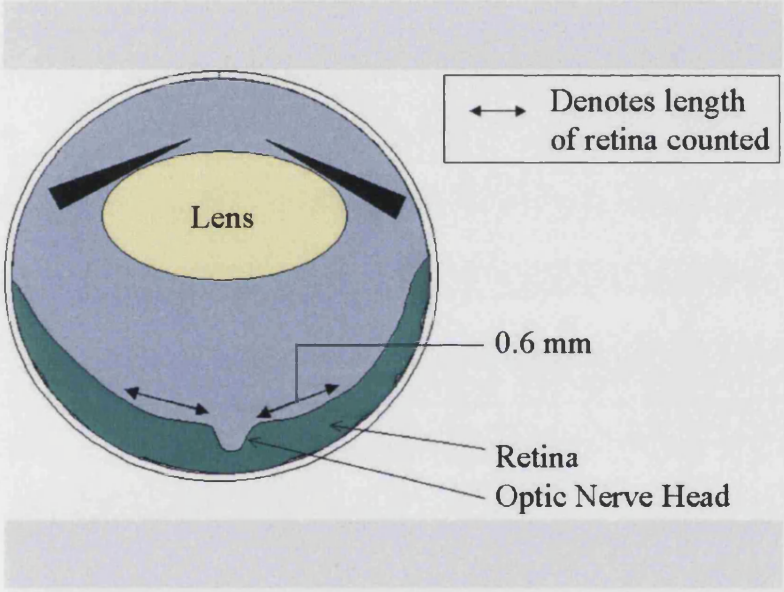

Figure 2.3 Schematic depiction of the region of retina analysed during most cell counts.

Defining a positive cell

All observers adhered to the same criteria for identifying cells that were positively stained. In the case of retinal microglia, the marked increase in their number and their ramified morphology precluded any attempts at counting cell numbers within the retinal parenchyma. As sub-retinal microglia were rounded, individual cell counts could be obtained, which corresponded to the semi-quantitatively assessed increase in

microglial numbers throughout the retina. Furthermore the sub-retinal space has been deemed by previous observers to be the destination of microglia as they migrate through the retina during retinal degeneration (towards the site of injury), so the counting of cells specifically in this location was considered to provide a good indication of the microglial response. Positively stained microglia were counted if they contained a nucleus or had a large enough area of cytoplasm to do so. Small segments and tufts of positively stained cytoplasm/membrane were not counted (*figure 2.4a*).

In the case of TUNEL staining, a photoreceptor nucleus (i.e. a nucleus residing in the outer nuclear layer) was counted as positive if it was densely stained and had evidence of staining throughout the nucleus. Nuclei that were encircled by a ring of peripheral staining without central nuclear staining were not counted (*figure 2.4b*).

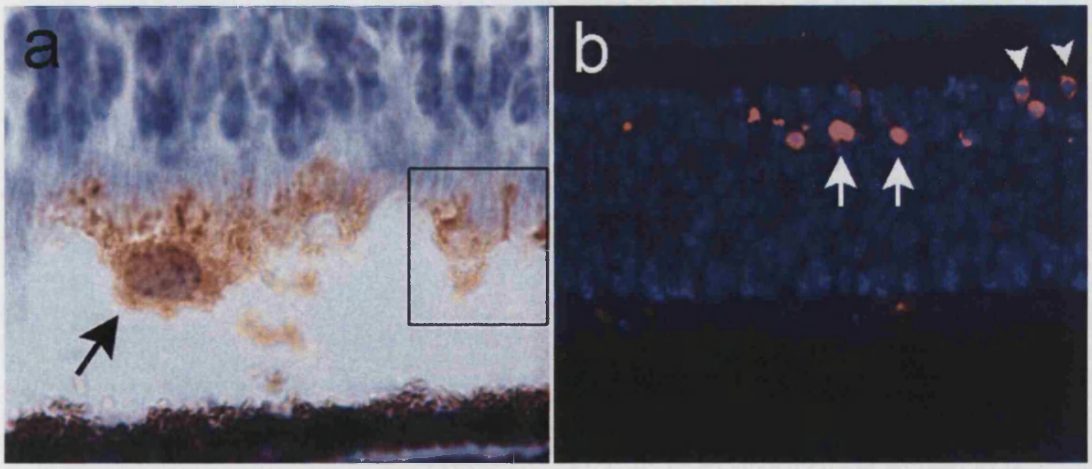

Figure 2.4 Defining a positive cell. Positively stained sub-retinal microglia were counted if they contained a nucleus or were large enough to do so (a, arrow). Tufts of positively stained membrane/cytoplasm were not counted (a, box). For TUNEL stained tissue, nuclei within the outer nuclear layer were counted if the were positively stained throughout the nucleus (b, arrows). A perinuclear halo was not considered to represent a TUNEL-positive cell (b, arrowheads).

Data Analysis and Statistics

Cell count data were entered into Microsoft Excel spread sheets. A mean cell count for each eye was obtained by taking the mean of the counts obtained from sections counted from that tissue. A mean of these means was then taken to give a value representative of a group of eyes with common features (e.g. same time point, same intervention etc.). Data are expressed as mean number of cell/unit length or area +/- standard error of the mean (SEM), and an independent samples T-test was used to determine statistical significance of differences between groups, where normality of the data was assumed and $p<0.05$ was considered significant. For this purpose a statistics package from SPSS (Chicago IL, USA) was used.

CHAPTER THREE

A DESCRIPTIVE STUDY OF MICROGLIAL BEHAVIOUR DURING RETINAL DEGENERATION IN THE *RDS* MOUSE

The first phase of this research was to describe the changes in microglial phenotype and activity during photoreceptor degeneration in the *rds* mouse. In the past the prodigious microglial reaction during photoreceptor degeneration has been noted, but there has been no detailed investigation of their functionality in these circumstances beyond a well characterised phagocytic role. Furthermore, although the temporal characteristics of photoreceptor apoptosis in this and other mouse models have been described(Chang et al. 1993; Portera-Cailliau et al. 1994), this has never been closely compared to the chronology of microglial activity. The earliest reports by Chang *et al* and Portera-Cailliau *et al*, documenting apoptosis as the mechanism of photoreceptor death in *rds* mice, noted a monophasic peak in photoreceptor death at P16-18 in *rds* mice, a finding since corroborated by other investigators studying the *rds* model(Ali et al. 1998). Should microglia be responsible for, or contributing to, photoreceptor demise one would expect that the peak in microglial activity should coincide with or directly precede any peak in photoreceptor apoptosis.

In this section we have therefore characterised the time course of microglial numbers, cell surface markers and markers of potential cytotoxicity during the most active phase of photoreceptor degeneration. Since the major mechanism of microglial cytotoxicity is through the production of nitric oxide (NO) and reactive oxygen species, we have concentrated on the ability of microglia to produce NO (through

inducible nitric oxide synthase, iNOS) and oxidative protein damage as indicated by nitrotyrosine accumulation in target tissue.

In terms of cell surface markers, it is well described that microglia are able to rapidly up-regulate their expression of certain molecules when activated, and while there is no specific marker of microglial 'activation' per se, knowledge of the functions of some of these markers provides clues to the behaviour of the microglia bearing them. The markers used are described below.

F4/80, first described by Austyn and Gordon(Austyn and Gordon 1981). The F4/80 antibody is a mouse macrophage-specific rat monoclonal IgG2b. The antigen recognised by this antibody is a 160kD glycoprotein with unknown function (the knockout mouse has normal phenotype(McKnight and Gordon 1998)), although it has some structural similarities to epidermal growth factor (EGF) and the family of Tm7 (seven transmembrane domain) hormone receptors(McKnight et al. 1996; Hume et al. 2002). There is significant (68%) sequence homology between the F4/80 antigen and human EGF module-containing mucin-like hormone receptor 1 (ERM1) and this is thought to be the possible human homologue of F4/80(McKnight and Gordon 1998). The epitope that F4/80 recognises has the advantage of being considerably resistant to fixative and, as a result the antibody has been extensively used as a marker of murine macrophages, including microglia of the CNS and retina(Hume et al. 1983; Perry and Gordon 1991).

Sialoadhesin, a member of the immunoglobulin superfamily and also known as CD169, is one of a group of macrophage-restricted cell surface sialic acid receptor proteins named siglecs (reviewed by Munday *et al*(Munday et al. 1999)) which has a high degree of conservation between rodents and humans. Although sialoadhesin is

not thought to be a phagocytic receptor(Crocker and Gordon 1986), its expression may facilitate other phagocytic receptors(Munday et al. 1999) and mediate cell-cell and cell-matrix interactions(van den Berg et al. 2001). Sialoadhesin is expressed on a discreet subset of macrophages mainly in secondary lymphoid organs. In the mouse spleen it is present only on macrophages in the marginal zone (*figure 2.3*), which may be involved in antigen handling and lymphocyte interactions(Martinez-Pomares et al. 1996; Steiniger et al. 1997; Geijtenbeek et al. 2002). Sialoadhesin is also expressed in other tissues under physiological conditions in both humans and mice, such as liver, gut and lung, and it is highly expressed in the inflamed joints of patients with rheumatoid arthritis(Hartnell et al. 2001). It is however notably absent, in both humans and mice, from CNS parenchymal microglia which reside behind the protection of the blood-brain barrier(Perry et al. 1992; Hartnell et al. 2001); and there is evidence that contact with a serum agent is a prerequisite of sialoadhesin expression(Crocker et al. 1988; Perry et al. 1992).

CD11b, also known as the complement receptor 3, is a β integrin that functions as a myeloid cell phagocytic receptor for complement opsonised particles and for direct interaction with some microbes (e.g. mycobacterium tuberculosis)(Gordon 2002). It is also involved in the clearance of apoptotic cells by macrophages and the recruitment of myeloid cells to sites of inflammation through binding to ligands such as intercellular adhesion molecule (ICAM-1)(Diamond et al. 1990).

CD11c, also known as complement receptor 4, is another β integrin involved in inter-cellular adhesion and endothelial trans-migration, and is often used as a marker of dendritic cells, which are the predominant cell type expressing this molecule(O'Doherty et al. 1994; De La Rosa et al. 2003). It may however also be

expressed on other myeloid cells such as monocytes, macrophages(Mevorach et al. 1998; Rezzonico et al. 2000) and microglia, especially when the latter are activated(Ulvestad et al. 1994; Dick et al. 1997; Schermer and Humpel 2002).

MHC class II, the key molecule of antigen presentation, may be expressed constitutively by human and rodent microglia(Lassmann et al. 1991; Penfold et al. 1993), but this is usually at low levels until inflammatory conditions prevail, during which microglia up-regulate their expression of MHC class II ten to twenty-fold(Sedgwick et al. 1998). As discussed in the introduction, the expression of MHC class II molecules by parenchymal microglia may provide for an immunoregulatory role rather than invoking primary immune responses.

CD205, also known as DEC205, is an endocytic receptor on dendritic cells (particularly the 'lymphoid' subset) and thymic epithelial cells(Jiang et al. 1995) that is involved in antigen processing. Like CD11c it is used as a marker of dendritic cells, but unlike CD11c, there are no reports of CD205 expression by microglia or macrophages.

PCNA (proliferating cell nuclear antigen), also known as cyclin, is a 36 kDa auxilliary protein for DNA polymerase δ, tethering the enzyme to its substrate by encircling the DNA and thereby increasing the processivity of the polymerase action. It is expressed by vertebrate cells undergoing DNA replication in S phase of the cell cycle but is absent or at nearly undetectable levels in resting cells (in G_0 phase)(Celis et al. 1987). Consequently it is now widely used as a marker of cell division in a variety of tissues and species, including murine microglia(Sedgwick et al. 1998).

iNOS. The nitric oxide synthase (NOS) isoenzymes are responsible for catalysing the production of nitric oxide (NO) from L-arginine. NO has a wide repertoire of biologic functions, and when released by endothelium (eNOS) and neurones (nNOS) it has important effects as a regulator of vascular tone and as a neurotransmitter respectively. It is however the inducible isoenzyme (iNOS) found in many cells but most prominently in macrophages and other myeloid derived cells that is of interest in terms of cytotoxicity. Whilst iNOS and NO are cornerstones of the innate immune system with vital defence roles against bacteria, fungi and tumours, NO also has unwanted, damaging effects on tissues and mediates cellular apoptosis through the production of DNA strand breaks(Muhl et al. 1996; Brune et al. 1999). Microglia readily upregulate expression of iNOS and production of NO under certain pro-inflammatory conditions(Possel et al. 2000) and evidence suggests that this leads to exacerbation of degenerative CNS disease(Liberatore et al. 1999; Law et al. 2001). Furthermore, after pharmacological inhibition of iNOS and in iNOS deficient mice, reduced neuronal loss is seen in both degenerative and inflammatory CNS disease(Nakanishi et al. 2001; Sasaki et al. 2001) and during experimental uveitis in rats(Thillaye-Goldenberg et al. 2000; Liversidge et al. 2002).

Nitrotyrosine. Tyrosine nitration is a covalent protein modification resulting from the addition of a nitro (-NO_2) group onto tyrosine residues, with nitric oxide providing the source of nitrogen(Ischiropoulos 1998). Anti-nitrotyrosine antibodies have been used extensively in a wide variety of tissues to detect NO and ROS mediated protein damage.

METHODS

Experimental design

A panel of antibodies were applied to whole eye sections from *rds* mice aged 8, 14, 16, 17, 19, 21, 30 and 40 days (P8, P14, etc). These time points cover the most aggressive phase of photoreceptor loss in the *rds* mouse. Three eyes were used for the P8, P14, P30 and P40 time points, and four eyes for the time points spanning peak disease activity: P16, P17, P19, P21. At least two non-adjacent sections per eye were counted for each stain. TUNEL detection of photoreceptor apoptosis was performed and compared with microglial activity in the same eyes. For MHC class II staining two eyes were used per time point.

Eyes from wild type CBA mice aged P8, P14, P21, P30 were also analysed with some stains for comparison with the *rds*. In particular, quantitative comparison was made at these time points for the presence of proliferating (dividing) microglia as detected by double staining for F4/80 and PCNA. For TUNEL staining only one wild type eye was used for P14, P21 and P30.

In addition two eyes from P3 CBA wild type and *rds* mice were analysed for microglial markers F4/80 and CD11b. Although initially TUNEL was used at this time point, quantitation of photoreceptor apoptosis was not possible due to the unification of the nuclear layers at this stage of development.

Immunostaining protocols

Single colour immunohistochemistry was employed as described in the previous chapter. For these experiments, the alkaline phosphatase immunohistochemical

TUNEL method was used. Variations on the protocols described above were as follows:

iNOS and nitrotyrosine

5% PBSA used as diluent for primary and secondary antibodies. Incubation times:

Block 60 minutes, 1° antibody 30 minutes, 2° antibody 15 minutes.

Reason: to reduce background staining.

F4/80 / Sialoadhesin two colour immunofluorescence

1) Slides out 30-60 minutes to dry
2) Encircling of sections with 'Immedge' hydrophobic pen
3) Wash 30 min in PBS
4) Blocking serum (goat, 15ul/ml 2% PBSA) 30 min
5) Tip off excess and add Primary antibody (Sialoadhesin) diluted in 2% PBSA overnight at 4°C
6) Wash 2x5 min in PBS
7) Goat anti rat FITC diluted in 0.1% PBSA 60 min
8) Wash 2x5 min in PBS
9) Biotinylated F4/80 primary in 2% PBSA for 2 hours
10) Wash 2x5 min in PBS
11) Streptavidin-TRITC 1:100 in 0.1% PBSA 60 min
12) Wash 2x5 min in PBS
13) DAPI mount

F4/80 / PCNA two colour immunohistochemistry

The PCNA antibody is a mouse monoclonal IgG. To reduce background staining of endogenous immunoglobulin while using this antibody on mouse tissue, a special kit from Vector, the MOM (mouse-on-mouse) kit was employed in this protocol.

1) Slides out 30-60 minutes to dry
2) Encircling of sections with 'Immedge' hydrophobic pen
3) Wash 30 min in PBS
4) Block endogenous peroxidase activity with 0.3% hydrogen peroxide in methanol for 15 min
5) Wash 2x5 min in PBS
6) Blocking serum 1.5% in 2% BSA for 30 min
7) Tip off excess blocking serum and add Primary antibody diluted in 2% PBSA overnight at 4°C
8) Wash 2x5 min in PBS
9) Secondary biotinylated antibody diluted 1:200 in 0.1% BSA
10) Wash 2x5 min in PBS
11) Add ABC for 30 min
12) Wash 2x5 in PBS
13) Add AEC for 30 minutes (checking for development)
14) Rinse in PBS 3 minutes then into running water briefly
15) Avidin block 15 min
16) Brief wash in PBS
17) Biotin block 15 min
18) Wash 2x5 min in PBS
19) Add 0.2% Triton-X 100 in PBS to slides for 1 minute to permeabilise
20) Wash 2x5 min in PBS
21) Vector MOM kit blocking serum 60 min
22) Wash 2x2 min in PBS
23) Add MOM diluent 5 min
24) Tip off excess and add mouse-anti-mouse antibody diluted in MOM diluent for 30 min
25) Wash 2x2 min in PBS

26) Add secondary antibody from MOM kit for 10 min

27) Wash 2x5 min in PBS

28) Add ABC for 30 min

29) Wash 2x5 min in PBS

30) Add DAB for approximately 90 secs (checking for development)

31) Rinse in PBS then into running water 2 min

32) Dip in haematoxylin, then running water 3 min

33) Aqueous mount (Dakomount, DAKO)*

*AEC is a red, alcohol-soluble substrate so alcohol dehydration is not possible.

RESULTS

General observations

The histopathological hallmarks of the *rds* model are the absence of photoreceptor outer segments and gradual thinning of the retina due to loss of photoreceptor from the outer nuclear layer. In the wild type outer segments are seen from about P12 and increase in length until fully formed at about one month.

Time Course Of Photoreceptor Apoptosis

TUNEL staining revealed a significant peak in photoreceptor apoptosis on P16 (*table 3.1 and figure 3.1, 3.2*), in keeping previous findings(Portera-Cailliau et al. 1994; Ali et al. 1998). Only scattered apoptotic photoreceptors were present at P8 and after P21, when there is a level of continued photoreceptor apoptosis not seen in the wild type. There was significantly more apoptosis at P16 compared to P21 (24.2+/- 5.2 and 7.6+/- 1.4 respectively, p=0.04) and at P17 compared to P21 (15.8 +/- 2.6 and 7.6+/- 1.4 respectively, p=0.04).

Age	Mean number apoptotic photoreceptors per 1.2mm retina	Standard Deviation	Standard Error of the Mean
P8	**3.5**	2.78	1.61
P14	**8.4**	2.69	1.56
P16	**24.2**	10.37	5.19
P17	**15.8**	5.12	2.56
P19	**10.6**	5.43	2.71
P21	**7.6**	2.86	1.43
P30	**2.7**	1.97	1.14
P40	**1.9**	1.54	0.89

P<0.05

Table 3.1: Number of apoptotic photoreceptors in *rds* retina

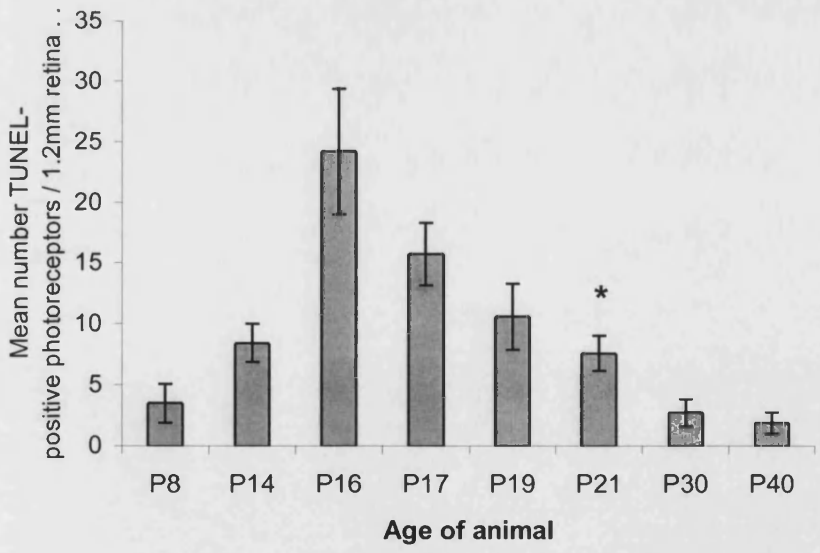

Figure 3.1. Time-course of photoreceptor apoptosis (TUNEL positivity - mean +/- SEM). Apoptotic rate peaks at the 16th post natal day (P16), significantly higher than at P21 (* p=0.020).

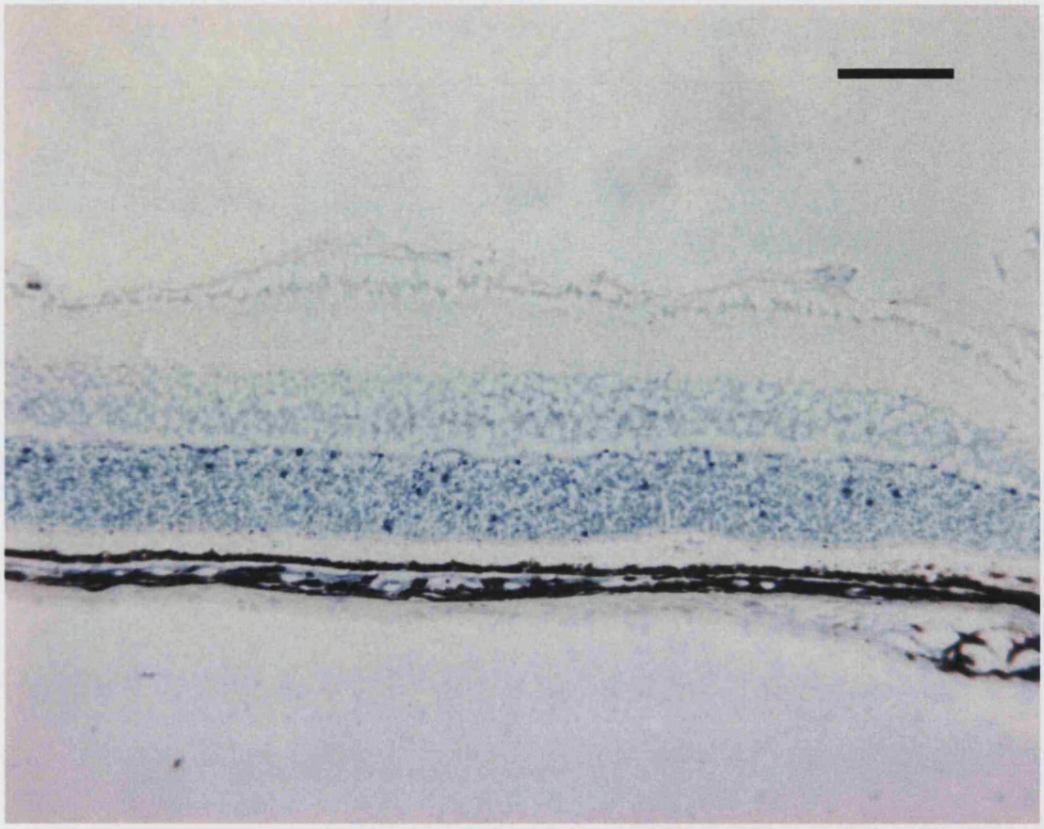

Figure 3.2 Immunohistochemical TUNEL staining of retina at P16, the peak of photoreceptor apoptosis in *rds* mice. Dark blue stained nuclei in the outer nuclear layer (TUNEL positive) are undergoing apoptosis. Counterstain: methyl green, scale bar: 100μm.

In the wild type only very occasional apoptotic photoreceptors were found at P14 (approximately 3 per entire retina) but none were found at later times, confirming previous findings (Hume et al. 1983), although a recent study on wild type C57Bl/6J mice found this 'developmental' photoreceptor loss to be more substantial at around P16 with infrequent photoreceptor apoptosis continuing after 1 month(Mervin and Stone 2002).

Increase in retinal and sub-retinal microglia during *rds* degeneration

At P3 no difference between wild type and *rds* mice could be found in terms of retinal morphology or microglial numbers. The retina at this age contains a ganglion cell layer and another common nuclear layer (*figure 3.3a,b*) which divides to become the inner and outer nuclear layer by P8.

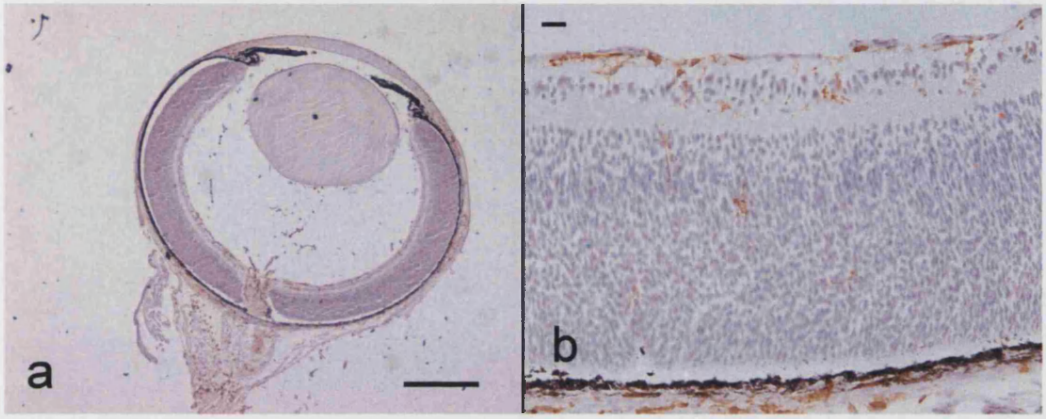

Figure 3.3 F4/80 immunohistochemistry at P3 in wild type (*rds* identical). The retina is still undergoing the final stages of development, with separation of the nuclear layer yet to occur. Hyaloid remnants are seen within the vitreous cavity near the optic nerve head, with a dense infiltration of macrophages within this embryological tissue (a). A modest infiltration of microglia (brown) is seen, predominantly in the inner retina, with occasional microglia within the common nuclear layer (b). Choroidal and scleral macrophages are also seen beneath the retinal pigment epithelium. Counterstain: haematoxylin, scale bar: (a) = 200μm, (b) = 20μm.

In wild type and *rds* animals microglia expressing F4/80 and CD11b were found predominantly in the inner retinal layers, with a few scattered within the common nuclear layer. In the wild type at later time points microglia were found only in the inner retinal layers, and, although initially in slightly increased numbers, a steady state is reached at around P21 when their numbers are few (*figure 3.4*). In the *rds*

mouse however, even as early as P8 microglia were present in greater numbers in the inner retinal layers and were also seen in the outer layers and in the sub-retinal space (7.1 +/- 1.0) (*figure 3.4*). The number of retinal microglia rose markedly and their distribution during the time course suggested that there was a migration from the inner to the outer retina, where their numbers peaked at P21 (20.3 +/- 2.7) and thereafter fell away. At P21 the outer retinal surface was often coated with a lining of cells adherent to the vestigial photoreceptor outer segments. By P30 the number of parenchymal and sub-retinal microglia is reduced (*figure 3.4*) but are still present at P40. The time-course of microglial numbers is shown in *table 3.2* and the temporal relationship to photoreceptor apoptosis in *figure 3.5* which shows that there is a distinct pattern of an apoptotic peak preceding maximal microglial numbers by at least five days. The number of sub-retinal microglia at P21 is significantly greater than at P16 ($p<0.01$), P17 ($p<0.01$) and P19 ($p<0.05$).

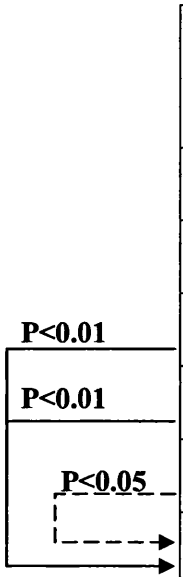

Age	Mean number sub-retinal microglia per 1.2mm retina	Standard Deviation	Standard Error of the Mean
P8	**7.1**	1.0	0.6
P14	**6.9**	0.8	0.5
P16	**10.8**	4.1	2.0
P17	**10.9**	3.8	1.9
P19	**10.6**	2.6	1.3
P21	**20.3**	2.7	1.4
P30	**7.9**	3.0	1.7
P40	**7.9**	1.9	1.1

Table 3.2 Number of Sub-retinal Microglia in *rds* Retina

Figure 3.4 (opposite) Comparison of distribution and numbers of F4/80-positive (brown) retinal microglia in wild type and *rds* mice aged P8-P30. Microglia appear to migrate from the inner to the outer retinal layers during *rds* photoreceptor degeneration and may be seen in the sub-retinal space as early as P8. Their numbers peak at P21, when they form an almost continuous layer of cells adherent to the vestigial photoreceptor outer segments. Sub-retinal microglia are not seen in the wild type and by P21, very few microglia remain and are restricted to the inner layers. A decent layer of photoreceptor outer segments is seen in the wild type by P21, but not in the *rds* retina. Counterstain: haematoxylin, scale bar: 20μm.

3.4

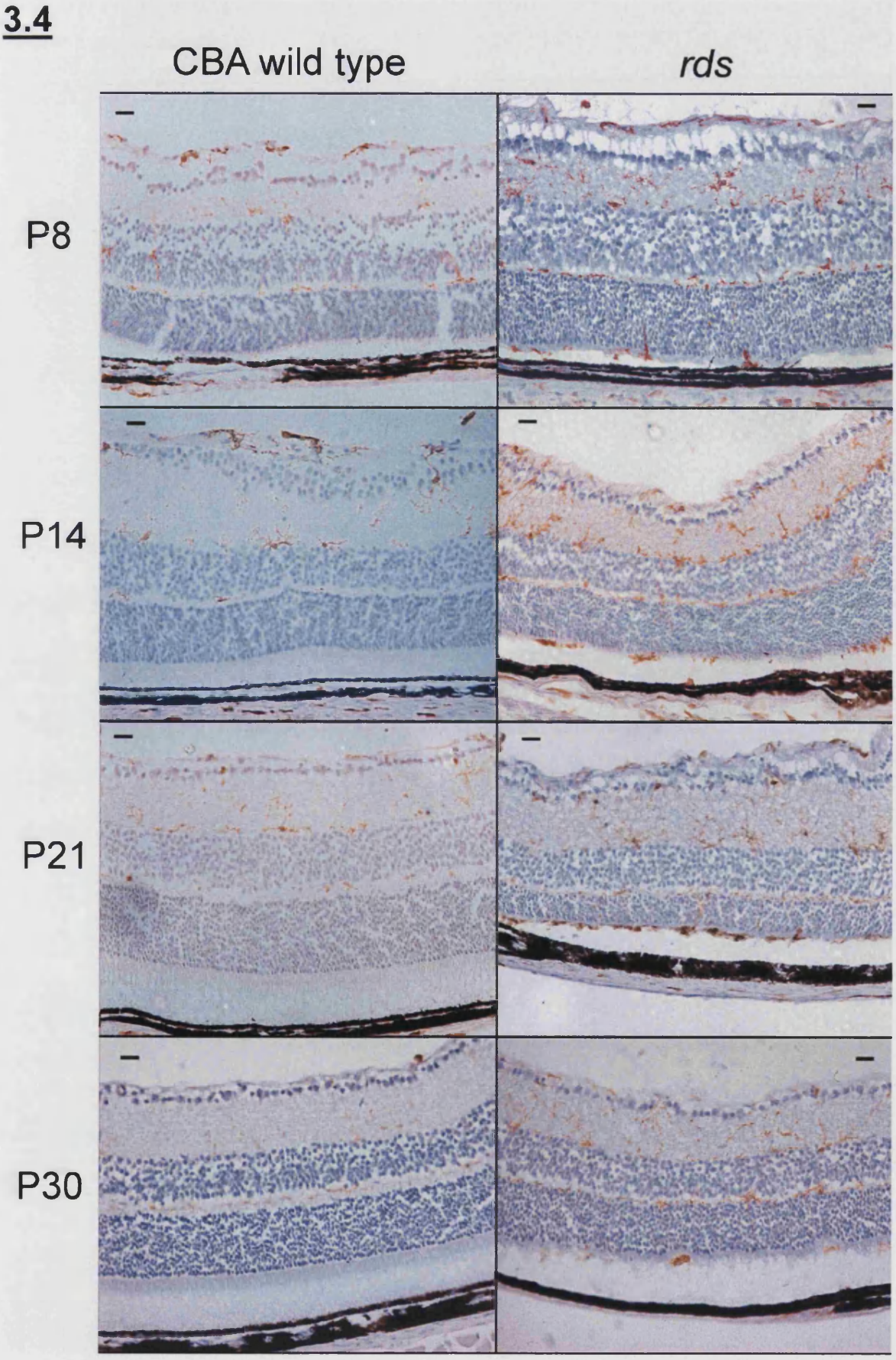

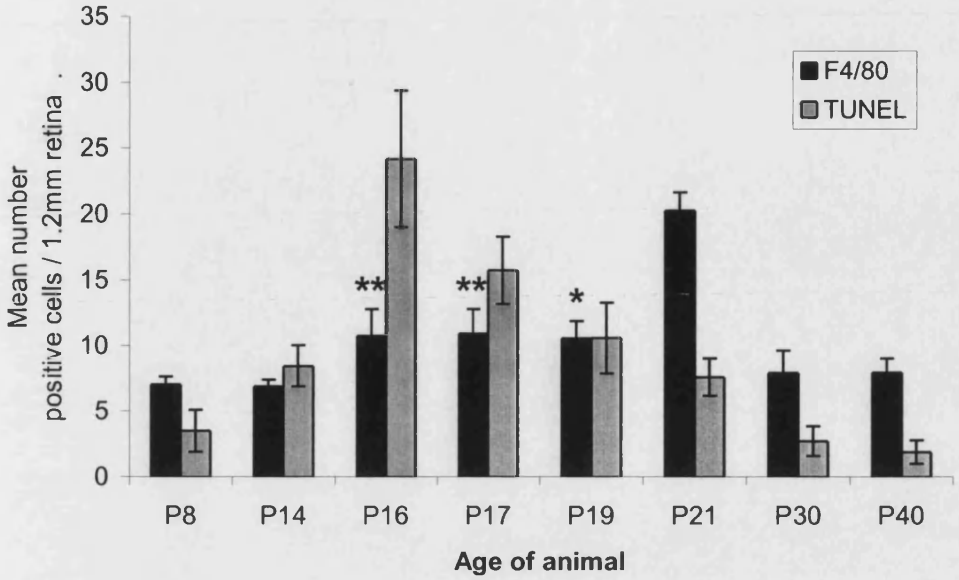

Figure 3.5. Temporal relationship between photoreceptor apoptosis and sub-retinal microglial numbers (mean +/- SEM). TUNEL staining of photoreceptors peaks at P16 while microglial numbers (stained for F4/80) peak at P21. Microglial numbers at P21 were significantly higher than at P16, P17 and P19. * $p<0.05$, ** $p<0.01$ relate to microglial numbers when compared with P21.

Changes in microglial morphology

Four distinct morphological identities can be found for cells expressing F4/80. Associated with blood vessels in the inner retinal layers there were elongated cells which were curved and slender; these are likely to be the perivascular macrophages or cells entering the retina from the intravascular compartment (*figure 3.6a)*. Within the plexiform layers parenchymal microglia adopted a typically ramified, highly arborised form (*figure 3.6b*), which has in the past been ascribed to a 'resting' state. The

processes of such ramified microglia were often extremely complex and might span 60 μm or more. En route from the inner retinal layers to the outer retina and sub-retinal space the microglia are required to cross the inner and outer nuclear layers, and during this transit they assumed a rod-like morphology, with few processes, often extending from the aspect of a nuclear layer to the outer (*figure 3.6c*). Finally, in the sub-retinal space microglia became more rounded and amoeboid in appearance (*figure 3.6d,e*), this morphology is thought to be associated with an activated and highly phagocytic state. In accordance with this, sub-retinal microglia/macrophages could often be seen to contain phagocytosed pigment granules shed by the RPE (*figure 3.6f*).

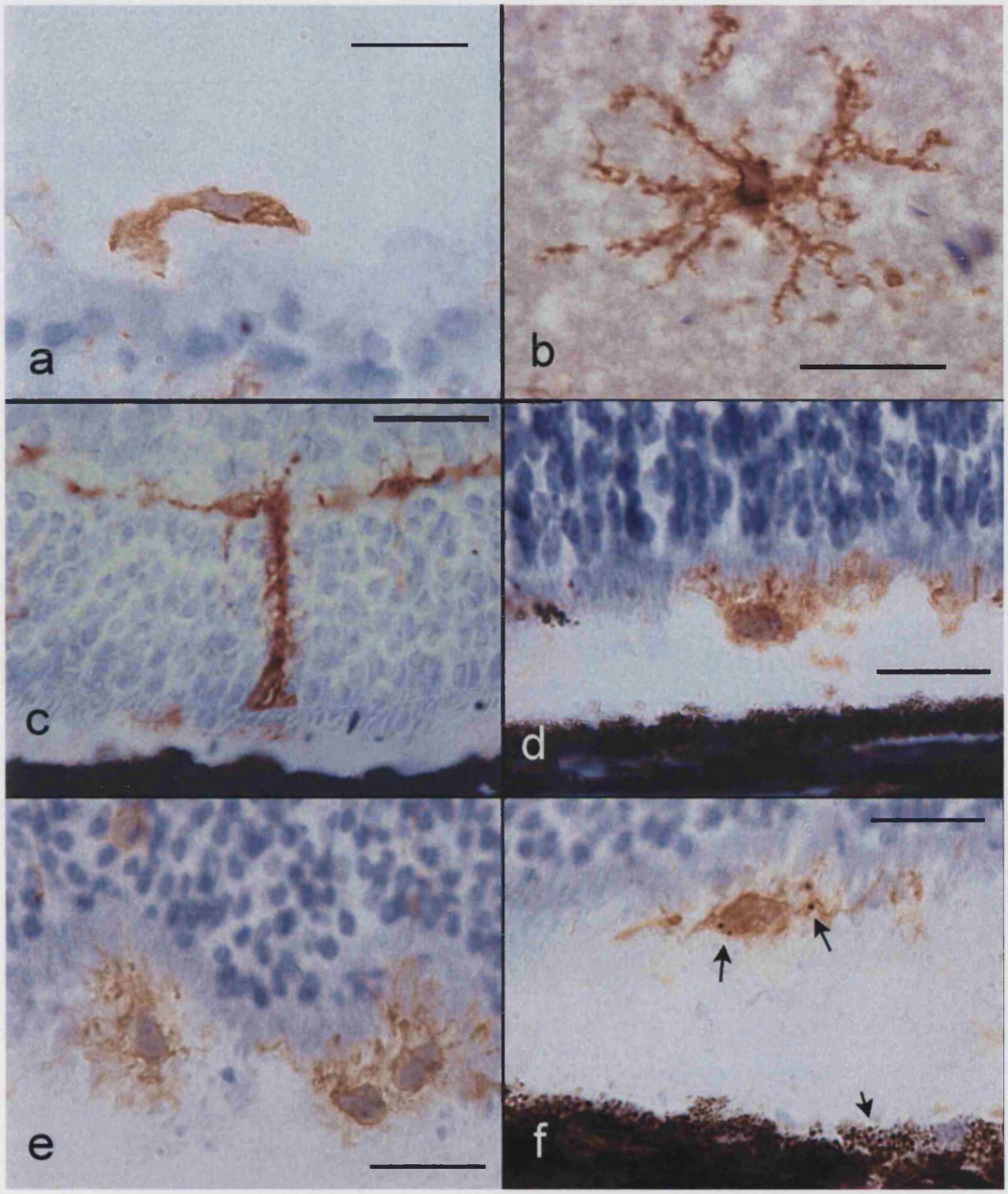

Figure 3.6 a-d represent the four distinct morphological appearances of retinal microglia during *rds* degeneration. Curved, smooth cells were found in the inner retinal layers, often near blood vessels (a). Highly complex, ramified cells were found within the plexiform layers (b). Rod shaped microglia could be seen crossing the nuclear layers (c) while in the sub-retinal space an 'amoeboid', rounded morphology was adopted (d, e) where they could occasionally be seen to have phagocytosed pigment from the retinal pigment epithelium (f). Counterstain: haematoxylin, scale bar: 20μm.

Expression of cell surface markers by microglia

Following the observation that there is a dramatic increase in microglia numbers and in particular, sub-retinal microglia with an activated morphology, we wished to assess if there was any change in phenotype indicating alterations in cellular activity. Macrophages display marked heterogeneity. They adapt to the local environment which regulates their development, differentiation, proliferation and activation. Monoclonal antibodies directed against cell surface antigens can highlight changes in macrophage function.

Throughout the examined time-course (P8-P40), microglia in both wild-type and *rds* retina express F4/80 and CD11b. MHC class II expression was found extremely infrequently and only on microglia in close proximity to the optic nerve head at P16. CD11c, a marker found on highly activated microglia and on dendritic cells, was only weakly expressed by a very small number of sub-retinal cells at the later time-points (P30 and P40) (*Figure 3.7*). The dendritic cell marker CD205 (DEC205) was not detected at any stage in the time-course.

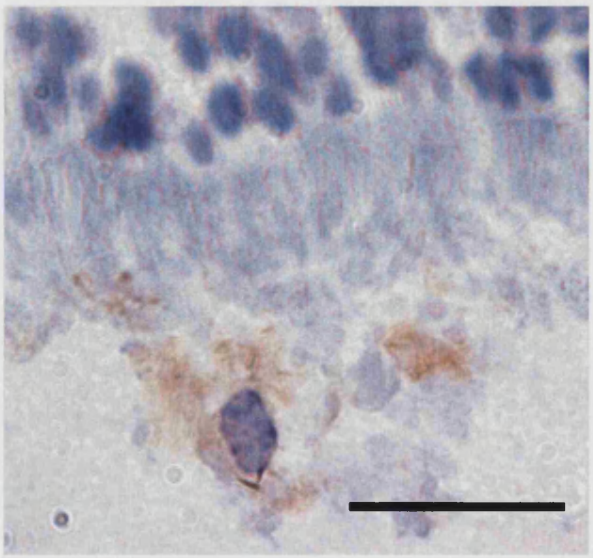

Figure 3.7 Very occasional weakly CD11c positive sub retinal cells could be found. Counterstain: haematoxylin, scale bar: 20μm.

Sialoadhesin (CD169) was absent from microglia in the wild type retina at all time points (excluding macrophages in the hyaloid remnants at P3) (*figure 3.8a-c*). This is consistent with current opinion on the distribution of sialoadhesin positive macrophages(Perry et al. 1992). However at P3 sialoadhesin was expressed by macrophages in hyaloid remnants at the optic nerve head (*figure 3.8a*). At later times this optic nerve head sialoadhesin expression disappears but some microglia within the retrobulbar nerve continue to express sialoadhesin. In the *rds* retina, no sialoadhesin expression was found at P8 despite increased microglial numbers (*figure 3.8d*). Indeed, only at P16 can a significant number of sialoadhesin positive macrophages be detected (2.0 +/- 2.2) contributing about 20% of the microglial population. At P16 the emergence of sialoadhesin positivity was seen predominantly in the inner retinal layers and around the vessels of the optic nerve head (*figure 3.8e-g*). By P21 sialoadhesin expression was florid and widespread, with approximately 40% of microglia expressing this marker (8.9 +/- 4.3) (*table 3.3 and figure 3.8h, 3.9*). Two-colour immunofluorescence confirmed that all sialoadhesin expressing microglia also expressed F4/80(*figure 3.10*). By P40 few microglia expressed sialoadhesin (*figure 3.8i*).

Figure 3.8 Apart from at the early stages of post-natal development when macrophages destroying hyaloid remnants expressed sialoadhesin (a), this marker was absent from the normal (wild type) retina (b, P3; c, P21). Sialoadhesin positive microglia (brown) could, however be seen in *rds* retina from P14 (d) to P16 (e-g), when they appeared to originate from the inner retinal layers and the blood vessels within the optic nerve head (e,f). By P21 there was florid and widespread expression of sialoadhesin from the inner retinal layers to the sub-retinal space (g). This had almost disappeared by P40 (h). Counterstain: haematoxylin, scale bar 20μm (except a, e: 200μm).

Age	Mean number sub-retinal sialoadhesin+ microglia per 1.2mm retina	Standard Deviation	Standard Error of the Mean
P8	**0.1**	0.14	0.08
P14	**0.4**	0.4	0.2
P16	**2.0**	2.2	1.1
P17	**3.1**	3.0	1.5
P19	**6.9**	2.5	1.3
P21	**8.9**	4.3	2.1
P30	**3.8**	2.6	1.5
P40	**0.7**	0.6	0.3

P<0.05

Table 3.3 Number of Sialoadhesin Positive Microglia in *rds* Retina

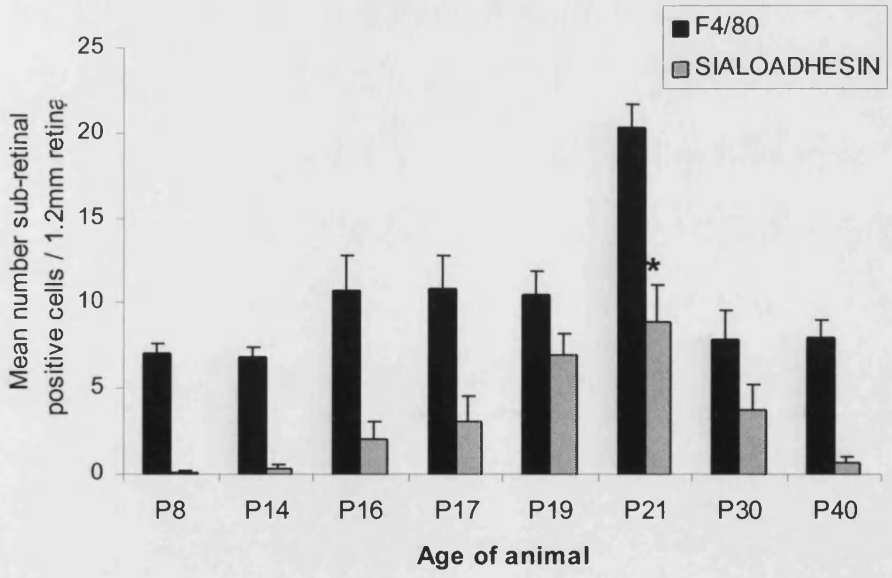

Figure 3.9. Sialoadhesin expression by sub-retinal *rds* microglia (mean +/- SEM). As with F4/80, peak expression occurs at P21, significantly greater than at P16 (* $p<0.05$).

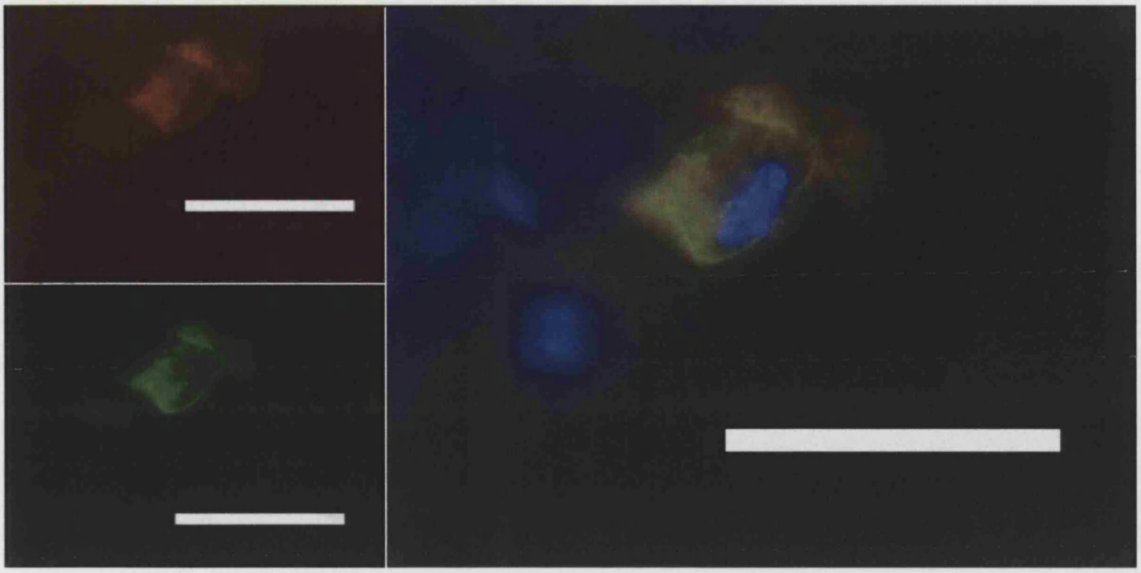

Figure 3.10 Two colour immunofluorescent staining for F4/80 (red) and sialoadhesin (green) demonstrating dual expression of these markers. Counterstain: DAPI, scale bar: 20μm.

No evidence of Nitric Oxide-mediated oxidative damage in *rds* retina

The production of nitric oxide (NO) and reactive oxygen species (ROS) is a major source of tissue damage following macrophage and/or microglial activation. Using polyclonal antibodies to inducible nitric oxide synthase (iNOS), the enzyme responsible for NO production, and nitrotyrosine, a marker of oxidative protein damage, I investigated the role of these molecules in *rds* retinal degeneration. Thymus from 14 day old mice was used as a positive control for both iNOS (expressed by thymic dendritic cells effecting clonal deletion of autoreactive thymocytes through NO(Tai et al. 1997; Aiello et al. 2000)) and for nitrotyrosine, found in thymocytes undergoing NO-mediated apoptosis (*figure 2.2*). No microglia expressed iNOS at any point in the time course studied including the period of

greatest microglial activity. In addition to this, no nitrotyrosine was detectable in the photoreceptors or any other cell in *rds* retina.

rds microglia proliferate in situ

Microglial numbers may rise in response to CNS pathology via *in situ* proliferation (Sedgwick et al. 1998) or by recruitment of monocytes from the circulation (Ling and Leong 1987; Giulian et al. 1989). An antibody to PCNA was used to determine the contribution of *in situ* proliferation to the increased numbers of retinal microglia. As well as neonatal thymus, an additional positive control was lens epithelial cells within each whole eye section, which allowed for an internal control for the strength of the PCNA staining. Lens epithelial cells undergo continual mitosis throughout life, but are particularly active *in utero* and in the neonatal period (*figure 3.11a*).

Double-staining of microglia with F4/80 and PCNA identified dividing microglia and showed that in both wild-type and *rds* mice proliferating retinal microglia could be found at P8 in the inner retinal layers (*figure 3.11b, 3.12 and table 3.4*). These proliferating cells were often found in clusters in the ganglion cell layer. By P14, very few proliferating microglia are present in the wild type and none were found after this time-point, reflecting the general reduction in microglial numbers. However there is sustained microglial proliferation in the *rds* retina at P14 and P21, when proliferating microglia can be found in the outer plexiform layer and on the outer retinal surface (*figure 3.11c,d*). Microglial proliferation in the *rds* model thereafter subsides and is minimal by P30.

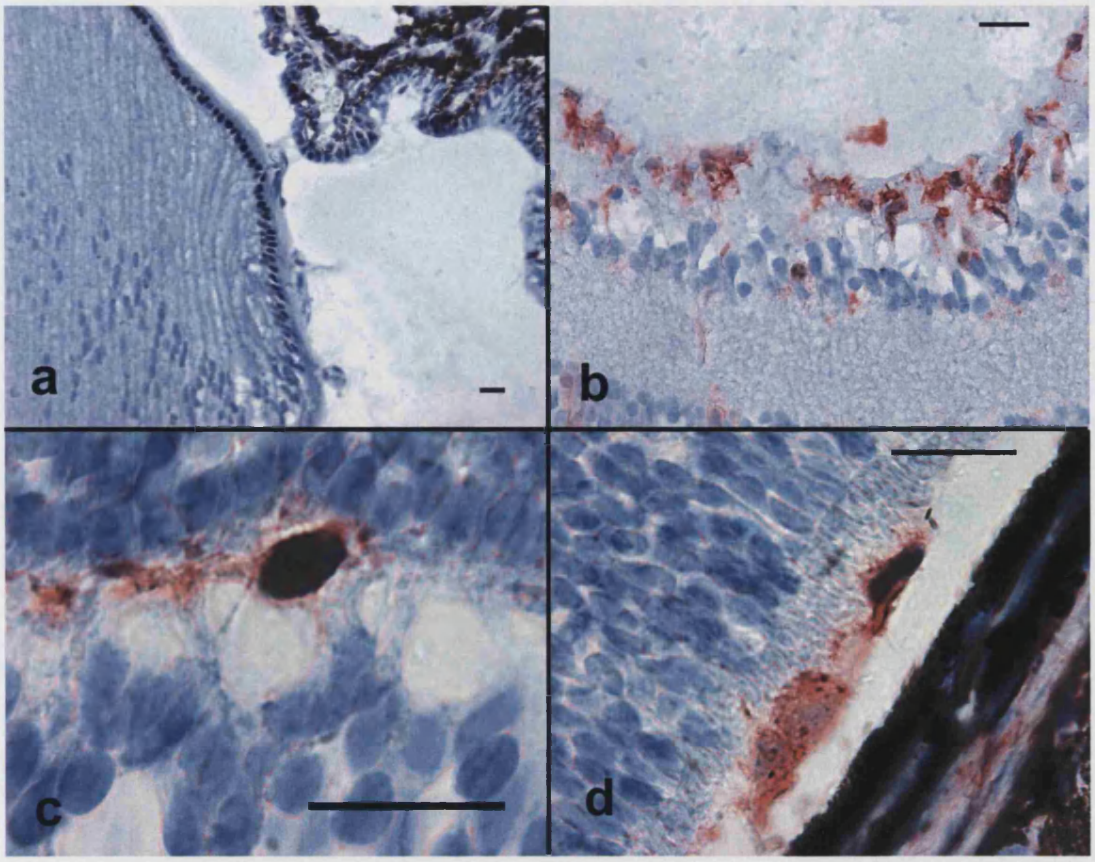

Figure 3.11 Two colour immunohistochemistry for PCNA (black/grey) and F4/80 (red). A convenient internal positive control were lens epithelial cells (black nuclei, a). Proliferating (double-positive) microglia could be found in clusters in the inner retinal layers at P8 (b) in both wild type and *rds* retina. At later time points in *rds* mice, they could be found in the outer plexiform layer (c) and sub retinal space (d, two non-proliferating microglia (blue nuclei) and one proliferating microglia (black nucleus)). Counterstain: haematoxylin, scale bar: 20μm.

Age	wild type	*rds*
P8	10.0	10.3
P14	0.4	11.2
P21	0	10.0
P30	0	0.3

Table 3.4 **Mean Number of PCNA / F4/80 Positive (proliferating) Microglia / mm^2 in *rds* and Wild Type Retina**

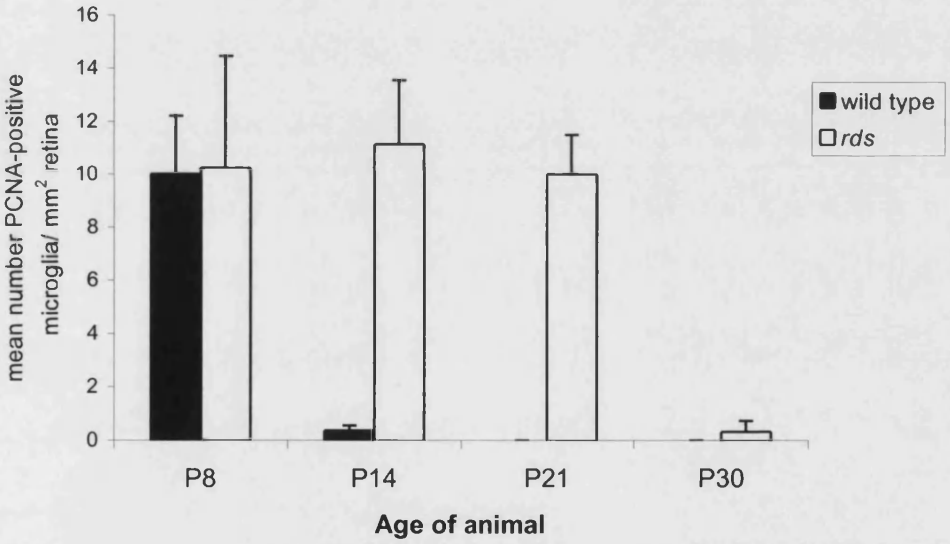

Figure 3.12. Comparison of retinal microglial proliferation (PCNA positivity, mean +/- SEM) in wild type and *rds* mice. Microglial proliferation is seen at P8 in *rds* and wild type equally, but while this is sustained in *rds* until P21, it is nearly absent by P14 in wild type mice.

DISCUSSION

The pattern of photoreceptor death in the *rds* mouse

A dramatic wave of photoreceptor apoptosis shortly after birth is a phenomenon recognised by others in their study of this and other mouse models of outer retinal degeneration, such as the *rd* mouse(Portera-Cailliau et al. 1994). In this study, in keeping with previous reports, I found the zenith of apoptosis to occur at P16 in the *rds* mouse. As a result of this cull, 50% of photoreceptors are lost by P42(Sarra et al. 2001) . There is no accepted explanation for this phenomenon, but clearly in this model the timing occurs shortly after the opening of the lids and the production of opsin (both occurring at around P10-12)(Usukura and Bok 1987; Schalken et al. 1990), suggesting that phototoxicity of some sort may be implicated. Since all the photoreceptors have the same genetic defect, why some photoreceptors should die and others survive until months later is a mystery. It is not the case that rods die early and cones die later in this model, Sanyal *et al.* observed in the central retina, simultaneous demise of both types of photoreceptor. Mathematical analysis of the kinetics of photoreceptor death in this and other inherited retinal degenerations fails to support a theory that accumulation of toxic products leads to eventual cellular demise(Clarke et al. 2000). The exponential decay in rate of photoreceptor death suggests that genetically defective photoreceptors are susceptible to sporadic insults which lead to random apoptosis, initially at greater frequency due to the larger number of cells available.

Therefore, as this dichotomy of survival time can not be explained by intrinsic photoreceptor differences, we must look for extrinsic reasons such as their location

within the outer nuclear layer. It was consistently observed following TUNEL (and Caspase 3) staining that the majority of the photoreceptor nuclei undergoing apoptosis at the peak time points were located at the inner aspect of the ONL (*figures 2.4b, 5.4, 5.7a+b*), and this raises the possibility that closer proximity to cells of the inner retinal layers, or greater distance from the choroid/RPE may be critical in dictating the fate of the photoreceptors. It may be possible that the more centripetal photoreceptor cell bodies are more prone to photic damage since incident light strikes them first.

The effect of light withdrawl and high intensity constant light conditions on albino and pigmented wild type and *rds* homozygotes was investigated by Sanyal and Hawkins(Sanyal and Hawkins 1986). Albino mice of both wild and *rds* genotypes underwent accelerated photoreceptor degeneration in the presence of continuous light exposure, signifying a natural and now well documented sensitivity of the albino photoreceptor. However neither wild type nor *rds* of pigmented background sustained increased photoreceptor loss in such conditions. Interestingly, rearing in total darkness had no protective effect on *rds* photoreceptors even in albino mice. Light therefore seems to be, at most, a trivial factor in the degeneration of this particular genetically defective photoreceptor.

Shortening of the outer segments in some models of photoreceptor degeneration led Travis *et al* to propose that increased proximity to the choroid led to photoreceptor death from oxidative damage. The pattern of photoreceptor loss observed in this work contradicts this hypothesis, since it is the photoreceptors furthest from the choroid that appear to die most frequently, raising the question whether it is in fact hypoxic stress that results in the demise of the most centripetal photoreceptors. Mervin and Stone have found that the low-level apoptosis of photoreceptors during

post natal development in the mouse is exacerbated by hypoxia and reduced by 50% in hyperoxic conditions(Mervin and Stone 2002), indicating that distance from the oxygen-rich choriocapillaris may well be an important determinant in photoreceptor apoptosis.

Microglial numbers and morphology in relation to photoreceptor apoptosis

Previous studies on animal models of photoreceptor degeneration have demonstrated microglial activity at approximately the same time as the phase of most rapid loss of photoreceptors. These findings can be interpreted in two ways: either as a phagocytic response to photoreceptor apoptosis, with microglia being attracted to the outer retina by unspecified chemotactic factors (released as a result of neuronal injury) to engage in the clearance of dead and dying cells, a phenomenon extensively studied within the CNS. Alternatively, the approximate coincidence of microglial activity with a surge of photoreceptor death, in conjunction with a knowledge of their cytotoxic potential, introduces the possibility that microglia are instrumental in, or at least contributing to, the apoptotic loss of photoreceptors.

By closely scrutinising the period of greatest disease activity in the *rds* mouse I have demonstrated that the peak rate of photoreceptor apoptosis (P16 in this set of experiments) precedes the peak in microglial numbers by at approximately 5 days. These novel findings indicate that microglia are unlikely to be the perpetrators of photoreceptor death, in which case one would expect that the maximal microglial activity would exactly coincide with or even precede maximal photoreceptor apoptosis.

It is possible however, that although not involved in the initial wave of photoreceptor cell death, an exuberant microglial response both potentiates and perpetuates the disease process. A self-perpetuating process of microglial cytotoxic activity, as is proposed in other models of CNS disease, may be one of the reasons why replacement of the missing peripherin gene by sub-retinal gene delivery has no discernable beneficial effect on the long term rate of photoreceptor loss in the *rds* mouse (Sarra et al. 2001). However, as photoreceptor apoptosis declines, so too (after a lag period) do microglial numbers, until only few are seen in the sub-retinal space by P40.

The comparison of apoptotic photoreceptors and microglial numbers therefore supports the hypothesis that microglia respond to, rather than induce photoreceptor injury and death, by migrating to regions where apoptosis is taking place to undertake phagocytosis of dead and dying cells to maintain tissue homeostasis. Following the peak of apoptosis the demand for cell debris clean-up is reduced and microglial numbers accordingly decline.

Microglial morphology varied according to location within the retina rather than in relation to the extent of photoreceptor apoptosis and microglial activity. Indeed, all four recognised morphological types could be identified throughout the time course studied in *rds* retina. Although different morphologies have, in the past been attributed to different activation states with amoeboid and ramified representing activation and resting respectively, it is possible that retinal microglia adopt a morphology depending on their surrounding cellular and extracellular environment rather than microglial function. For example, the crossing of a nuclear layer might be easier if the cells adopt a rod or spear shape. Microglia in the sub-retinal space are amoeboid in shape. This may be the morphology they adapt in the absence of

neuronal contact (i.e. similar to a tissue macrophage), or it may indeed be an indication, as suggested in the literature, that sub-retinal microglia are the most 'activated' and phagocytic.

Cell surface marker expression

As expected, microglia readily expressed both F4/80 and CD11b in the degenerating retina. Since little is known about the function of F4/80 we cannot draw conclusions from the presence of this marker, but the strong presence of CD11b, which as previously discussed may be involved in the clearance of apoptotic cells, is in keeping with the clean-up' role of microglia. CD11c (a marker of dendritic cells and activated macrophages/microglia) was generally not expressed, although faint staining could be seen on a very small number of sub-retinal microglia at P30. Although this marker may be present on dendritic cells, their presence in this condition in the sub-retinal space seems unlikely and the absence of the dendritic cell marker CD205 supports this.

The pattern of sialoadhesin expression by *rds* microglia is of great interest. Sialoadhesin is a member of a group of macrophage-restricted cell surface sialic acid receptors termed siglecs. The function of sialoadhesin and other siglecs is yet to be fully characterised, but cell-matrix and cell-cell interactions and in particular adhesion to lymphocytes have been noted(van den Berg et al. 1992). CD45 has been identified as a T cell counter receptor for sialoadhesin(van den Berg et al. 2001) and the presence of sialoadhesin on macrophages in the splenic marginal zone, which may be involved in antigen handling (Martinez-Pomares et al. 1996; Steiniger et al. 1997; Geijtenbeek

et al. 2002) suggests a possible role in the bridging of innate and adaptive immunity. The presence of sialoadhesin on a proportion (40%) of microglia at P21 may therefore imply some up-regulation of T cell interaction capability. However microglia were almost always MHC class II negative.

Another explanation for the presence of sialoadhesin positive microglia in *rds* retina is that the expansion of microglial numbers involves recruitment of myeloid precursors from the blood, and that these blood derived elements represent the sialoadhesin positive microglial faction. The observation that sialoadhesin positivity originates from the inner retina and around blood vessels supports this notion, but on the other hand, it has been found that monocytes do not express sialoadhesin(Hartnell et al. 2001).

The observation of sialoadhesin-positive microglia might also be explained by blood-retinal barrier breakdown. In the healthy CNS and retina, microglia being protected by the blood-brain-barrier are sialoadhesin negative (sialoadhesin was not present in wild type retina). During the early stages of retinal degeneration in the *rds* mouse when there is already significantly increased microglial activity there was no sialoadhesin expression but by P21 nearly half the microglia were sialoadhesin-positive. In view of the findings of Perry *et al*, that contact with serum is required for sialoadhesin expression(Crocker et al. 1988; Perry et al. 1992) one possible explanation of our findings is that there is break-down of the blood-retinal barrier, leading to exposure of microglia to serum proteins. Breakdown of the blood-retinal barrier in retinal dystrophies, as has long been suggested in retinitis pigmentosa(Fishman et al. 1981), has implications for future gene therapeutic strategies where evasion of systemic immune responses is of paramount importance.

It is hoped that the anatomical and immunological properties of the eye will be advantageous, yet exaggerated systemic immune responses can be found when injecting into the sub-retinal space of a dystrophic murine retina when compared with normal mice(Suber et al. 2001).

In situ proliferation contributes to increased microglial numbers

Under normal conditions parenchymal microglia are a stable population of cells with little or no turnover (Hickey et al. 1992). In the retina of wild type animals microglial proliferation is restricted to a short period (P8-P14) when there is neuronal remodelling in the inner retinal layers(Hume et al. 1983; Mervin and Stone 2002).

The source of the increased pool of microglia seen in CNS disease has been disputed: proliferation *in situ* or recruitment from blood? Our findings demonstrate that microglia in the *rds* mouse proliferate *in situ* in far greater numbers than wild type at day 14 and 21 post natal (P14 and P21) but to the same extent at P8. Although proliferating microglia were found only in the inner retinal layers in the wild type, by P21 they were situated throughout *rds* retina, including in the sub-retinal space. Maximal proliferation in the *rds* retina occurs before the greatest microglial presence so this phenomenon cannot be explained merely by greater cell numbers. As with the burst of microglial proliferation around P8 in wild type animals, once the stimulus of cell death has abated microglial proliferation declines.

However the presence of microglial proliferation does not exclude additional recruitment of myeloid precursors from blood. Indeed, without preventing one or the

other, it is impossible to quantify the contribution each make to the overall expansion of the microglial population. This will be discussed further in the next chapter.

Lack of oxidative damage and iNOS

The importance of iNOS and NO in macrophage and microglia-induced tissue damage in the context of disease exacerbation has been discussed. Within activated macrophages, L-arginine may be metabolised via iNOS to NO or via arginase to urea, and the activation phenotype dictates which pathway is followed. iNOS upregulation and NO release are considered part of a spectrum of phenotypic alterations seen with 'classical' activation of macrophages induced by bacterial LPS and IFNγ released by Th1 lymphocytes and natural killer cells. Classical activation of macrophages is seen during acute inflammation and leads to the release of pro-inflammatory cytokines (IL6, IL1, TNFα) as well as NO, and the upregulation of MHC class II expression. Alternative activation, a concept introduced by Gordon and colleagues(Stein et al. 1992) and reviewed by Gordon(Gordon 2003) and Goerdt and Orfanos(Goerdt and Orfanos 1999), is induced by Th2 lymphocyte-associated cytokines IL4 and IL13, and involves an up-regulation of the macrophage mannose receptor and other scavenger receptors with enhanced endocytosis and phagocytosis. There is also an up-regulation of MHC class II expression and such alternatively activated macrophages may be able to induce differentiation of naïve T cells into a Th2 phenotype(Cua and Stohlman 1997). In alternatively activated macrophages arginase activity predominates over iNOS, which is down-regulated, so it seems that the arginase/iNOS balance is competitively regulated in the context of Th1 vs Th2-driven responses(Munder et al. 1998).

The lack of iNOS expression by microglia during *rds* retinal degeneration is supported by the absence of nitrotyrosine in the dying photoreceptors, and taken together these findings eliminate a major mechanism of microglial cytotoxicity. Furthermore, in view of such florid microglial activity, their phagocytic role and the lack of iNOS expression, it might be deduced that *rds* retinal microglia are activated in an 'alternative' manner with reduced cytotoxic and enhanced immunomodulatory functions. Indeed, some investigators have found that the ingestion of (non-opsonized) apoptotic cells by macrophages leads to their down-regulation of 'classical' activation phenotype with reduced pro-inflammatory cytokine release (including the potentially cytotoxic IL-1β and TNFα), and enhances secretion of the immunoregulatory Transforming Growth Factor-β1 (TGF-β1)(Fadok et al. 1998; Barker et al. 1999). Furthermore, addition of apoptotic cells to bacterial LPS-stimulated lungs reduces pro-inflammatory cytokine levels and inflammatory cell counts, an effect which may be blocked by neutralizing antibodies to TGF-β1(Huynh et al. 2002).

So in terms of our neurodegenerative model, research on bone marrow-derived macrophages implies that in their role of phagocytosis of non-opsonized apoptotic photoreceptors, microglia would adopt an alternative activation phenotype and tend to suppress inflammatory responses.

Summary

The data presented in this chapter provide circumstantial evidence that microglia respond to, rather than induce photoreceptor apoptosis in the *rds* mouse. In addition, I

have demonstrated that the expansion of retinal microglial numbers in response to photoreceptor death is at least partly generated by *in situ* proliferation. Microglial sialoadhesin expression may indicate blood retinal barrier breakdown and the absence of iNOS and nitrotyrosine eliminates a major mechanism of microglial cytotoxicity. However, as discussed earlier, several mechanisms of microglial cytotoxicity have been described including the release of cytokines(Chao et al. 1995; Jeohn et al. 1998), prostaglandins(Araki et al. 2001) and excitatory amino acids(Piani et al. 1992; Giulian 1999) and although unlikely in view of the temporal relationship between microglial activity and photoreceptor death, a cytotoxic role for microglial in the *rds* model can not be ruled out on the basis of these findings alone.

CHAPTER FOUR

THE USE OF CLODRONATE LIPOSOMES TO DEPLETE RETINAL MICROGLIA

To clarify whether microglia exert a cytotoxic effect in the *rds* model of retinal degeneration, a radical approach was adopted: microglial depletion in order to observe any effect upon the rate of photoreceptor apoptosis. If microglia are responsible for cytotoxicity, then a significant reduction in their numbers might result in a significant decrease in photoreceptor apoptosis. On the other hand, if microglia confer a protective effect, perhaps through the maintenance of extracellular homeostasis then their depletion would be expected to increase photoreceptor cell death.

Clodronate Liposomes

Prior to the mid 1980's, the experimental approaches for *in vivo* selective removal of macrophages included the administration of silica and asbestos(Pomeroy and Filice 1988). However neither technique resulted in very thorough depletion effects. Liposome encapsulated dichloromethylene diphosphonate (Cl_2MDP, clodronate), developed by van Rooijen is much more effective at depleting macrophages and has been widely used in the study of macrophages and inflammatory disease(Van Rooijen 1989). Clodronate is a member of a family of drugs called bisphosphonates (*figure 4.1*), several of which are in current clinical use for the treatment of osteoporosis, hypercalcaemia and other conditions involving pathologic bone resorption including multiple myeloma(Ashcroft et al. 2003). Bisphosphonates have calcium chelating properties, inhibit osteoclast activity and have been shown to inhibit macrophage

migration(Stevenson and Stevenson 1986). Generally they have poor bioavailability after oral administration and are excreted unmetabolised by the kidney. They persist in plasma only very briefly owing to rapid uptake by the skeleton (these drugs avidly bind hydroxyapatite in bone), and in the case of clodronate the plasma half life in humans and rodents is 90 minutes(Lin 1996).

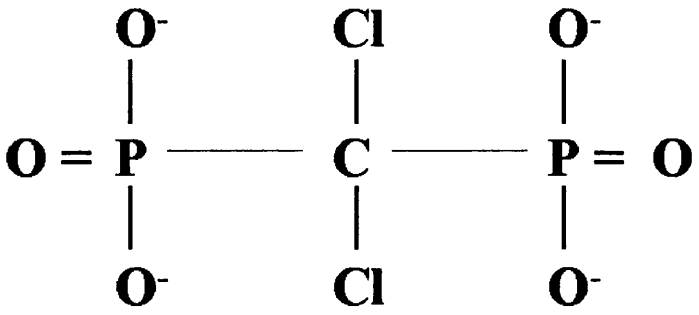

Figure 4.1. Chemical Structure of Dichloromethylene Diphosphonate (Clodronate)

Liposome-encapsulation of clodronate has allowed specific targeting of macrophages, whose phagocytic nature leads them to ingest the liposomes, whereas other cells are prevented from accessing the enclosed drug. Once within the cytoplasm of the macrophage, phospholipase-containing lysosomes fuse with the phagosome and break down the liposomal membranes encasing the drug, thereby releasing it into the cell(Van Rooijen and Sanders 1994). High concentrations of the drug within macrophages leads to their apoptosis(van Rooijen et al. 1996) through an as yet undefined mechanism. Although calcium chelation resulting in depletion of intracellular calcium would be a logical cause, some other bisphosphonates do not have the same toxic effect(van Rooijen and Kors 1989) and furthermore, neither does the calcium chelator ethylenediaminetetraacetic acid (EDTA) (van Rooijen et al.

1996). Calcium replacement in cells treated with clodronate *in* vitro marginally reduces its cytotoxic effect but increases its migration inhibitory effect(Stevenson and Stevenson 1986). It has been suggested that the two chlorine groups (*figure 4.1*) may contribute to the cytotoxicity of clodronate, but since many other non-toxic agents have chlorine groups this is unlikely to be the sole apoptosis-inducing feature. PBS-containing liposomes and free clodronate have no macrophage-depleting effect(van Rooijen and van Nieuwmegen 1984).

The effect of liposomal clodronate depends on its site of administration. Intravenously administered in rodents, it will effectively clear both liver and spleen of almost all macrophages, with those in the splenic marginal zone (metallophilic macrophages) being particularly sensitive and taking up to two weeks to repopulate after a single injection(van Rooijen et al. 1989; Van Rooijen et al. 1990). Intra-tracheal/nasal administration depletes macrophages in the lungs(Thepen et al. 1989; Cheung et al. 2000), injection into the ventricles of the brain removes meningeal and perivascular macrophages(Polfliet et al. 2001) and subcutaneous foot pad administration leads to macrophage depletion in draining politeal lymph nodes(Delemarre et al. 1990).

Intra-peritoneal administration, the only systemic route available to me in the study of neonatal mice (tail vein cannulation almost impossible) had originally been thought only to clear the peritoneum(Van Rooijen 1989) but has more recently been shown to have an additional systemic depletion effect similar to intravenous administration(Biewenga et al. 1995).

Through the depletion of the systemic myeloid reserve, liposomal clodronate administered both intravenously and intraperitoneally has also been successfully used to prevent recruitment of macrophages/monocytes in models of inflammatory disease

including those affecting the CNS and eye(Forrester et al. 1998; Pouvreau et al. 1998; Tran et al. 1998; Koennecke et al. 1999; Baatz et al. 2001). Most studies of the effects of liposomal clodronate administration on CNS and ocular inflammation have made the assumption that prevention of macrophage recruitment is the mechanism of tissue macrophage depletion, rather than an effect on macrophages *in situ*, because liposomses are assumed not to cross the blood-brain barrier. It is worth noting however that in most of these conditions the blood-brain barrier will be compromised.

In studies of experimental autoimmune uveoretinitis (EAU), although reduced infiltrate of the anterior chamber has been noted after liposomal treatment(Pouvreau et al. 1998; Baatz et al. 2001), mixed reports of the success of depletion of macrophages from the retina can be found. Pouvreau *et al* found no diminution in macrophage infiltrate in retina during endotoxin induced uveoretinitis (despite good response in iris and ciliary body and to some extent the choroid)(Pouvreau et al. 1998), but Forrester *et al* noted a marked attenuation of chorioretinal infiltrate and clinical parameters during retinal extract induced EAU(Forrester et al. 1998). The main reason for this discrepancy probably relates to the severity of retinal involvement in the two models, which was mild in the former (endotoxin induced) and severe in the latter (retinal extract induced).

It was unclear whether it would be possible to deplete the developing, degenerating retina of microglia. Bauer *et al* observed a reduction in the number of spinal cord ED1+ resident microglia with systemic administration of clodronate liposomes during experimental allergic encephalomyelitis (EAE) in the rat(Bauer et al. 1995). Comparison was made to control EAE rats only and not naïve animals, so it was unclear whether microglial numbers had been reduced to normal levels or even lower, but it was noted that although spleen sections from clodronate liposomes-

treated animals contained numerous apoptotic macrophages, no microglia were undergoing apoptosis within the CNS parenchyma, implying that depletion was not occurring *in situ*.

Cogniscent of the increase in retinal microglial numbers in the early post-natal period associated with development and tissue remodelling, I decided to initiate clodronate liposomes treatment as early as possible after birth. With this approach I hoped to maintain low levels of retinal microglia until the key time points of P16 and P21, representing the peak in photoreceptor apoptosis and microglial numbers respectively, as determined by work shown in the previous chapter.

MATERIALS AND METHODS

Materials

Clodronate liposomes were acquired from the laboratory of Dr Nico van Rooijen, Department of Molecular Cell Biology, Research Institute of Immunology & Inflammation, Vrije Universiteit Van der Boechorststraat, Amsterdam, The Netherlands and ordered via their website(http://www.clodronateliposomes.com.). Detailed description of the preparation of multilamellar liposomes containing dichloromethylene-diphosphonate (CL_2MDP) (Clodronate, a kind gift of Roche Diagnostics GmbH, Mannheim, Germany) may be found in a review article by Dr van Rooijen, 1989(Van Rooijen and Sanders 1994), but a brief outline follows.

75 mg of phosphatidylcholine (Lipoid KC, Ludwigshafen, Germany) and 11 mg of cholesterol (Sigma, Poole, UK) were dissolved in 20 mg methanol/chloroform (1:1). The organic phase was removed by low vacuum rotary evaporation (37°C), and the lipid film was dispersed in 10 ml of phosphate buffered saline (PBS) for the preparation of PBS-containing liposomes (PBS-Lip). To enclose the CL_2MDP, 2.5 g of Clodronate were dissolved in 10 ml of PBS in which the lipid film was dispersed and the preparations were kept for 2 h at room temperature, sonicated for 3 min, and resuspended in 4 ml of PBS. Each 2 ml of CL_2MDP-Liposomes (CL_2MDP-Lip) suspension contained 10 mg of clodronate. In this manner clodronate would be enclosed in multiple layers of phospholipid bilayers (multilamellar liposomes).

PBS-containing liposomes were not used in control animals, since there is evidence that they induce and then inhibit macrophage phagocytosis(http://www.clodronateliposomes.com.), thereby not proving a true control. Control animals therefore received no injection. Clodronate liposomes were

stored at 4°C under nitrogen for up to one month after preparation. Storage for longer than this period is said to compromise efficacy due to leeching of clodronate out of the liposomes(http://www.clodronateliposomes.com.). Prior to use, since the liposomes had often settled, they were resuspended by gentle shaking and warmed to room temperature to reduce stress to the injected animals.

Experimental design

Four experimental designs were used in the process of developing the method for microglial depletion. All protocols involved intraperitoneal injection of clodronate liposomes commencing from P2. Doses of clodronate liposomes are given as µl per gram of animal weight. Each animal was weighed prior to injection to ensure consistent dosing. As a guideline, P2 mice weighed approximately 2g and by P21 weight had increased to approximately 10g. At time points where histology was to be performed, animals were killed and tissue taken as described in chapter two. Both eyes and the spleen were taken from control and treated animals for immunohistochemical analysis. Unless otherwise stated, only one eye per animal was used for immunostaining.

Experiment 1: (Pilot study) January 2002

Dose	10 µl / g
Frequency	Every 5-6 days
Time points analysed	P5, P8, P16, P19, P21
Number of animals	P5: 1, P8-P21: 2 each
Controls	Previously analysed eyes

Experiment 2: February/March 2002

Dose	20 µl / g
Frequency	Every 2 days
Time points analysed	P8, P16, P21
Number of animals	P8:1, P16:3, P21:3
Controls	Uninjected mice from a parallel litter

Experiment 3: June 2002

Dose	20 µl / g
Frequency	Every 2 days
Time points analysed	P16, P21
Number of animals treated	P16:5, P21:2
Controls	Uninjected mice from a parallel litter

NB a further two animals per time point in this experiment were left un-injected until two days prior to sacrifice when they then received liposomes daily for those two days.

Experiment 4: July/August 2002

Dose	20µl / g
Frequency	Every 2 days
Time points analysed	P16
Number of animals treated	6
Controls	6 uninjected littermates

Immunohistochemistry

Tissue was fixed, embedded and sectioned as described in chapter two. Spleen and retinal sections from treated and control mice were analysed for macrophage markers F4/80 and sialoadhesin to confirm macrophage/microglial depletion (method described in chapter two). Retinal sections were also stained with the TUNEL, initially by the alkaline phosphatase method, then by fluorescent TUNEL TMR, in order to determine photoreceptor apoptosis (methods described in chapter two). In addition, to determine the extent of microglial apoptosis within the retina after clodronate liposomes treatment, double immunofluorescent labelling for TUNEL and F4/80 was performed as described below. At least six non-adjacent retinal sections were counted per stain per eye as described before.

F4/80 / TUNEL two colour immunofluorescence

1) Slides out 30-60 minutes to dry
2) Encircling of sections with 'Immedge' hydrophobic pen
3) Wash 30 min in PBS
4) Blocking serum (goat, 15ul/ml 2% PBSA) 30 min
5) Tip off excess and add Primary antibody (F4/80) diluted in 2% PBSA overnight at 4°C
6) Wash 2x5 min in PBS
7) Goat anti rat FITC diluted in 0.1% PBSA 60 min
8) Wash 2x5 min in PBS
9) Permeabilise in Triton x-100 for 2 minutes
10) Wash 2x5 min
11) TUNEL-TMR for 1 hour at 37°C
12) Wash 3x5 min
13) DAPI mount

RESULTS

EXPERIMENT 1: Pilot study

Design Summary: 10 µl/g clodronate liposomes every 5-6 days

The spleen from one animal was analysed at P5 (three days after the initial clodronate liposomes injection to determine extent of macrophage depletion. Marked depletion of F4/80 positive cells was observed in comparison with an untreated P21 mouse (*figure 4.2a,b*). One further animal was analysed at P8 (six days after the initial injection). This revealed that the spleen was nearly fully replenished with F4/80 positive cells (*figure 4.2c*) although sialoadhesin depletion was still profound.

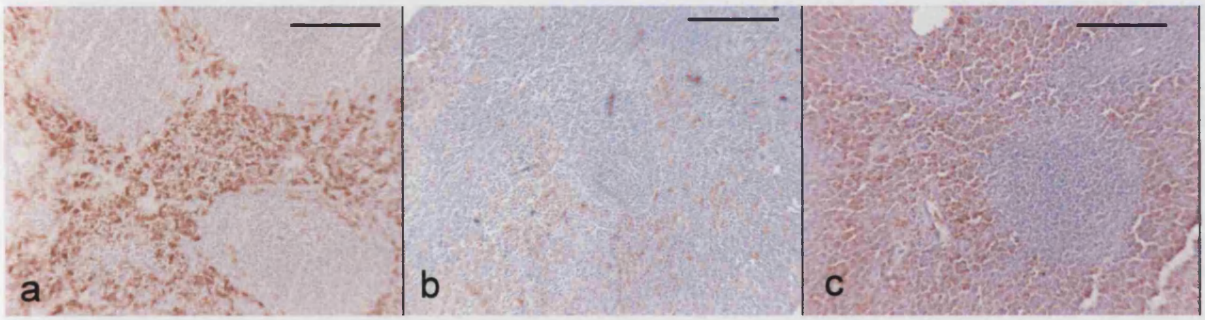

Figure 4.2 Immunohistochemical detection of the macrophage surface marker F4/80 in the spleen. In contrast to the normal dense population of (brown stained) F4/80 positive macrophages occupying, predominantly the inter-follicular regions (a), three days after a single intraperitoneal injection of clodronate liposomes at P2, the spleen is profoundly depleted of these cells (b). Six days after the clodronate liposomes treatment (P8) repopulation of macrophages bearing F4/80 is almost complete (c). Counterstain: haematoxylin, scale bar: 200µm.

There was some evidence of microglial depletion in the retina at P8 with slightly reduced inner retinal microglia in comparison with previously analysed eyes (from untreated animals) and no sub-retinal microglia were present (in contrast with eyes from untreated P8 *rds* mice, *figure4.3*). At later time points (P16, P19, P21) there appeared to be no significant effect on the numbers of retinal microglia.

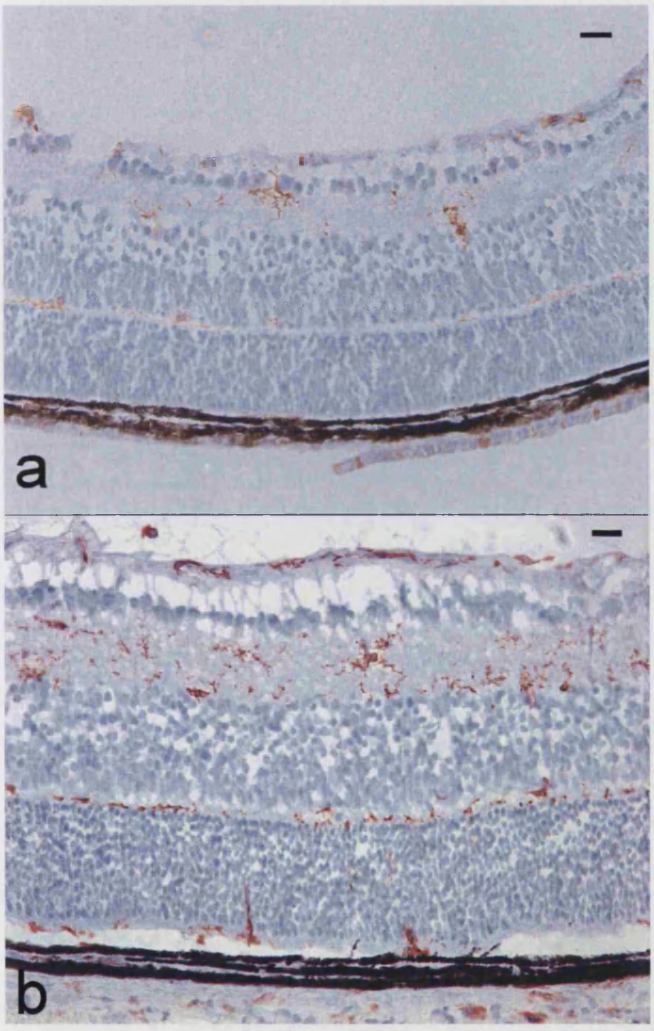

Figure 4.3 Fewer retinal microglia were seen at P8 after a single injection of clodronate liposomes at P2 (a), when compared with an untreated animal from a parallel litter (b). Χουντερσταιν: ηαεματοξψλιν, σχαλε βαρ: 20μm.

These results suggested that the clodronate liposomes can be effective at depleting the systemic myeloid pool, but this effect was much reduced by 6 days post-injection. Although there was some suggestion of retinal microglial depletion in one eye at P8, the results from later time points and the rapid splenic repopulation indicated that more frequent injections might be required. For that reason subsequent experiments were conducted using an increased frequency of clodronate liposomes injections; given on alternate days.

EXPERIMENTS 2 + 3: Optimisation of protocol for depletion or retinal microglia

Design summary: 20 µl/g clodronate liposomes every 2 days

Experiment 2

A single animal was analysed at P8 to confirm splenic macrophage depletion with the new batch of clodronate liposomes. At P16, no significant depletion of F4/80 positive retinal microglia was observed in comparison to uninjected controls from an age-matched litter (not counted). Furthermore, splenic F4/80 depletion was not profound at this time point.

At P21 however, dramatic depletion of both splenic and retinal F4/80 and sialoadhesin positive cells was noted in comparison with P21 controls from an age-matched litter (*figure 4.4a-d*). The results of cell counts for P21 were pooled with P21 animals in experiment 3 and will thus be presented together below.

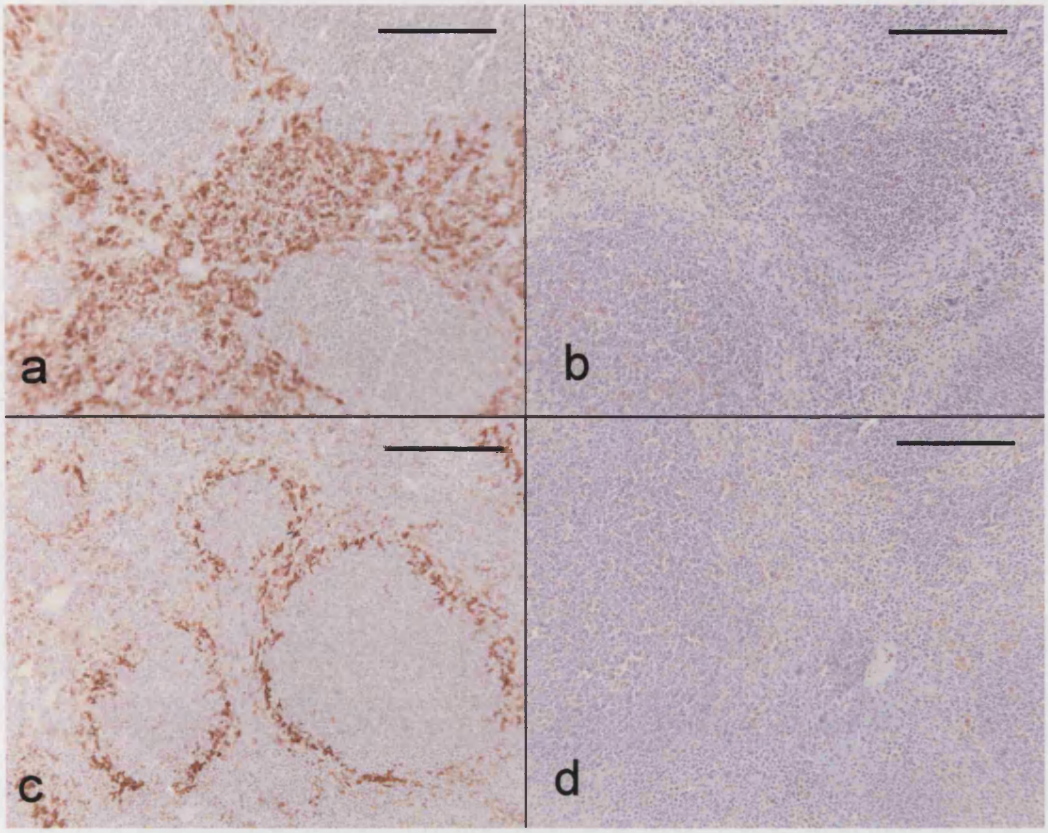

Figure 4.4 Demonstration of the effect of continued, alternate day administration of clodronate liposomes on splenic macrophages. At both P16 and P21 time points splenic depletion for F4/80 (a, normal; b, clodronate liposomes-treated) and sialoadhesin (c, normal; d, clodronate liposomes-treated) was confirmed in each animal. Counterstain: haematoxylin, scale bar: 200μm.

There are a number of possible explanations why P16 showed minimal depletion compared with P21. The first possibility is that clodronate liposomes penetrate the retina and deplete retinal microglia *in situ*, but only after some breakdown of the blood retinal barrier occurring after P16. However, in view of the reduced depletion of spleen at P16, it seemed more likely that there had been a failure in the efficacy of the clodronate liposomes. Two possible reasons for this existed:

a) Due to unforeseen circumstances (a delay in the delivery of fresh clodronate liposomes), an injection was not possible on P14, but was given on P15 instead (a three day interval). If an alternate day interval was critical, then this delay may explain the reduced affect at P16.

b) The liposomes used at the start of the experiment were at the end of their one month life and were replaced with a fresh batch on P15. Reduced efficacy in the first half of the experiment may have been due to leeching of clodronate out of the liposomes.

For these reasons the experiment was repeated with fresh liposomes throughout and a strict alternate day injection programme.

Experiment 3

Splenic macrophage depletion was confirmed in each animal at P16 and P21. Comparison between untreated mice from an age-matched litter showed significant depletion (by >60%) of F4/80 positive retinal microglia in the treated group at P16 (*table 4.1, figure 4.5, 4.6 a+b*). Although only sub-retinal microglia were counted (see chapter two), retinal microglial numbers appeared to be reduced throughout the retina.

Time point: P16, Marker: F4/80

Animal	Controls	Liposome-treated	
1	14.1	0.5	
2	14.2	5.3	
3	16.6	4.8	
4	19.0	10.1	
5	13.7	7.2	
Mean	**15.5**	**5.6**	P < 0.001
SD	2.3	3.5	
SEM	**1.0**	**1.6**	

Table 4.1 **Comparison of mean number of sub-retinal microglia (F4/80 positive) per 1.2 mm retina in clodronate liposomes-treated and control mice at P16.**

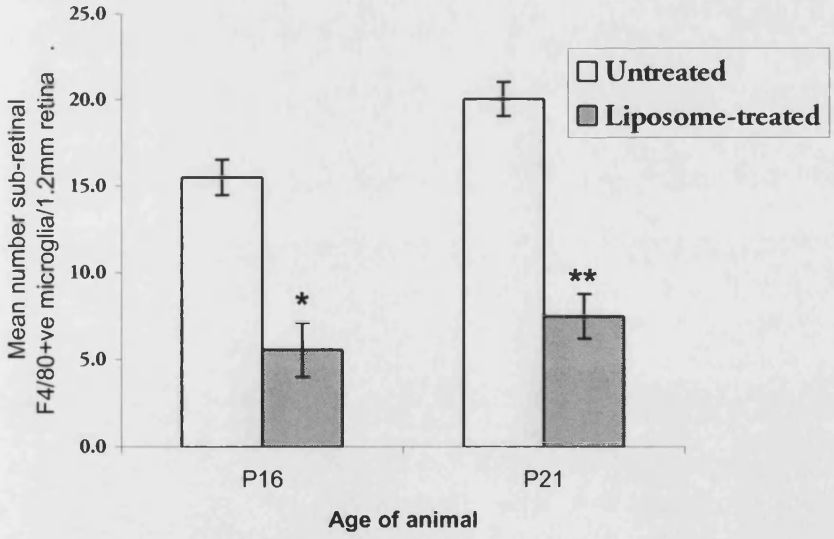

Figure 4.5. Treatment with clodronate liposomes resulted in a greater than 60% reduction in the number of sub-retinal F4/80 positive microglia at P16 and P21. *p<0.001, **p<0.0001.

Figure 4.6 Clodronate liposomes-mediated depletion of retinal microglia (F4/80, brown). a and c show the normal complement of retinal microglia in *rds* mice at P16 and P21 respectively. After alternate day clodronate liposomes treatment, markedly reduced microglial numbers were seen at both time points (b, P16; d, P21). Counterstain: haematoxylin, scale bar: 20μm.

Although sialoadhesin expression on retinal microglia at P16 is limited in control *rds* mice, in clodronate liposomes treated animals it was virtually non-existent at this time (*table 4.2, figure 4.7*).

Time point: P16, Marker: sialoadhesin			
Animal	**Controls**	**Liposome-treated**	
1	3.1	0	
2	2.6	0	
3	2.4	0	
4	12.2	0.3	
5	0.3	0	
Mean	**4.3**	**0.1**	NS
SD	4.9	0.1	
SEM	**2.2**	**0.1**	

Table 4.2 **Comparison of mean number of sub-retinal microglia (sialoadhesin positive) per 1.2 mm retina in clodronate liposome-treated and control mice at P16.**

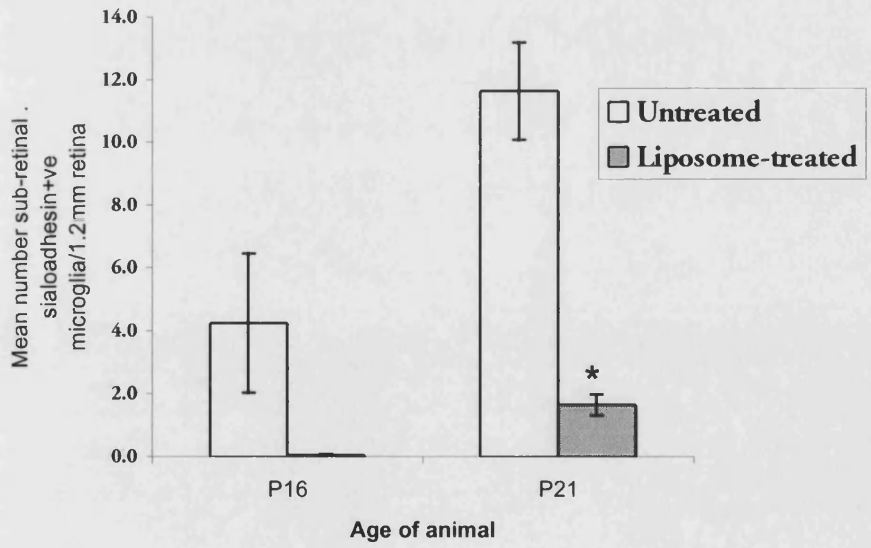

Figure 4.7. Treatment with clodronate liposomes reduced sialoadhesin expression at P16 to almost undetectable levels and caused an 85% reduction in the number of sialoadhesin positive sub-retinal microglia at P21. *$p<0.005$.

At P21 in this experiment, as with the previous one, good depletion of retinal and splenic myeloid cells was achieved in clodronate liposomes treated animals (*figure 4.6c+d*). Cell counts were pooled with those from experiment 2 and are shown in *table 4.3* and *figure 4.5*. Overall a >60% reduction in microglial numbers was seen with clodronate liposome treatment.

Time point: P21, Marker: F4/80			
Animal	**Controls**	**Liposome-treated**	
1	20.4	10.3	
2	19.0	8.7	
3	18.3	3.7	
4	18.8	5.3	
5	23.8	9.5	
Mean	**20.1**	**7.5**	P< 0.0001
SD	2.2	2.9	
SEM	**1.0**	**1.3**	

Table 4.3 **Comparison of mean number of sub-retinal microglia (F4/80 positive) per 1.2 mm retina in clodronate liposome-treated and control mice at P21.**

The depletion effect on sialoadhesin-expressing retinal microglia at P21 was even more profound with an 85% reduction in their numbers as shown by *figures 4.7, 4.8a,b and table 4.4.*

Time point: P21, Marker: sialoadhesin			
Animal	**Controls**	**Liposome-treated**	
1	12.1	2.1	
2	10.5	1.8	
3	10.8	0.4	
4	8.4	1.7	
5	16.5	2.3	
Mean	**11.6**	**1.7**	$P < 0.005$
SD	3.0	0.7	
SEM	**1.4**	**0.3**	

Table 4.4 Comparison of mean number of sub-retinal microglia (sialoadhesin positive) per 1.2 mm retina in clodronate liposomes-treated and control mice at P21.

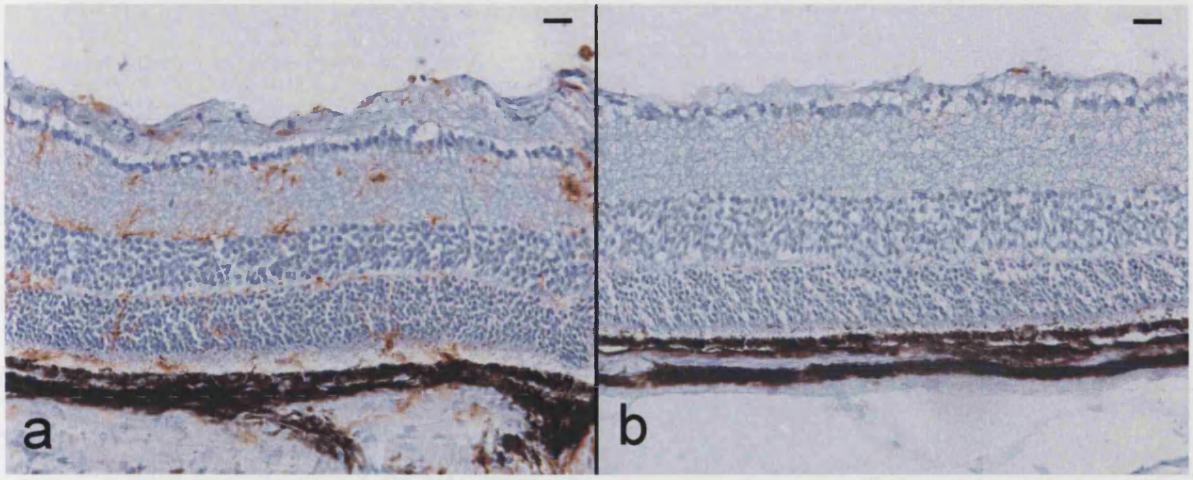

Figure 4.8 Even more profound depletion of sialoadhesin-expressing microglia (brown) was seen with clodronate liposomes administration. At P21 in the control *rds* mice, retinal microglial sialoadhesin expression was widespread (a), whereas in clodronate liposomes-treated animals at the same age sialoadhesin was almost completely absent. Counterstain: haematoxylin, scale bar: 20μm.

In contrast to the successful depletion of retinal microglia with alternate day clodronate liposomes injections from P2, animals receiving injections only on the two days preceding sacrifice had at best only a partial effect (not formally counted) at both P16 (injected on P14 and P15) and P21 (injected on P19 and P20). The depleting effect on sialoadhesin expression, however, after only two days of clodronate liposomes, was quite marked at P21 (only one eye counted).

Experiment 3: Effect of microglial depletion on photoreceptor apoptosis

Having established a protocol for depleting retinal microglia, TUNEL was used to determine any effect this depletion might have on photoreceptor apoptosis. P16 eyes

were analysed by the alkaline phosphatase TUNEL method, whereas for P21 the fluorescent method was used. The reasons for this are detailed below.

TUNEL staining at P16 showed a non-significant reduction in photoreceptor apoptosis in clodronate liposomes treated mice (19.4 +/-1.1 and 14.4 +/- 9.6 in controls and treated mice respectively, *table 4.5 and figure 4.9*).

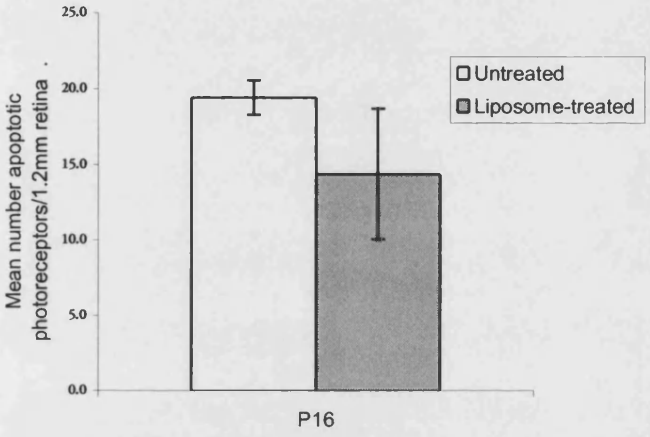

Figure 4.9. After microglial depletion with clodronate liposomes, reduced photoreceptor apoptosis was seen at P16, compared with the untreated age-matched litter (not significant).

Time point: P16, Marker: TUNEL (alk phos)		
Animal	**Controls**	**Liposome-treated**
1	18.5	8.5
2	18.2	31.0
3	17.0	14.5
4	19.9	10.1
5	23.6	7.9
Mean	**19.4**	**14.1**
SD	2.5	9.6
SEM	**1.1**	**4.3**

Table 4.5 Comparison of mean number of TUNEL positive photoreceptors per 1.2 mm retina in clodronate liposome-treated and control mice at P16.

The shaded data value (mouse 2 in clodronate liposomes treated group) was noted to be an eccentric value, without which a statistically significant difference between the groups would exist. The value was verified by repeat staining of this and the other eye of this animal. In considering the reason for this widely outlying data point it became apparent that due to the rapid nature of the surge of photoreceptor apoptosis at around P15-18 from very low to very high levels within 24 hours or so, even a slight difference in age between the two litters might result in differences in TUNEL scoring. This outlying data value might have represented the most advanced

individual in the litter in terms of development, and it is conceivable that within 12 hours, the remainder of the litter would have risen to such high values.

So, presented with this argument, the study design of the clodronate liposomes experiments to this point were deemed flawed in their use of a separate age-matched litter for controls, particularly when analysing P16, at which time the rate of change of photoreceptor apoptosis rate is so high that small differences between litter ages might result in significant differences in levels of photoreceptor apoptosis. Therefore it was decided to repeat the experiment for P16 using untreated siblings as controls (see experiment 4).

.

In the course of this experiment, for the purposes of double immunofluorescent labelling for TUNEL and F4/80 it was noted that the fluorescent TUNEL TMR method provided much cleaner staining than its alkaline phosphatase counterpart. The numbers of apoptotic photoreceptors detected were also higher with this method. For these reasons the fluorescent TUNEL TMR method was used for all subsequent TUNEL analysis, including the P21 eyes for this clodronate liposome experiment 3. TUNEL staining demonstrated a significant increase in photoreceptor apoptosis after retinal microglial depletion with clodronate liposomes at P21 (14.3 +/- 1.5 and 23.6 +/- 3.0 for control and treated mice respectively, $p<0.05$). The data are shown in *table 4.6 and figure 4.10.*

Time point: P21, Marker: TUNEL (TMR)			
Animal	**Controls**	**Liposome-treated**	
1	9.9	33.4	
2	14.6	15.9	
3	16.1	20.2	
4	18.4	21.1	
5	12.8	27.1	
Mean	**14.3**	**23.6**	$p < 0.05$
SD	3.2	6.8	
SEM	**1.5**	**3.0**	

Table 4.6 Mean numbers of apoptotic photoreceptors per 1.2mm retina in clodronate liposomes-treated and control mice at P21.

The difference however between these two groups, which only just reached significance, has to be considered potentially artifactual due to the lack of sibling controls for this experiment, as discussed above.

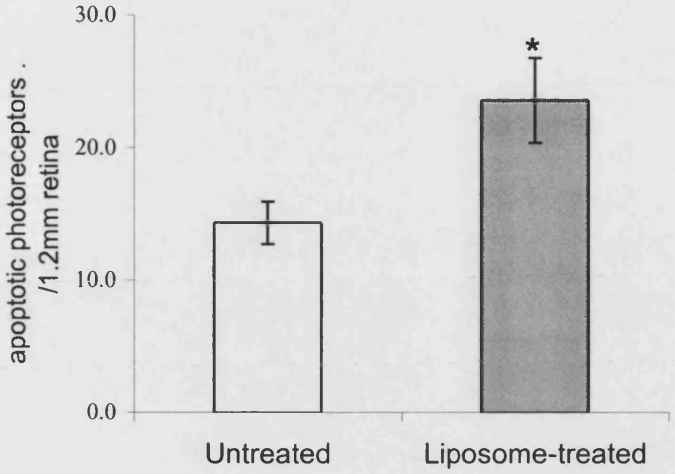

Figure 4.10 An increase in the number of TUNEL positive photoreceptors was seen after microglial depletion with clodronate liposomes at P21. $p<0.05$.

EXPERIMENT 4: Microglial depletion at P16 with littermate controls

Design summary: 20 µl/g clodronate liposomes every two days. Sibling controls.

Splenic macrophage depletion was confirmed in each animal. Clodronate liposomes treatment again led to a significant depletion of retinal microglia in treated mice when compared with their untreated littermates (controls: 8.1 +/- 0.5, liposome-treated: 3.0 +/- 0.9, $p<0.005$. *Table 4.7 and figure 4.11a,b and 4.12).* One animal from the treatment group had a mean value of 7.4 microglia per 1.2 mm retina and was deemed to have had failed depletion. That individual was therefore excluded from the data set.

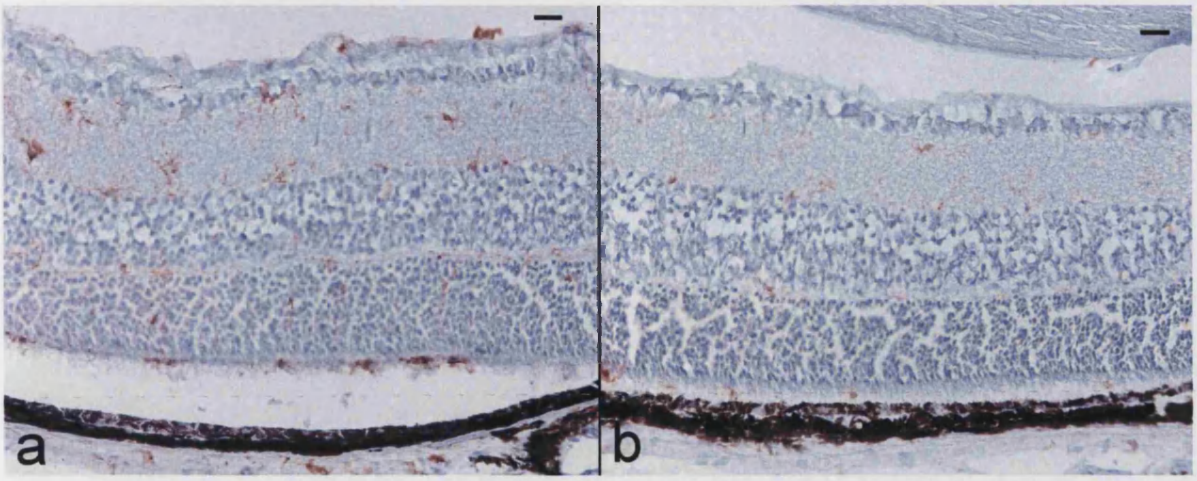

Figure 4.11 Clodronate liposomes-mediated depletion of retinal microglia (F4/80, brown) at P16 in experiment 4. Littermate controls had significantly more retinal microglia (a) than their clodronate liposomes-treated siblings (b). Counterstain: haematoxylin, scale bar: 20μm.

Time point: P16, Marker: F4/80			
Animal	**Sibling Controls**	**Liposome-treated**	
1	7.9	0.8	
2	7.2	0.9	
3	9.2	4.4	
4	7.4	4.9	
5	7.3	3.8	
6	9.8		
Mean	**8.1**	**3.0**	$p < 0.005$
SD	1.1	2.0	
SEM	**0.5**	**0.9**	

Table 4.7 **Mean numbers of sub-retinal microglia (F4/80) in clodronate liposomes-treated and sibling control mice at P16.**

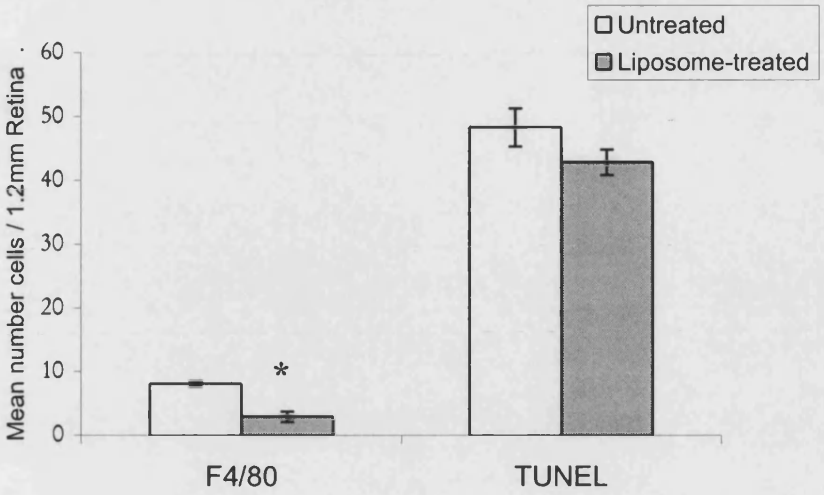

Figure 4.12. Clodronate liposomes treatment depleted sub-retinal retinal microglia (F4/80) by >60% compared with untreated littermates at P16. This, however, resulted in no change in rate of photoreceptor apoptosis. * $p<0.005$.

Despite marked (63%) depletion of retinal microglia in the treatment group, no difference was seen in photoreceptor apoptosis between clodronate liposomes-treated animals and their littermate controls (*table 4.8 and figure 4.12*). Indeed, even in animals whose microglia had been depleted to profoundly low levels, photoreceptor apoptosis was not influenced (*table 4.8*). For example, animal 2 in the treated group has slightly greater photoreceptor apoptosis than control animal number 3, despite having only 10% the complement of microglia.

	Controls		Liposome-treated	
Animal	**Microglial Numbers**	**Photoreceptor Apoptosis**	**Microglial Numbers**	**Photoreceptor Apoptosis**
1	7.9	62.6	0.8	40.0
2	7.2	47.1	0.9	45.4
3	9.2	42.1	4.4	42.5
4	7.4	49.4	4.9	44.5
5	7.3	45.8	3.8	49.8
6	9.8	43.1		

Table 4.8 **Comparison between mean microglial numbers and mean photoreceptor apoptosis within treated animals and littermate controls at P16.**

Retinal Microglial Apoptosis

To deduce the mechanism of retinal microglial depletion I compared the number of apoptotic microglia in liposome-treated and control retina, on the premise that if the liposomal clodronate was crossing the blood-retinal barrier and acting *in situ*, more apoptotic microglia would be seen in treated retinas. TUNEL and F4/80 double immunofluorescent labelling was used on eyes from experiments 3 (P21) and 4 (P16). Very few apoptotic microglia (*figure 4.14*) were found in either treated or control retina (treated 0.4/mm^2 +/- 0.3, controls 0.3/mm^2 +/- 0.1, not significant. *Table 4.9, figure 4.13*), implying that the depleting effect on retinal microglia is mediated by preventing recruitment of systemic myeloid cells to the retina.

	P16		P21	
Animal	**Controls**	**Liposome-treated**	**Controls**	**Liposome-treated**
1	0	0	1.3	0
2	0.7	0.3	0.4	0
3	0	0.6	0	0
4	0.6	0	0	0
5	0.6	1.6	0	1.5
6	0	0		

Table 4.9 **Mean number of apoptotic retinal microglia per mm^2 retina in clodronate liposomes-treated and control mice.**

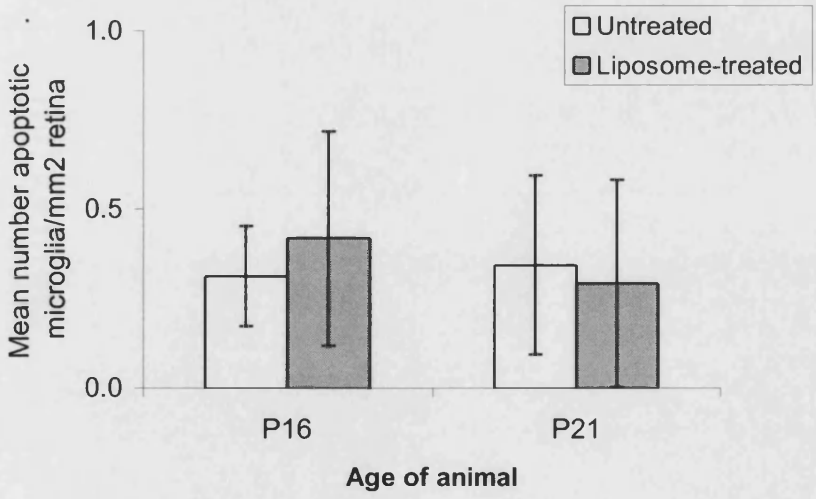

Figure 4.13. No difference was found between clodronate liposomes-treated and control mice in the number of apoptotic retinal microglia.

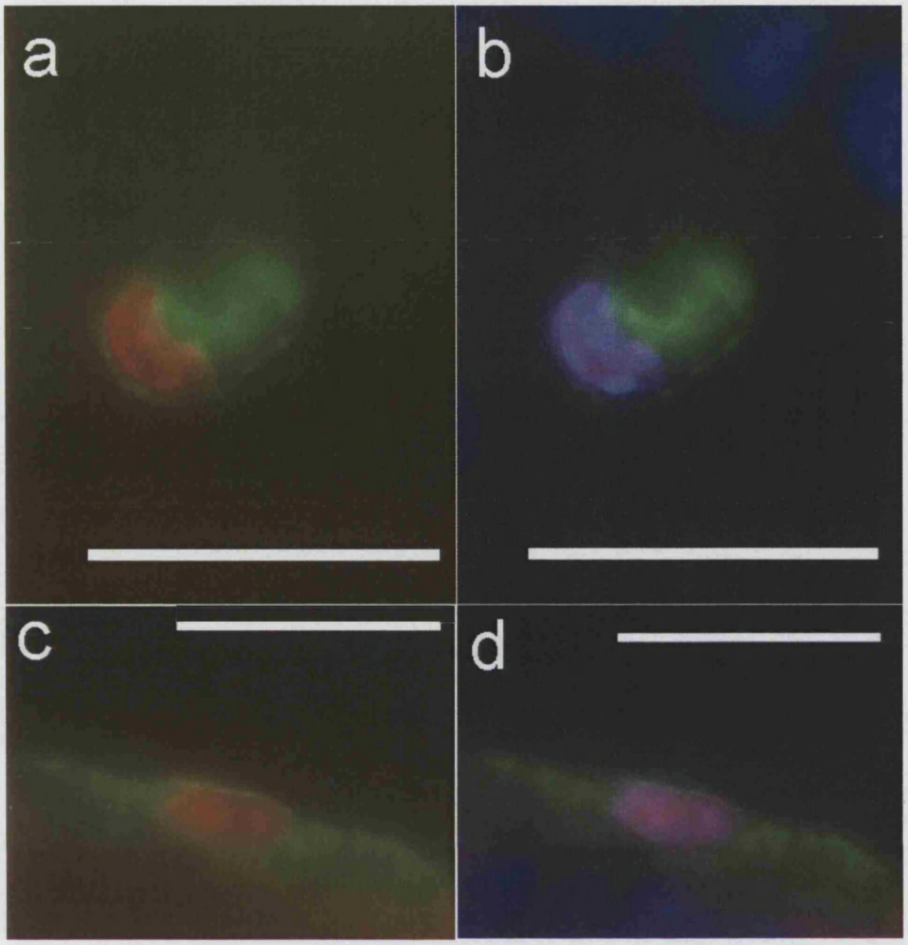

Figure 4.13 Two colour immunofluorescence for F4/80 (green, cell surface) and TUNEL (red, nucleus) demonstrating scarce apoptotic retinal microglia in both clodronate liposomes-treated and control mice. a and c show apoptotic microglia on outer and inner retinal surfaces respectively. Nuclear staining with DAPI (blue) is overlaid on the same images in b and d. Scale bar: 20μm.

DISCUSSION

The findings of the four clodronate liposomes experiments provide insight into the biological mechanisms of photoreceptor apoptosis and degeneration, microglial responses to CNS injury and of the clodronate liposomes themselves. The experiments represent, to my knowledge, the first successful depletion of microglia from the retina during retinal degeneration.

Mechanism of action in this model

Four key pieces of evidence indicate that intraperitoneally administered clodronate liposomes reduce the number of retinal microglia during *rds* degeneration by preventing recruitment of myeloid precursors from the systemic pool, rather than by an *in situ* action on the resident microglia.

- Firstly, and of fundamental importance is that I (and many others) have documented a profound depletion effect systemically (spleen). This effect seems to have been stronger and longer lasting on sialoadhesin positive macrophages normally resident in the marginal (perifollicular) zones of the spleen.

- Secondly, there appears to be no induction of microglial apoptosis within the retina of clodronate liposomes-treated mice at both P16 and P21. It is unknown whether the eventual decline of microglial numbers at later time points results from *in situ* apoptosis later on or migration out of the eye.

- Thirdly, injection of clodronate liposomes only on the two days preceding analysis (as opposed to alternate days from P2) has only a mild, if any

depletion effect. If clodronate liposomes were penetrating the retina one would expect to see as potent an effect as with chronic administration. The fact that only chronic, continued administration works implies that maintaining the systemically depleted state, continues to prevent recruitment to the retina.

- Fourthly, the almost complete absence of sialoadhesin expressing microglia from clodronate liposomes-treated mice. Immunohistochemical staining suggests that the emergence of sialoadhesin expression within the retina of *rds* mice is attributable to recruited macrophages, since sialoadhesin positivity is initially observed around the retinal vessels at P16. Furthermore, although P21 animals receiving clodronate liposomes only on the two days preceding analysis had poor depletion of F4/80 positive microglia, sialoadhesin expression appeared to be far more profoundly reduced, to levels nearly equal to those seen with chronic alternate day administration (only formally assessed in one tissue sample). A possible explanation for this is that sialoadhesin positivity is lost from recruited microglia after a couple of days within the retina. Two days of clodronate liposomes administration may have prevented the recruitment of fresh (sialoadhesin expressing) myeloid cells during that period but not for long enough to significantly reduce overall retinal microglial numbers.

Prevention of recruitment of myeloid cells to the CNS and eye during inflammatory pathologies has been studied before with the use of clodronate liposomes. Most notably, Bauer *et al* used this approach in the setting of experimental allergic encephalomyelitis (EAE, a model of demyelinating CNS disease) in rats. They noted

a marked reduction in the numbers of both infiltrating macrophages and resident microglia within the spinal cord of EAE rats treated with clodronate liposomes in comparison to control EAE rats. No indication was given of how microglia levels in the cord of clodronate liposomes treated EAE rats compared to normal rats (in the absence of EAE), but since no apoptotic microglia were found *in situ* in the cord, it was suggested that the liposomes were not acting directly on the resident cells. It is known that microglia proliferate *in situ* in response to neuropathology (chapter 3 and (Streit and Kreutzberg 1988; Sedgwick et al. 1998)), so one might expect if clodronate liposomes had no effect on the resident microglia, that numbers of these cells would be greater in EAE than in physiological conditions, even after systemic myeloid depletion.

Ischaemic brain insults also result in up-regulated microglial activity and the effect of clodronate liposomes on this process was studied by Schroeter *et al*(Schroeter et al. 1997; Schroeter et al. 2001). Prevention of recruitment of systemic myeloid cells led to a marked reduction in microglial numbers in the region of photochemically induced infarction, although in the early stages the lesion characteristics did not differ from un-depleted animals, suggesting that resident microglia undertake the initial response to injury, but that recruitment is also required to manifest the full microglial response to CNS injury.

We demonstrated in experiments presented in chapter three that enhanced microglial proliferation occurs within the retina of *rds* mice. The experiments presented in this chapter demonstrate that prevention of recruitment of myeloid cells significantly attenuates the microglial response indicating that recruitment is a substantial component of the microglial expansion seen during retinal degeneration.

Clearly the proliferation capacity of resident microglia is inadequate to propagate the numbers required and is unable to compensate for the withdrawal of recruited support from the systemic circulation.

Thus, a combination of *in situ* proliferation and recruitment from the blood appears to be a consistent feature of microglial responses throughout the brain, spinal cord and retina, regardless of the invoking pathology (inflammatory, ischaemic or degenerative).

Retinal microglial involvement in photoreceptor degeneration

The main purpose of the experiments described in this chapter was the assessment of the effect that microglial depletion had on photoreceptor apoptosis. The most robust data that was obtained was from experiment four, since this involved the use of littermate controls. No alteration to the rate of photoreceptor death was observed despite >60% depletion of microglia at the height of photoreceptor apoptosis. Furthermore, no correlation existed between microglial numbers and photoreceptor apoptosis within individual retinas. Although an increased amount of photoreceptor apoptosis was observed in experiment two/three with clodronate liposomes treatment at P21, this effect only just achieved significance and, more importantly littermate controls were not used. The potential differences between litters in terms of disease severity casts doubt over the validity of the finding, and one cannot exclude the possibility that small variations in the ages of treated and control animals accounted for the difference in levels of apoptosis.

No evidence has been found for a microglial cytotoxic effect (in which case photoreceptor apoptosis should have been reduced with depletion of microglia) and in conjunction with the findings outlined in chapter three, the findings of the clodronate liposome experiments indicate this role is extremely unlikely. Furthermore there was some suggestion that microglial activity might even be protective. Whilst additional experiments (using littermate controls) would be required to confirm this, there are a number of possible reasons why this might be the case:

- the withdrawal of tissue homeostasis and microglia-derived trophic factors

- a build up of sub-retinal debris preventing oxygenation from the choroid and the diffusion of nutrients. This is an important consideration since it has not been possible to quantify the relative contributions of the retinal pigment epithelium (RPE) and infiltrating microglia to the removal of apoptotic debris from the sub-retinal space. If indeed the main role of microglia in the outer retina and sub-retinal space in this model is a phagocytic one with the purpose of clearing up cellular remains, then depletion of microglia could significantly over-burden the phagocytic capacity of the RPE and lead to accumulation of material in the sub-retinal space as occurs in the RCS rat.

- the failure of phagocytosis of apoptotic cells prior to their lysis, leading to local accumulation of toxic substances such as IL1β and free radicals that may be released by dying cells and cause 'contagious apoptosis'(Friedlander 2003).

CHAPTER FIVE

THE EFFECT OF MINOCYCLINE ON PHOTORECEPTOR DEGENERATION

During literature review of the subject of microglial cytotoxicity, searching for methods of inhibiting microglia *in vivo,* I became interested in studies utilising minocycline to manipulate microglial responses to neurodegeneration. Minocycline is a semi-synthetic, second generation tetracycline antibiotic first introduced in the early 1970s. Despite a broad spectrum of antibacterial action, its clinical use has been limited mainly to the treatment of acne, but it has also been used with good effect in a wide variety of infections including atypical respiratory infections, sexually transmitted diseases, meningococcal prophylaxis and periodontal disease(Brogden et al. 1975). It has excellent bioavailability after oral administration, is cleared by both liver metabolism and excretion unchanged in the urine and has a serum half life of 12 to 16 hours after a single dose, increasing on repeated administration. Unlike other tetracyclines it benefits from excellent penetration of the blood-brain barrier (owing to its lipophilicity) and has recently been shown to have a remarkable neuroprotective role in models of neurodegeneration(Chen et al. 2000; Du et al. 2001; Sanchez Mejia et al. 2001; Wu et al. 2002; Zhu et al. 2002) and brain ischaemia (Yrjanheikki et al. 1999; Arvin et al. 2002). The mechanism of this apparent neuroprotective property is not yet fully defined, but evidence suggests that it may arise through two separate mechanisms, distinct from the drug's antibiotic attributes. The first of these mechanisms is a proposed direct anti-apoptotic effect, possibly acting on the caspase cascade or further up-stream in the apoptotic pathway.

Caspases are the central executioners in apoptosis, and are highly conserved through evolution, being found in humans down to insects and nematodes. About twelve caspases exist, the majority of which are involved in apoptosis, during which they cleave specific sites on vital cell proteins usually causing disassembly, but occasionally activating them as in the case of nucleases that then go on to fragment the nuclear DNA(Hengartner 2000; Yuan and Yankner 2000; Friedlander 2003).

Caspases normally lie redundant within the cytoplasm and require cleavage for activation. This is closely regulated by upstream mechanisms which fall into two basic categories of apoptosis initiation (*figure 5.1*). The mitochondrial pathway results from internal cellular insults such as DNA damage, which leads to activation of a pro-apoptotic member of the bcl2 family that causes release of cytochrome c and other mediators, such as apoptosis inducing factor, from mitochondria. Cytochrome c then forms an 'apoptosome' with procaspase 9 and Apaf1 which in turn leads to activation of caspase 9 which cleaves caspase 3 into activated p12 and p17 subunits.

The cell death receptor pathway requires activation of cell surface receptors such as CD95 (Fas) and the TNFα receptor, which bind to and cleave procaspase 8. Activated caspase 8 then cleaves caspase 3 and Bid with the latter acting as a bridge between the two pathways by then inducing mitochondrial cytochrome c release. Both pathways converge at caspase 3 activation, which is a key step in the execution of apoptosis and plays a major role in the both developmental (physiological) and pathological apoptosis. For example, caspase 3-null mice have severe defects in developmental neuronal cell death with the development of a variety of hyperplasias and disorganized cell deployment in the brain resulting in perinatal death(Kuida et al. 1996). In these mice retinal development was also markedly affected, with the development of ectopic masses of neuroretinal tissue (all layers involved), growing

into the vitreous cavity and compressing the lens, indicating the importance of this enzyme in development and remodelling of the retina. Interestingly in these caspase 3-null mice, other cells outside the CNS, such as thymocytes had normal apoptosis thresholds in response to pro-apoptotic ligands like Fas, when compared to wild types, suggesting a differential of importance of caspase 3 as an executioner of apoptosis in different tissues, with a dominant role within the brain and retina. In keeping with this, caspase 3 has been shown to have a particularly important role in photoreceptor apoptosis during models of retinal degeneration(Liu et al. 1999; Tezel and Wax 1999; Jomary et al. 2001; Kim et al. 2002).

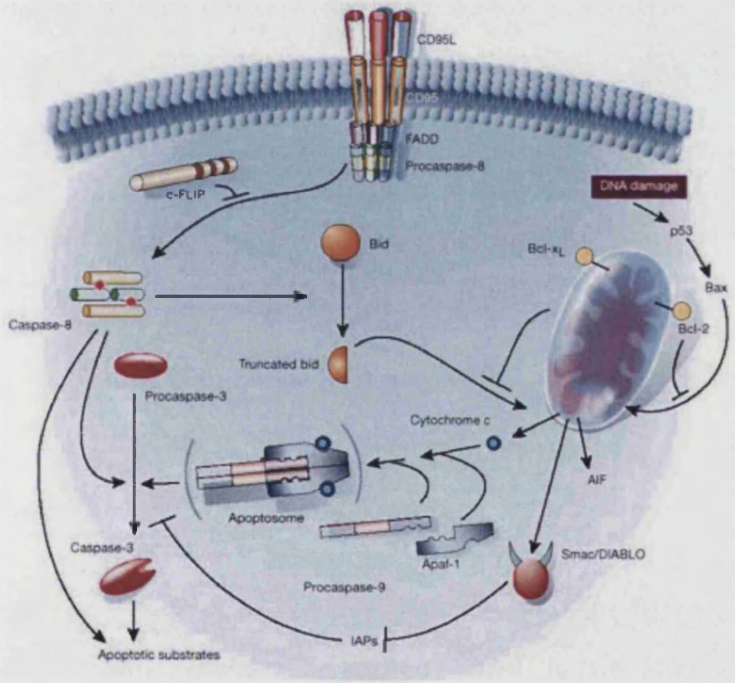

Figure 5.1 Schematic depiction of the two major apoptotic pathways: via binding of cell death receptors e.g. by Fas and TNFα (left hand side) and via mitochondrial pathway with release of proapoptotic factors such as cytochrome c and apoptosis inducing factor (AIF) in response to internal cellular injury such as DNA damage (right hand side). The two paths are bridged by the process of Bid cleavage and converge on the fundamental execution step of caspase 3 activation. From Hengartner M.O. The Biochemistry of Apoptosis. *Nature* 2000: **407**; 770-776.

It should be noted that some species differences exist in the molecular mechanisms of apoptosis and that therefore not all rodent work can correlate directly with human disease. An example of this is caspase 12 which is believed to play a key role in murine apoptosis (Nakagawa et al. 2000) but in humans is involved in proteolytic events in inflammatory cascades such as cytokine maturation (Saleh et al. 2004). However, in this work I have focussed on caspase 3 which is an important apoptosis executioner in both rodents and humans.

The elucidation of the biochemistry of apoptosis has led to the development of caspase inhibitors which have been tested in a variety of animal models in an attempt to reduce pathological apoptosis. In the eye, specific inhibitors of caspases 1 and 3 have had mixed success in the treatment of ganglion cell and photoreceptor apoptosis of various aetiologies including ischaemic, toxic and genetic insults(Chaudhary et al. 1999; Katai et al. 1999; Katai and Yoshimura 1999; Lam et al. 1999; Lam et al. 1999; Liu et al. 1999; Yoshizawa et al. 2000; Yoshizawa et al. 2002).

Marked inhibition of caspase 3 up-regulation and activation has also been demonstrated in studies documenting the neuroprotective effect of minocycline, both after brain ischaemia(Arvin et al. 2002) and during neurodegeneration (a mouse model of Huntington's disease)(Chen et al. 2000), and although its precise primary target was not found, it was shown not to act directly as a caspase enzyme inhibitor(Chen et al. 2000). More recently work by Zhu and Friedlander *et al* has demonstrated that minocycline probably works by inhibiting release of cytochrome c from mitochondria. They showed this at three distinct levels: *in vivo* during neurodegenerative and brain ischaemic models, during cell based death models and also by using cell-free mitochondrial preparations in which minocycline prevented Bid- and calcium-induced cytochrome c release(Zhu et al. 2002).

Another observation during minocycline-mediated neuroprotection has been the inhibition of microglial activity with reduced expression of iNOS and IL1β(Yrjanheikki et al. 1999; Du et al. 2001; Wu et al. 2002) and this has led to the proposal of a second mechanism of neuroprotection: through prevention of microglial cytotoxicity. It is difficult *in vivo*, however, to discern direct inhibition of microglial activation from consecutive reduction in the activity of these cells as a result of minocycline-mediated neuronal rescue. Nevertheless, Tikka *et al* have demonstrated direct microglial inhibition by minocycline *in vitro*(Tikka et al. 2001; Tikka and Koistinaho 2001). They showed that in both mixed spinal cord and microglial cultures and pure microglial cultures, excitotoxins kainate and glutamate induced microglial p38 mitogen-activated protein kinase (MAPK) activity and proliferation as well as the release of NO and IL1β from microglia, which were cytotoxic to the spinal cord neurones. Minocycline inhibited the up-regulation of p38MAPK and proliferation of microglia and their release of NO and IL1β, with consequent rescue of the neurons, a result which could be mimicked by a pure p38MAPK inhibitor but not by a P44/42MAPK inhibitor. They concluded that minocycline prevents microglial activation through inhibition of p38MAPK.

We decided to test the effect of minocycline administration in *rds* mice, to ascertain whether neuroprotective effects observed in the brain could be conferred on photoreceptors. To our knowledge its effect on retinal disease had not been previously studied and, having characterised microglial behaviour and photoreceptor apoptosis me hoped to determine the mechanism of any beneficial effect provided by the drug.

MATERIAL AND METHODS

Materials

Minocycline hydrochloride ($C_{23}H_{27}N_3O_7 \cdot HCl$, Mw 493.9) was obtained from Sigma, Poole, UK (product number M9511) in crystalline form and subsequently dissolved in distilled water.

Other materials used are described in previous chapters.

Experimental design

50mg/kg minocycline hydrochloride was injected intraperitoneally into *rds* mice daily from P2 until sacrifice, with un-injected littermates providing controls. The dose of minocycline was chosen after review of articles using minocycline for neuroprotection(Arvin et al. 2002). Mice were sacrificed and spleen and eyes taken as described above at P16, P18, P21, P24, P27 for immunohistochemical and immunofluorescent analysis. *Table 5.1* details the numbers of mice used per time point.

Time Point	**Number of Animals**	
	Minocycline-treated	*Un-treated littermates*
P16	**6**	**6**
P18	**5**	**5**
P21	**5**	**4**
P24	**5**	**5**
P27	**4**	**3**

Table 5.1 Numbers of control and treated animals used per time point.

Immunohistochemical and immunofluorescent staining

Assessment of retinal microglial numbers (F4/80) and extent of photoreceptor apoptosis (fluorescent TUNEL TMR) was performed as described above. Further immunohistochemistry was employed to determine the extent of photoreceptor caspase 3 activation using a polyclonal antibody (Asp175, Cell Signalling Technology, Beverly MA, USA) against the larger cleaved (activated) subunit (17/19kDa) of caspase 3. The antibody does not recognise full length (inactive) caspase 3 or other cleaved caspases. Both single colour immunohistochemistry and immunofluorescence and two colour immunofluorescence (TUNEL/Caspase 3) were employed for activated caspase 3 detection and the methods are described below. For all three stains (F4/80, TUNEL and caspase 3) eight non-adjacent retinal sections per eye were counted as described before.

Single Colour Immunohistochemistry/Immunofluorescence

1) Slides out 30-60 minutes to dry
2) Encircling of sections with 'Immedge' hydrophobic pen
3) Wash 30 min in PBS
4) Block endogenous peroxidase activity with 0.3% hydrogen peroxide in methanol for 15 min (not for immunofluorescence)
5) Wash 2x5 min in PBS
6) Wash 2x5 min PBS/0.1% Triton-X100
7) Blocking serum (goat, 15ul/ml PBSA+ 0.1%Triton-X 100) 30 min
8) Tip off excess blocking serum and add caspase 3 antibody diluted in 2% PBSA/0.1% Triton-X100 overnight @ 4°C
9) Wash 2x5 min in PBS
10) Add biotinylated goat anti rabbit 2^0 antibody (5ul/ml in 0.1% PBSA) 30 min
11) Wash 2x5 min in PBS
12) i) ABC 30 min or ii)Streptavidin TRITC 1 hour

13) Wash 2x5 min in PBS

14) i) DAB 3 minutes or ii)DAPI mount

15) Rinse in PBS then into running water 3 min

16) Haematoxylin dip

17) Running water 3 min, distilled H2O 1 min, 75% Alcohol 2 min, 100% Alcohol 2x2 min, Histoclear 2x2 min.

18) Histomount

Two colour immuofluorescence (TUNEL / Activated Caspase 3)

1) Slides out 30-60 minutes to dry
2) Encircling of sections with 'Immedge' hydrophobic pen
3) Wash 2x5 min PBS/0.1% Triton-X100
4) Blocking serum (goat, 15ul/ml PBSA+ 0.1%Triton-X 100) 30 min
5) Tip off excess blocking serum and add caspase 3 antibody diluted in 2% PBSA/0.1% Triton-X100 overnight @ 4°C
6) Wash 2x5 min in PBS/0.1% Triton-X100
7) Goat anti rabbit FITC 2° antibody (1:10 in 0.1% PBSA/0.1% Triton-X100) 60 min
8) Wash 2x5min in PBS/0.1% Triton-X100
9) TUNEL-TMR for 1 hour at 37°C
10) Wash 3x5 min in PBS
11) DAPI mount

Outer Nuclear Layer thickness measurement

To determine any potential neuroprotective effect of minocycline, as well as comparing numbers of apoptotic and activated caspase 3-expressing photoreceptors between treated and control animals, the thickness of the outer nuclear layer (ONL) at P27 was measured, giving an indication of the number of surviving photoreceptors. This was performed on a Leica fluorescent inverted microscope using Leica Qfluoro image analysis software. A box was drawn around a length of ONL either side of the

optic nerve head at a distance of both 200 μm and 600 μm as shown in *figure 5.2*. The area of the box was divided by its length to give the mean thickness of that sample of ONL. For this purpose, only retinal sections passing directly through the optic nerve head were analysed and three non-adjacent sections per eye were used.

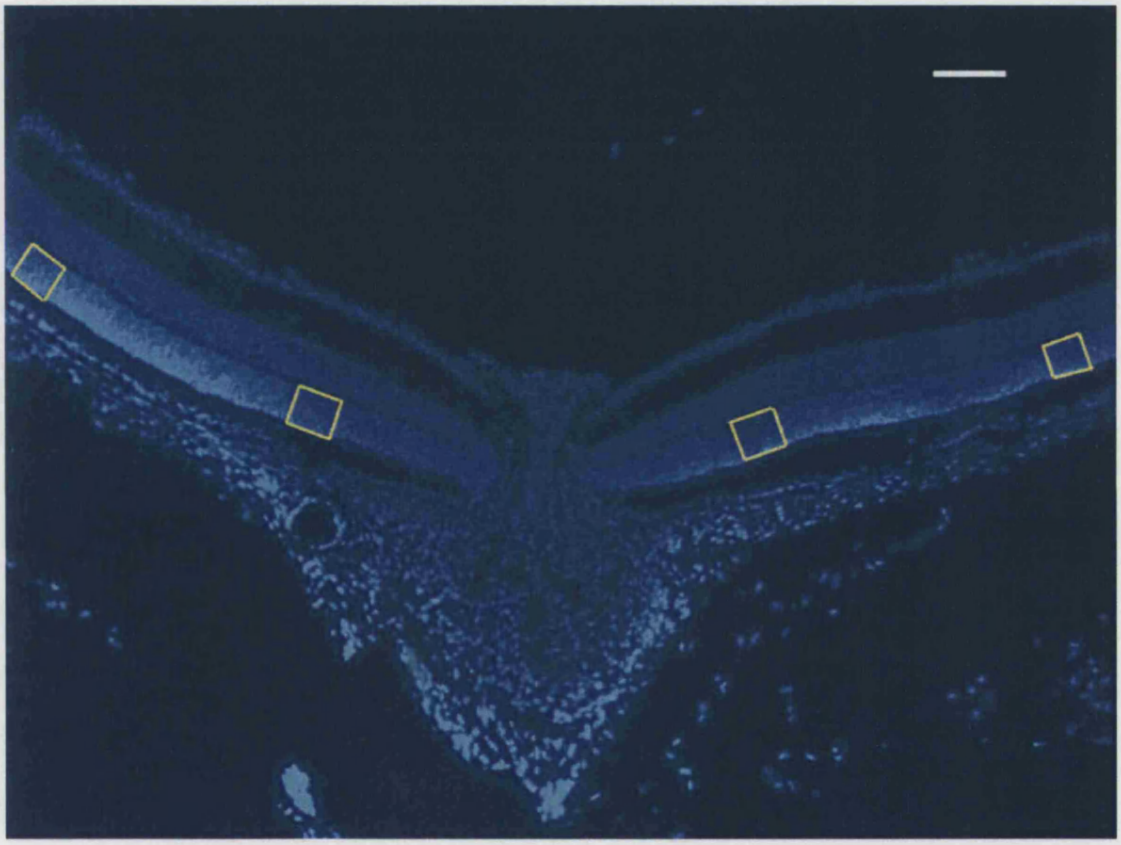

Figure 5.2 Measurement of outer nuclear layer (ONL) thickness at P27. Only retinal sections passing through the optic nerve head were used (as shown). Using image analysis software, boxes were drawn around the ONL at 200μm and 600μm either side of the optic nerve head, and the area within the box divided by its length. Counterstain: DAPI, scale bar: 100μm.

RESULTS

In order to examine whether administration of minocycline influenced the course of photoreceptor degeneration in the *rds* mouse, sections of retina from mice treated with daily intraperitoneal minocycline were analysed and compared with untreated littermates.

Minocycline reduces photoreceptor apoptosis at P16

During these experiments, photoreceptor apoptosis peaked at P18 in control and treated mice, two days later than found in experiments detailed in chapters three and four. This differences may be attributable to variability in disease expression between litters and also inaccuracy in the determination of the precise age of the litters. Administration of minocycline produced a profound (65%) reduction in the extent of photoreceptor apoptosis at P16 (treated: 15.1 +/- 2.6, controls: 44.1 +/- 3.1, $p<0.0005$) but this effect was not sustained (*table 5.2 and figures 5.3, 5.4*). By P18, the extent of photoreceptor apoptosis was the same in treated and control animals, suggesting that minocycline delayed, rather than prevented apoptosis, although me did not see a compensatory increase in apoptosis in the treated group at later time points. However, me analysed time points at three day intervals from P18-P27, and it may be that photoreceptor apoptosis was significantly higher in the minocycline-treated animals at points between those analysed.

Time Point	Apoptotic photoreceptors/1.2mm retina (+/-SEM)		
	Un-treated littermates	*Minocycline-treated*	
P16	**44.1** (+/- 3.1)	**15.1** (+/- 2.6)	p<0.0001
P18	**69.6** (+/- 3.9)	**66.2** (+/- 4.0)	ns
P21	**25.7** (+/- 8.0)	**26.1** (+/- 4.4)	ns
P24	**8.8** (+/- 0.7)	**13.3** (+/- 2.3)	ns
P27	**11.1** (+/- 1.7)	**9.4** (+/- 0.8)	ns

Table 5.2 **Mean number apoptotic photoreceptors per 1.2mm retina in minocycline-treated and control mice.**

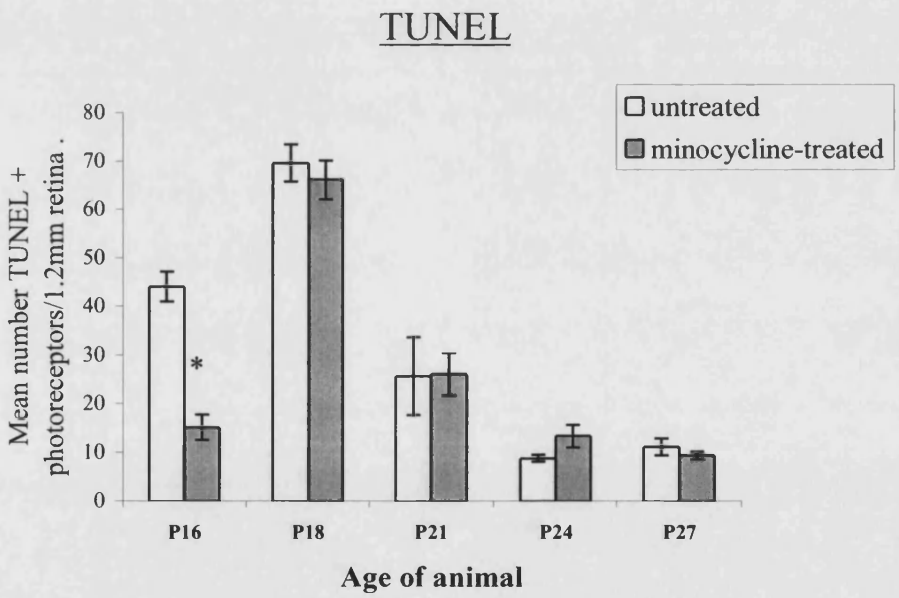

Figure 5.3. Extent of photoreceptor apoptosis (TUNEL) in minocycline-treated *rds* mice and littermate controls. Marked reduction in photoreceptor apoptosis at P16 was seen with minocycline treatment, although this effect was not sustained. * p<0.0001.

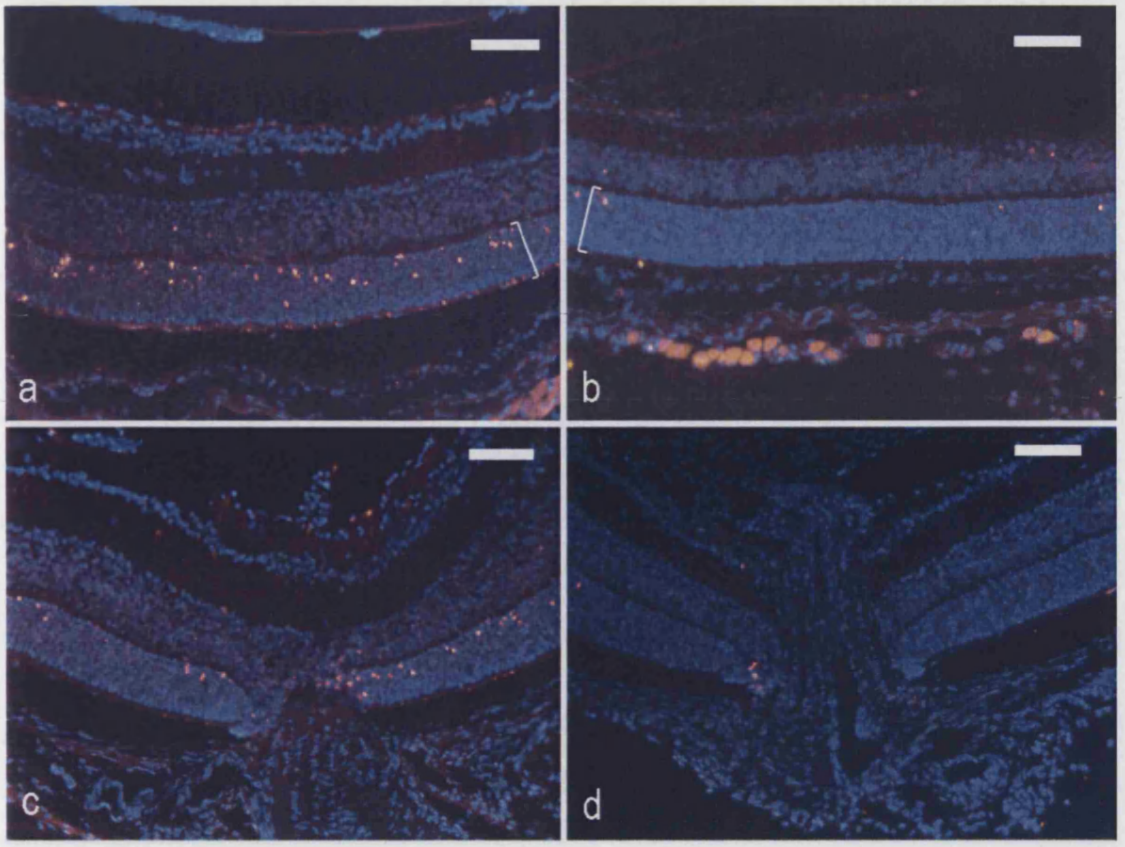

Figure 5.4 Immunofluorescent TUNEL (red nuclear stain) staining demonstrated a dramatic reduction in the number of apoptotic photoreceptors in P16 *rds* mice treated with minocycline (b, d) in comparison with controls (a, c). The effect was evident throughout the retina (a and b show mid-peripheral retina, c and d are centred on the optic nerve head). Counterstain: DAPI, scale bar: 100μm. Brackets denote the outer nuclear layer.

The hypothesis that photoreceptor apoptosis is merely delayed, rather than prevented (in some photoreceptors) with minocycline treatment is supported by ONL measurements at P27. These were used to establish whether the observed beneficial effect of minocycline treatment at P16 translated to an overall reduction in the number of photoreceptors lost. There was no difference between ONL thickness at 200μm and

600μm from the optic nerve head in treated and control animals (*table 5.3 and figures 5.2, 5.5*), indicating that by P27, minocycline treatment had not reduced the total number of photoreceptors lost.

Distance from Optic Nerve Head	ONL thickness at P27 (μm +/-SEM)	
	Un-treated littermates	*Minocycline-treated*
200 μm	**55.5** (+/- 3.4)	**54.7** (+/- 3.1)
600 μm	**52.2** (+/- 2.4)	**49.9** (+/- 0.7)

Table 5.3 Comparison of ONL thickness at P27 between minocycline-treated and untreated mice.

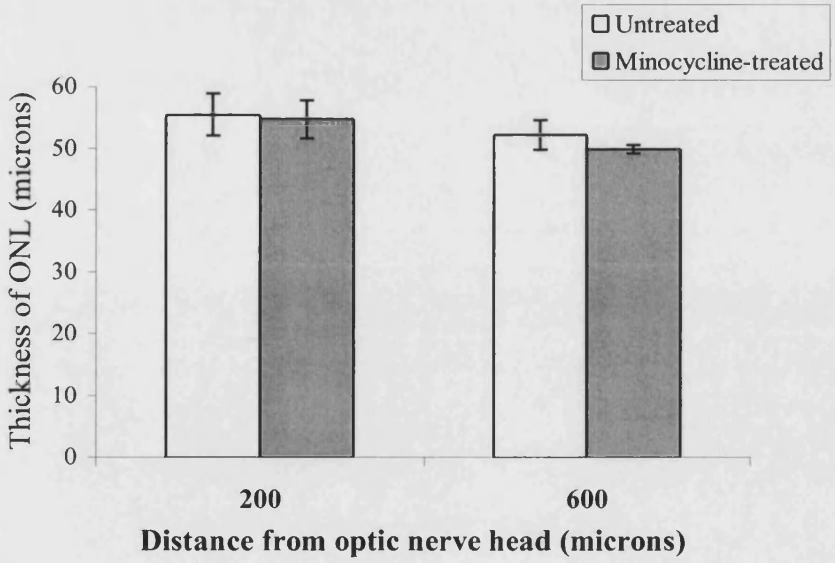

Figure 5.5. No difference was found between ONL thickness in minocycline-treated and control *rds* mice at P27.

The effect of minocycline on photoreceptor apoptosis, as detected by TUNEL, was mirrored by the effect on activation of caspase 3 in photoreceptors (*table 5.4 and figures 5.6, 5.7a,b*) with a similar 60% inhibition at P16 (treated: 16.9 +/- 1.7, controls: 42.0 +/- 3.9, $p<0.001$) but no effect at later time points. Double staining for TUNEL and activated caspase 3 revealed that the great majority of apoptotic photoreceptors were positive for both markers simultaneously (*figure 5.7c-f*).

Time Point	Activated caspase 3-expressing photoreceptors/1.2mm retina (+/-SEM)		
	Un-treated littermates	*Minocycline-treated*	
P16	**42.0** (+/- 3.9)	**16.9** (+/- 1.7)	p<0.0005
P18	**52.7** (+/- 9.0)	**55.2** (+/- 5.1)	ns
P21	**19.7** (+/- 8.2)	**14.5** (+/- 3.6)	ns
P24	**5.3** (+/- 0.9)	**5.7** (+/- 1.6)	ns
P27	**5.1** (+/- 1.5)	**3.9** (+/- 0.8)	ns

Table 5.4 **Mean number of photoreceptors expressing activated caspase 3 in minocycline-treated and control *rds* mice.**

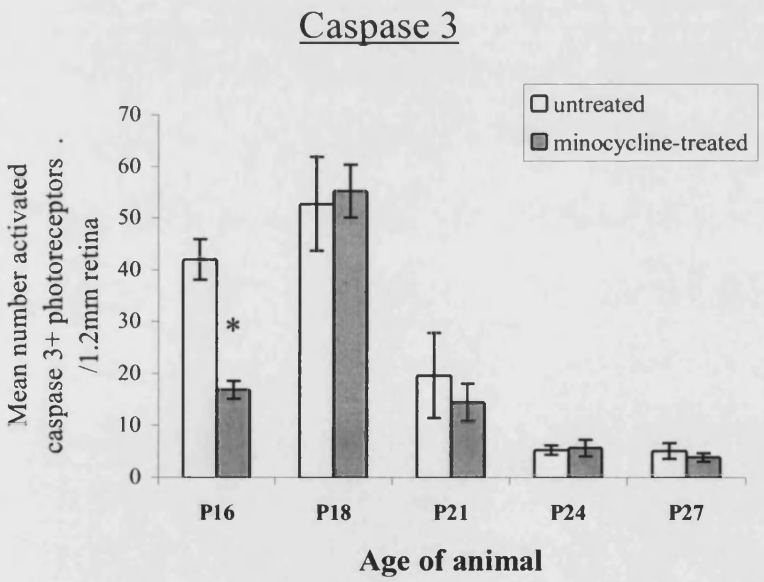

Figure 5.6. Number of activated caspase 3-expressing photoreceptors in minocycline-treated and control mice. Mirroring the TUNEL scoring, at P16 a profound reduction in activated caspase 3 expression is seen with minocycline treatment, but this reduction is short-lived, with no difference seen at later times. *p<0.0005

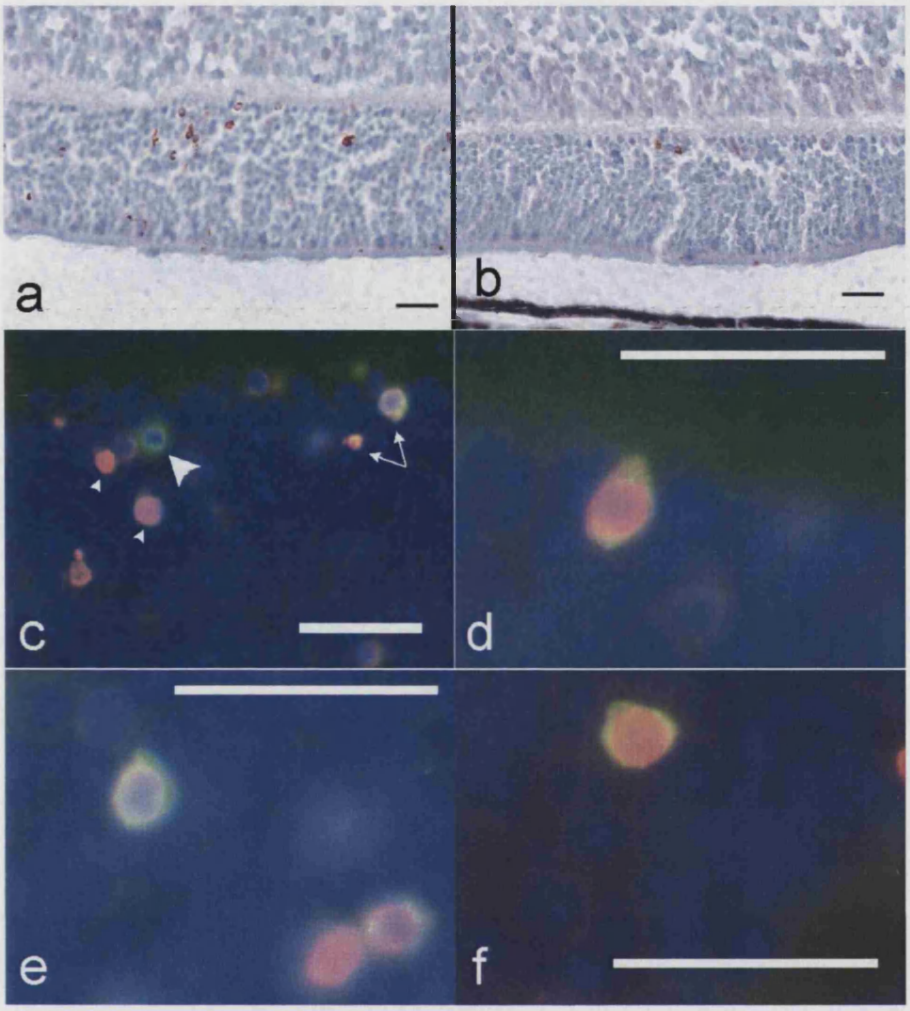

Figure 5.7 In accordance with the reduced TUNEL scoring of the ONL at P16 with minocycline treatment, photoreceptor expression of activated caspase 3 (brown cytoplasmic staining) was also markedly attenuated in minocycline-treated *rds* mice (a) compared with their untreated littermates (b). Two colour immunofluorescence for activated caspase 3 (green, cytoplasm) and TUNEL (red, nucleus) revealed that the great majority of TUNEL-positive photoreceptors also expressed activated caspase 3 and vice-versa (c, arrows and d-f). There were, however occasional photoreceptors positive only for caspase 3 (c, large arrowhead) or only for TUNEL (c, small arrowheads). Activated caspase 3 staining could occasionally be made out to be particularly intense in round cytoplasmic collections, possibly lysosomes (d, e). Counterstain: DAPI, scale bar: 20μm.

Minocycline treatment delays the microglial response

Minocycline-treated mice had a 52% reduction in sub-retinal microglial numbers at P16 (treated: 5.2 +/- 0.7, controls: 10.9 +/- 1.5, $p<0.01$. *Table 5.5 and figure 5.8*) and microglial numbers peaked later (P24) than in controls (P21). As was observed in earlier experiments (chapter three), in both treated and control groups microglial numbers peaked several days after the time of maximal photoreceptor apoptosis. Analysis of splenic sections showed no difference between minocycline-treated and control mice for F4/80 positivity.

Time Point	Sub-retinal microglia (F4/80) / 1.2 mm retina		
	Un-treated littermates	*Minocycline-treated*	
P16	**10.9** (+/- 1.5)	**5.2** (+/- 0.7)	p<0.01
P18	**8.7** (+/- 1.2)	**12.4** (+/- 1.9)	ns
P21	**16.4** (+/- 1.1)	**16.6** (+/- 0.6)	ns
P24	**6.2** (+/- 1.0)	**18.4** (+/- 3.4)	p<0.05
P27	**4.8** (+/- 0.8)	**6.6** (+/- 1.3)	ns

Table 5.5 Mean numbers of sub-retinal microglia in minocycline-treated and untreated control *rds* mice.

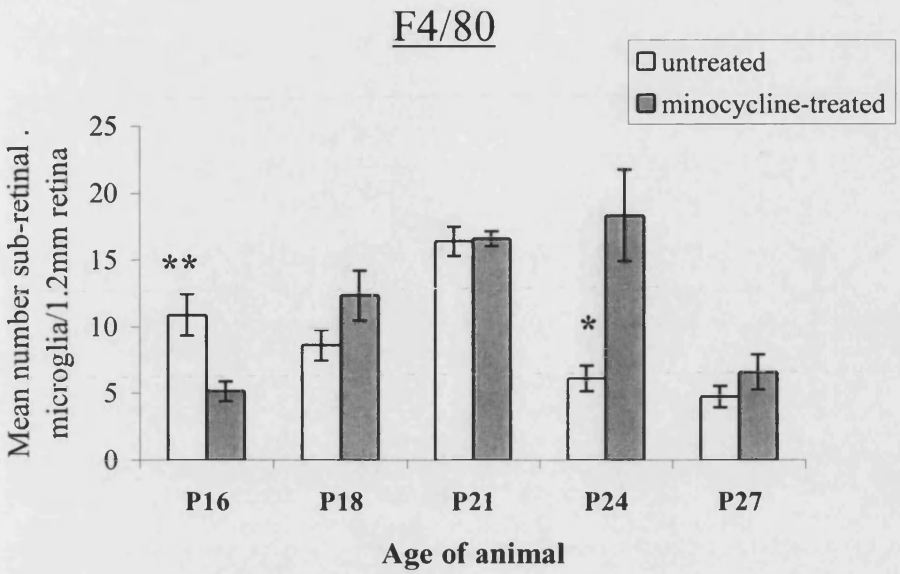

Figure 5.8. Minocycline treatment resulted in reduced sub-retinal microglial numbers at P16, and number peaked later (at P24) than in controls (at P21). Therefore minocycline appears to delay the microglial response, with delayed ingress and delayed egress. *$p<0.05$, **$p<0.01$

DISCUSSION

The beneficial effect of minocycline and its mechanism

Minocycline treatment appears to delay the onset of both photoreceptor apoptosis and microglial activation in this model of inherited photoreceptor degeneration, although there was no effect on the thickness of the outer nuclear layer at the end of the experiment (P27), indicating that photoreceptors were not ultimately saved.

The findings of the minocycline experiment may be explained by two hypotheses: either that minocycline treatment exerts a direct inhibitory effect on photoreceptor apoptosis, perhaps through an action on the caspase cascade or its regulators. This might result in less photoreceptor death and thereby lessen the stimulus for the microglial response to injury, accounting for the observed delay in microglial up-regulation. Alternatively minocycline treatment might suppress microglia directly and thereby reduce photoreceptor death from microglial cytotoxicity.

Three main points contradict the second hypothesis:

- As shown in chapter three and in the results presented here, microglial activity reaches a peak 3-5 days after the peak in photoreceptor apoptosis and 8 days after the time of reduced photoreceptor apoptosis with minocycline treatment. This temporal relationship is not consistent with a microglial role in photoreceptor apoptosis in the early stages of *rds* degeneration. Furthermore, if microglia were responsible for photoreceptor death, then we might expect that the delayed peak in microglial numbers seen following minocycline administration would be associated with a delayed peak in photoreceptor apoptosis. This is not the case – the peak is at P18 in both control and treatment groups.

- As shown in chapter three, no evidence of microglia-mediated oxidative damage can be found in *rds* retina.

- Most importantly, since the clodronate liposomes experiment (chapter four) revealed that an even greater reduction in microglial numbers at P16 than that seen following minocycline administration had no effect on photoreceptor apoptosis, it is unlikely that a direct effect on microglia accounts for the effects on photoreceptor apoptosis.

Therefore, the second hypothesis as a mechanism for minocycline-mediated delay in photoreceptor apoptosis may be rejected in this model. Clearly, rejection of the second hypothesis in this model does not exclude its applicability to other neurodegenerative models such as MPTP-induced Parkinson's disease in the mouse(Du et al. 2001).

A direct action of minocycline on apoptosis or its initiating mechanisms is supported (but not proven) by the observed reduction in caspase 3 activation seen after minocycline treatment, which almost exactly matched the profile of TUNEL positivity. Specific caspase 3 inhibitors such as Ac-DEVD-CHO have been tested in various models of retinal pathology. Yoshizawa *et al.* demonstrated in rats treated with the photoreceptor toxin N-Methyl N-nitrosurea (MNU, a direct acting alkylating agent), a 45% reduction in the extent of retinal damage, with significantly reduced photoreceptor death in those receiving concomitant intravitreal Ac-DEVD-CHO (Yoshizawa et al. 2000). Similar protection has been conferred, with the same caspase 3 inhibitor, on retinal ganglion cells after optic nerve transection (35%

protection)(Chaudhary et al. 1999) and inner nuclear layer neurons (60% protection) after retinal ischaemia(Katai and Yoshimura 1999). Other caspase inhibitors have also been employed intravitreally, including a broad spectrum peptidyl caspase inhibitor (YVAD-CMK) which protects inner retinal neurons from ischaemia-reperfusion injury and damage mediated by intravitreally injected excitotoxins(Lam et al. 1999; Lam et al. 1999).

The outcome has been somewhat different, however, when caspase inhibitors have been used to prevent photoreceptor death in models of inherited outer retinal degeneration. Intraperitoneally administered Ac-DEVD-CHO had only a transient effect in *rd* mice, with no amelioration of disease in the longer term(Yoshizawa et al. 2002) as was the case with intravitreal injection of the caspase 1 inhibitor, Ac-YVAD-CHO in RCS rats(Katai et al. 1999). An exception to this is a report of an irreversible caspase 3 inhibitor (z-DEVD-fmk) partially rescuing photoreceptors in transgenic rats with a rhodopsin mutation after a single intravitreal administration at P9(Liu et al. 1999). There was a sustained reduction in photoreceptor loss, such that by P20 when the ONL of untreated rats was one nucleus thick, it was four of five nuclei thick in those treated with the caspase 3 inhibitor mice at P20 (12 nuclei thick in wild types). The difference between these three studies may relate to the efficacy of the three drugs. Although all three are considered potent inhibitors of their target enzyme, Ac-DEVD-CHO and Ac-YVAD-CHO are reversible inhibitors, while z-DEVD-fmk is irreversible. Although the study on *rd* mice by Yoshizawa *et al* did treat the animals with alternate day intraperitoneal administration of Ac-DEVD-CHO over the ten day study period, it may be that with longer lasting insults arising from genetic disease, irreversible inhibition of caspase is required.

The success of caspase inhibitors to treat retinal disease is paralleled by their use in models of brain disease, such as the ALS mouse model(Li et al. 2000), the rat brain ischaemia model(Han et al. 2002; Mouw et al. 2002) and a mechanical spinal cord injury model(Li et al. 2000). Furthermore caspase 1 deficient mice are resistant to Huntington's disease and mechanical spinal cord injury(Ona et al. 1999; Li et al. 2000). So, since caspase inhibitors have similar neuroprotective effects to minocycline in similar brain models the proposed mechanism of action of minocycline through prevention of caspase activation (as discussed at the beginning of this chapter) seems plausible.

The transient delay in photoreceptor apoptosis in the *rds* mouse is disappointing when compared to the success seen following administration of minocycline in brain ischaemia models in which sustained protection from injury is seen(Yrjanheikki et al. 1999; Arvin et al. 2002). Both Yrjanheikki *et al* and Arvin *et al* demonstrated an impressive (70-76%) reduction in cortical infarct size after temporary occlusion of the internal carotid artery in rats treated with minocycline in comparison with untreated controls. As with the use of caspase inhibitors in models retinal disease, in which pathologies resulting from temporary insults respond better than genetic defects, minocycline has less profound effects in chronic degenerative brain models such as ALS and Huntington's disease, in which symptom onset is delayed and survival extended by only 10-14%(Chen et al. 2000; Zhu et al. 2002).

Perhaps the limited efficacy of minocycline for the treatment of inherited neuropathies should be expected, particularly if minocycline acts on the execution of apoptosis. It seems unlikely that apoptosis can be indefinitely held at bay by pharmacological means when the cellular injury is continuous. Any clinical neuroprotective benefit of drugs such as minocycline will probably be realised in

conditions featuring transient cellular insults, such as ishaemia, trauma and toxins. In these situations short term inhibition of apoptosis may be enough to protect cells until the stimulus has passed. The brain infarct/ischaemia models indicate that this might be the case. The penumbra surrounding the central zone of necrotic cell death in an infarct may be reduced in size following administration of apoptosis inhibitors(Friedlander 2003), indicating that cells in this region are not irreversibly damaged and may be 'rescued'.

In contrast genetic cellular lesions such as that seen in the photoreceptors of the *rds* mouse are less likely to be significantly improved by such treatment approaches. However, human outer retinal degenerations are rarely as severe as the *rds* phenotype, and it may be that more substantial and clinically relevant delay in disease progression would be conferred on human RP which progresses over decades rather than days. There would be important considerations, nevertheless, in contemplating chronic adminstration of a drug such as minocycline which has long term safety concerns including vestibular and gastro-intestinal disturbances, rashes and drug-induced autoimmune diseases such as systemic lupus erythematosis and hepatitis. There are, nonetheless, clinical trials in progress assessing the benefit of minocycline in patients with ALS and Huntington's disease, and no doubt trials of its efficacy in stroke will shortly follow.

CHAPTER SIX

GENERAL DISCUSSION

The primary goal of this project was to determine whether microglia exert a cytotoxic effect on photoreceptors in the *rds* model of inherited retinal degeneration. Although there is evidence in other neurodegenerative conditions that activation of microglia is detrimental and causes tissue damage, the findings of this research do not support this concept in the context of inherited retinal degeneration. This is the first detailed description of the relative temporal aspects of photoreceptor apoptosis and microglial numbers(Hughes et al. 2003). The chronological profiles of photoreceptor apoptosis, with a monophasic peak at P16-18; and microglial numbers and sub-retinal location, peaking several days later at around P21 are consistent with microglia responding to, rather than initiating photoreceptor apoptosis. In support of this is the absence of oxidative damage within *rds* mouse retina as demonstrated by the absence of iNOS and nitrotyrosine expression throughout the time course studied. In addition, the clodronate liposome experiment has shown that even a significant depletion of retinal microglia does not ameliorate photoreceptor apoptosis, as might be expected if these cells exerted a cytotoxic effect.

Microglia are clearly involved in the pathological processes of photoreceptor degeneration and as previously discussed, their phagocytic role has been demonstrated in several models of retinal degeneration(Sanyal 1972; Sanyal et al. 1980; Thanos 1992; Roque et al. 1996; Ng and Streilein 2001). Phagocytosis of photoreceptors undergoing apoptosis is probably crucial to the maintenance of tissue homeostasis and the prevention of release of noxious cell contents(Savill et al. 1993; Savill and Fadok

2000). Indeed, it could be argued that any potential photoreceptor salvage with clodronate liposomes-mediated microglial depletion might be counteracted by the detrimental results of inadequate apoptotic cell clearance. This does, however, become a somewhat circular argument, since if microglia were responsible for photoreceptor death, their depletion would lead to fewer apoptotic cells and less demand for phagocytic clear-up. Nevertheless, three distinct findings presented in this thesis argue against microglia cytotoxicity in photoreceptor degeneration, and in concert provide strong evidence against this role in the *rds* mouse model.

The possibility that microglia might in fact exert a protective influence on photoreceptors during retinal degeneration has been suggested by findings in this project. The slight increase in photoreceptor apoptosis at P21 after clodronate liposomes-induced retinal microglial depletion, suggests that the ingress of microglia to the outer retinal layers is in some way responsible for the slowing of photoreceptor loss. In other words, without the microglial response, photoreceptor apoptosis might proceed unchecked at the rate seen at P16-P18 until all photoreceptors were lost by P40. Unfortunately this experiment was methodologically flawed (lack of sibling controls), but this should be an area of further study and in the first instance, the experiment should be repeated with the same design except that untreated littermates should be used as controls.

Sialoadhesin

The expression of sialoadhesin on microglia during the peak of microglial activity is an interesting finding. Since the function of sialoadhesin is still not fully defined, the importance of its presence is uncertain but it may imply blood-retinal barrier

breakdown which has implications for future sub-retinal gene therapeutic strategies where evasion of systemic immune responses is of utmost importance. Furthermore, the observation that sialoadhesin-expressing cells seem to arise from the inner retinal layers in which retinal blood vessels are located, and from the vessels of the optic nerve head suggests that they represent a population of cells recruited from the systemic circulation. Weight is added to this notion by the clodronate liposomes experiments which, as discussed, appeared to prevent recruitment of myeloid cells and were particularly effective in eradicating sialoadhesin-positive microglia from the retina.

Macrophage depletion

Liposomal clodronate is clearly a very valuable research tool in the evaluation of macrophages and microglia and its use in this model served the intended purpose of determining the effect of profoundly reduced microglial numbers on photoreceptor apoptosis. The ability of the drug to markedly reduce retinal microglial numbers through prevention of recruitment provides valuable information about microglial biology: namely that a microglial response to photoreceptor injury involves both proliferation and recruitment from blood, with recruitment appearing to be the most important in terms of numbers produced. Microglia were not completely eradicated, and it may be argued that a 60-65% reduction in microglial numbers may not impair cytotoxicity to the same extent if the remaining microglia were capable of up-regulating their production of noxious mediators. However, in models of CNS inflammatory disease microglial/macrophage depletion (but not eradication) with clodronate liposomes has had beneficial effects on extent of tissue damage and clinical

parameters, indicating that a reduction in their numbers has a significant effect on macrophage and microglial functionality during disease states(Bauer et al. 1995; Forrester et al. 1998; Tran et al. 1998).

CD200

Another potential method for determining the role of microglia in photoreceptor degeneration would be to deliver an activating or disinhibiting signal and observe the effect on the progress of the retinal degeneration. As discussed in chapter one, the CD200-R is a myeloid-restricted cell surface receptor, whose ligand (CD200), expressed on lymphocytes, endothelium and neurons, has an inhibitory effect on macrophages and microglia and serves to dampen down and regulate myeloid cell activation. CD200 knockout mice have a constitutive level of microglial activation and accelerated CNS inflammatory disease(Hoek et al. 2000; Broderick et al. 2002). Back-crossing of CD200 knockout C57/Bl6 mice with *rds* mice is currently being undertaken at the Institute of Ophthalmology, London. With this back-cross, it will be possible to observe the effect of deregulated and exaggerated microglial function on photoreceptor degeneration. However, since constitutive iNOS expression appears to be a feature of $CD200^{-/-}$ microglia, it may be that the activation profile of microglia in this mouse may sway more towards the 'classical' type than the 'alternative' type seen in $CD200^{+/+}$ *rds* mouse (see chapter3, discussion).

The location of apoptotic photoreceptors

The observation that the majority of apoptotic photoreceptors nuclei are located in the inner part of the ONL is not, as far as I am aware, a finding published by other research groups. This phenomenon may have relevance to the mechanisms underlying photoreceptor death and therefore merits further investigation. Formal assessment of this in different animal models of photoreceptor degeneration would indicate whether this is characteristic of a peripherin mutation alone, or represents a broader susceptibility of centripetal photoreceptors regardless of genetic defect. The possible reasons for enhanced susceptibility to apoptosis in this location were discussed in chapter 3, and an oxygen gradient from the choroid may be a factor with centripetal photoreceptors occupying a watershed position between the inner retinal circulation and the choriocapillaris. Therefore experiments similar to those used by Mervin and Stone, with the effect of oxygen levels set at 21% (normoxic), 10 or 11% (hypoxic) or 70% (hyperoxic) on the rate of photoreceptor apoptosis observed(Mervin and Stone 2002), may provide insight into the cause of this phenomenon.

The signal for microglial activation and migration

Several things remain unclear about microglial biology in retinal degeneration. It has been proposed that the recognition and phagocytosis of an apoptotic cell by macrophages requires cell-cell contact via receptors for ligands expressed on apoptotic cells such phosphatidyl serine and exposed sugars, yet in the absence of degeneration, microglia reside in the inner retinal layers, well away from the photoreceptors. What then is the signal for microglial migration? Although not assessed during this work,

some investigators have found that microglial activation occurs prior to neuronal apoptosis, during the stage of neuronal dysfunction(Boillee et al. 2001). A diffusible chemotactic factor released by injured, pre-apoptotic neurons seems likely and fractalkine(Harrison et al. 1998), IL6(Streit et al. 2000) and monocyte chemoattractant protein 3(Zhang 2003) have been studied in rodents and found to have a possible role in microglial recruitment.

This would be another interesting area of further study. Using the techniques outlined in this study, it would be interesting to analyse microglial activation between P3 and P10 in both *rds* and wild type mice in order to determine whether microglial behaviour (i.e. migration to the sub-retinal space) in *rds* mice diverges from the normal prior to the wave of photoreceptor apoptosis. If this is the case then it can be assumed that pre-apoptotic signalling is occuring to attract microglia to the ONL. Further investigation of the chemoattractants involved would also be desirable. This might include a comparison between *rds* and wild types of the quantities of chemokines such as macrophage chemoattractant protein by ELISA of homogenised retina. If raised levels of chemokines are found in *rds* retina, then the next step would be to determine whether there is production of these within photoreceptors or nearby cells. This might be done by three methods; in situ hybridisation on retinal sections, isolation of photoreceptors and rt-PCR, demonstrating (by ELISA of supernatant) the release of chemokines by a photoreceptor cell line in culture after stressing stimuli.

In this project me have demonstrated that the increased number of microglia seen in the *rds* mouse retina are generated by both *in situ* proliferation and recruitment from the systemic pool, but the eventual fate of microglia is unclear. Retinal microglial numbers declined rapidly after P21 in line with the reduced rate of

photoreceptor apoptosis, yet very few apoptotic microglia were found at P16 and P21. From these studies me cannot exclude that at later time points, when microglial numbers are on the decline, apoptotic microglia would be found, but this was not investigated. Alternatively, rather than dying *in situ*, microglia may migrate from the retina either into the blood via the retinal or choroidal circulation, or to regional lymph nodes. Since there is a lack of conventional lymphatic drainage from the internal ocular structures(Perry 1998; Streilein 2003), the blood stream route seems more likely. In view of the possible immunoregulatory role of microglia (induced in macrophages by ingestion of apoptotic cells(Fadok et al. 1998; Barker et al. 1999)), this migration (if it existed) with potential subsequent contact with cells of the adaptive immune system, might serve to regulate T cell responses against self antigens exposed by blood-retinal barrier breakdown, or against 'neo-autoantigens' created by the cleavage of cellular proteins during apoptosis.

Minocycline

The effect of minocycline administration on the progress of *rds* photoreceptor degeneration was interesting because it was able to delay photoreceptor apoptosis, but disappointing because the delay was brief, with no long term beneficial effect in terms of photoreceptor loss. More benefit may be realised from minocycline treatment in conditions such as retinal ischaemia and toxic injury, as has been found with specific caspase inhibitors, with which significant retinal neuronal rescue has been achieved after such transient insults. Retinal ischaemia may be induced in rats by raising the intraocular pressure to 110mmHg for 60 minutes using a needle introduced to the anterior chamber and connected to a saline column(Katai and Yoshimura 1999; Lam et

al. 1999). The effect of intraperitoneal minocycline treatment during and after ischaemia on the rate of apoptosis of retinal ganglion cells would easily be observed by immunohistochemical TUNEL techniques and subsequently functional benefits may be estimated by visually evoked cerebral potentials.

Further mechanistic information about the neuroprotective effect of minocycline would also be desirable. Levels of caspases 1, 3 and 8, cytochrome c and both full-length and cleaved Bid in ganglion cells could be detected immunohistochemically on retinal sections and by western blotting of retinal cytosolic fractions(Jomary et al. 2001; Zhu et al. 2002) (see *figure 5.1*). Should significant rescue of retinal ganglion cells and retinal function occur with minocycline, then a case would be made for the short-term use of this agent during and after retinal ischaemic events in patients, avoiding the potential problems of chronic administration of minocycline (chapter 5, discussion).

The question remains to be answered, whether pharmacological treatment is ever likely benefit patients with inherited photoreceptor degenerations. This will no doubt depend upon the genetic mutation, as exemplified by the *rd* mouse, whose phosphodiesterase mutation with subsequent continual opening of the cGMP gated cation channel, may be amenable to effective treatment with calcium channel blockers already in clinical use for cardiovascular conditions(Frasson et al. 1999). However the majority of mutations underlying human photoreceptor degeneration do not have such simple mechanistic rationale for photoreceptor death and dysfunction, and until the unclear pathways from genetic miscoding to apoptosis are elucidated, pharmacological intervention is likely only to delay, rather than prevent disease progression. Most RP

patients see perfectly well in their youth, only to slowly lose sight later. The implication is that despite their genetic mutation, the photoreceptors initially survive and perform their function of phototransduction, but, after a variable period succumb to apoptosis. Perhaps with greater trophic support from growth factors, these photoreceptors could be encouraged to survive and function past their predestined time of demise. For example Brain-derived Neurotrophic Factor (BDNF) and Ciliary Neurotrophic Factor (CNTF) have both been shown to prolong the survival of degenerative photoreceptors(LaVail et al. 1998; Caffe et al. 2001; Liang et al. 2001; Okoye et al. 2003), yet surprisingly neurotrophin receptors (tyrosine kinase receptors: TrkA, B, C and the $p75^{NTR}$) are thought to be absent from photoreceptors themselves in rodents(Ugolini et al. 1995; Harada et al. 2000; Harada et al. 2002).

Work by Harada *et al.* has unravelled some of the complexities of the provision of trophic support by Müller cells to the outer retina. They found that in light induced photoreceptor degeneration in rats, expression of the TrkC and $p75^{NTR}$ neurotrophin receptors are up-regulated on different parts of Müller cells, with TrkC localising to the inner retinal aspect and $p75^{NTR}$ to the outer retina in and around the ONL. Blockade of the $p75^{NTR}$ led to increased bFGF production by Müller cells and protected photoreceptors from light-induced apoptosis. In addition $p75^{NTR}$ knockout mice were similarly protected against light damage. Conversely, blockade of TrkC led to reduced bFGF production and enhanced photoreceptor death, demonstrating that Müller cells have the ability, through the production of growth factors such as bFGF and regulated by neurotrophins, to determine photoreceptor survival in pathological conditions(Harada et al. 2000). More recent work by these authors has demonstrated that microglia, through the production of neurotrophins including Nerve Growth Factor (NGF) and neurotrophin 3 (NT-3) may be the regulators of Müller cell bFGF

release. Indeed, medium from cultures of retinal microglia from light-reared animals led to a significant reduction in Müller cell bFGF production, an effect that could be blocked by anti $p75^{NTR}$ antibodies but not by Trk blockers(Harada et al. 2002) implying that NGF was the factor responsible for inhibition of bFGF release. Paradoxically, exogenous NT-3 was shown to increase Müller cell bFGF production through Trk receptors, so while microglia in light-reared animals produced increased levels of a variety of neurotrophins (including both NT-3 and NGF), the overall effect on photoreceptors, may ultimately be dictated by the differential up-regulation of neurotrophin receptors on different parts of Müller cells. Clearly the complexities of these microglial-glial interactions need to be unravelled further before concrete conclusions about the relative protective or damaging effects of this interplay can be made, but therapeutic options for promoting photoreceptor survival are increasing as this line of research progresses.

APPENDIX

ANATOMY OF THE POSTERIOR SEGMENT OF THE EYE

Human Anatomy

The posterior segment of the eye consists of the wall of the globe and its contents, posterior to the lens, overall comprising 4/5 the volume of the eye (*figure A.1*).

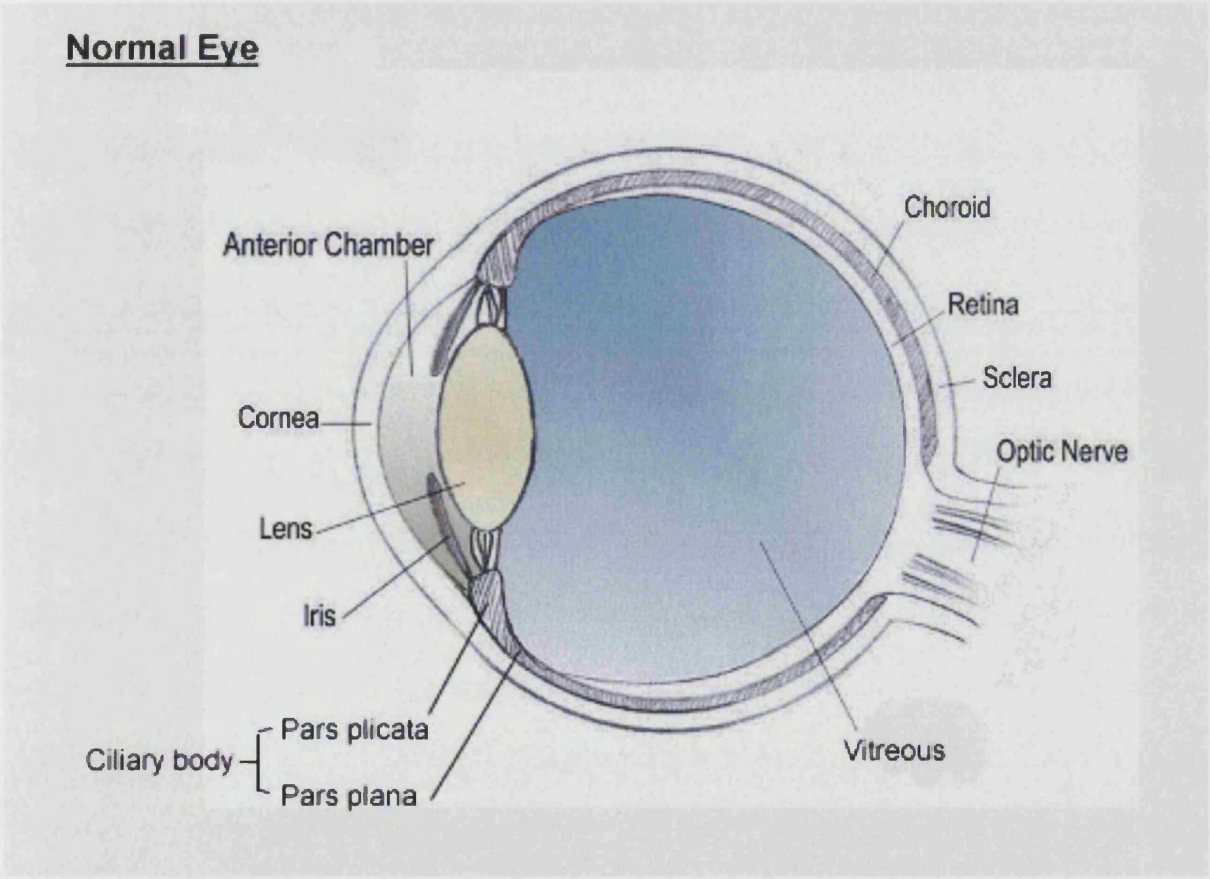

Figure A.1 Schematic depiction of the anatomy of the human eye (not to scale). Artist: Geraldine Murphy.

The outer layer of the wall is the sclera; a tough, collagenous and largely acellular protective coat that overlies the choroid posteriorly and ciliary body anteriorly. The

choroid is highly vascular and possesses a capillary network (choriocapillaris) serving the metabolic demands of the adjacent outer retina. The ciliary body is composed of two continuous segments: the pars plana, which is a direct continuation of the choroid, and the pars plicata which is responsible for the anchoring of the lens and the production of the aqeous humour that bathes the anterior segment. The retina lies between the inner-most layer of the choroid (the retinal pigment epithelium) and the vitreous gel which fills the posterior segment. The retinal pigment epithelium is involved in the recycling of visual pigments and its tight junctions form the outer blood-retinal barrier.

The retina

The retina is a thin layer of nervous tissue with a surface area of about 266mm^2 (Bron 1997). It is approximately 0.5mm thick around the optic nerve, gradually thinning to 0.1mm at the extreme periphery (ora serrata) where it meets the pars plana of the ciliary body. The neurons of the retina are organized into discreet layers with the photoreceptors outermost (in contact with the retinal pigment epithelium) and the ganglion cells and nerve fibre layer innermost (*figure A.2*). The centre of the retina is termed the macula where the densest population of cone photoreceptors (responsible for colour vision and fine visual discrimination) is found. This 3 mm^2 area corresponds to the area at the centre of the visual field which is responsible for fine visual discrimination and colour vision. At the centre of the macula lies the fovea which is occupied exclusively by cone photoreceptors. Damage to this area has profound impact on visual acuity. More peripherally the photoreceptors are predominantly rods providing visual field, motion detection and night vision.

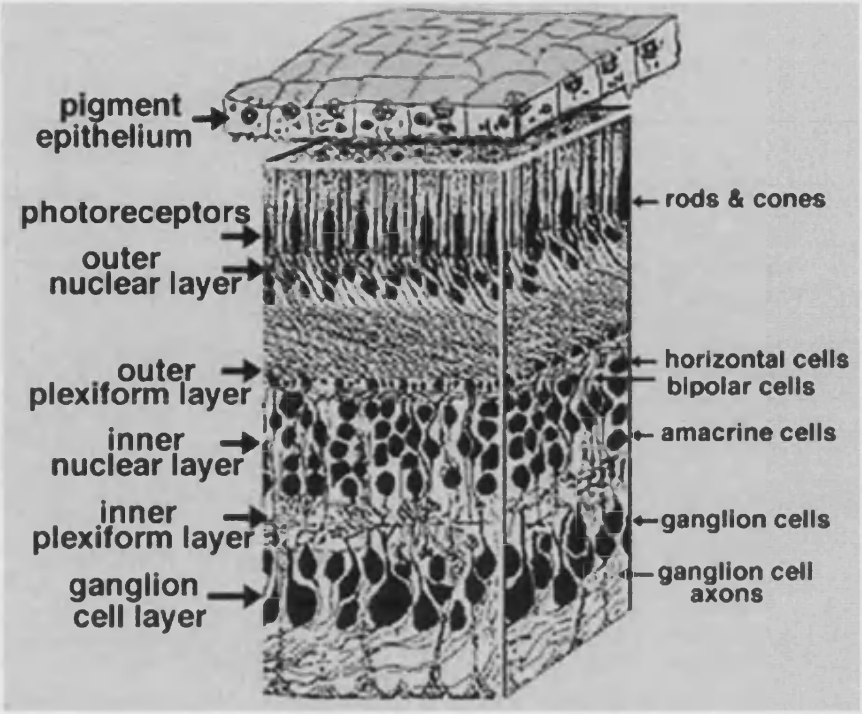

Figure A.2 Schematic depiction of retinal neuronal anatomic relationships. Uppermost in the picture is the retinal pigment epithelium, which is the innermost part of the choroid and forms the outer blood-retinal barrier. The adjacent photoreceptors, whose cell bodies reside in the outer nuclear layer, synapse with bipolar cells which make synaptic contact with several different cell types including ganglion cells (vertical transmission), and horizontal and amacrine cells (horizontal neuronal processing).

The vasculature of the retina stems from the central retinal artery (a branch of the ophthalmic artery), and drains via the central retinal vein. These enter and leave the eye via the optic nerve and divide within the optic nerve head to form four major arcades: superotemporal, superonasal, inferotemporal and inferonasal. These vessels branch out on the surface of the retina and within the nerve fibre layer before penetrating the inner retina to form capillary complexes serving the inner half of the retina, the outer half being served by the choriocapillaris. The central 0.35mm of the

retina is avascular (foveal avascular zone). Tight endothelial junctions in the retinal capillaries form the inner blood retinal barrier.

Mouse Ocular Anatomy

Subtle differences exist between mice and humans in the anatomy of the posterior segment. The first, and most obvious is that owing to the increased proportions of the mouse lens (relative to the rest of the eye), the vitreous cavity occupies a smaller percentage of the eye contents. The retina of the mouse is far more rod-dominated than in humans with rod photoreceptors outnumbering cones even at the centre of the retina although there is a relative increase in cone density centrally(Jeon 1998). Although the mouse does not possess a foveal pit, there is a concentration of cones around the centre of the retina, although not as exaggerated as in the human. All the other cell types seen in human retinas, including bipolar horizontal, amacrine, ganglion and Müller cells are also represented in the mouse.

REFERENCES

Abler, A. S., C. J. Chang, et al. (1996). Photic injury triggers apoptosis of photoreceptor cells. Res Commun Mol Pathol Pharmacol **92**(2), 177-89.

Aiello, S., M. Noris, et al. (2000). Thymic dendritic cells express inducible nitric oxide synthase and generate nitric oxide in response to self- and alloantigens. J Immunol **164**(9), 4649-58.

Ali, R. R., M. B. Reichel, et al. (1998). Absence of p53 delays apoptotic photoreceptor cell death in the rds mouse. Curr Eye Res **17**(9), 917-23.

Aloisi, F. (2001). Immune function of microglia. Glia **36**(2), 165-79.

Aloisi, F., F. Ria, et al. (1999). Relative efficiency of microglia, astrocytes, dendritic cells and B cells in naive CD4+ T cell priming and Th1/Th2 cell restimulation. Eur J Immunol **29**(9), 2705-14.

Aloisi, F., F. Ria, et al. (1998). Microglia are more efficient than astrocytes in antigen processing and in Th1 but not Th2 cell activation. J Immunol **160**(10), 4671-80.

Araki, E., C. Forster, et al. (2001). Cyclooxygenase-2 inhibitor ns-398 protects neuronal cultures from lipopolysaccharide-induced neurotoxicity. Stroke **32**(10), 2370-5.

Arvin, K. L., B. H. Han, et al. (2002). Minocycline markedly protects the neonatal brain against hypoxic-ischemic injury. Ann Neurol **52**(1), 54-61.

Ashcroft, A. J., F. E. Davies, et al. (2003). Aetiology of bone disease and the role of bisphosphonates in multiple myeloma. Lancet Oncol **4**(5), 284-92.

Austyn, J. M. and S. Gordon (1981). F4/80, a monoclonal antibody directed specifically against the mouse macrophage. Eur J Immunol **11**(10), 805-15.

Baatz, H., J. Puchta, et al. (2001). Macrophage depletion prevents leukocyte adhesion and disease induction in experimental melanin-protein induced uveitis. Exp Eye Res **73**(1), 101-9.

Barker, R. N., L. Erwig, et al. (1999). Differential effects of necrotic or apoptotic cell uptake on antigen presentation by macrophages. Pathobiology **67**(5-6), 302-5.

Bauer, J., I. Huitinga, et al. (1995). The role of macrophages, perivascular cells, and microglial cells in the pathogenesis of experimental autoimmune encephalomyelitis. Glia **15**(4), 437-46.

Becher, B. and J. P. Antel (1996). Comparison of phenotypic and functional properties of immediately ex vivo and cultured human adult microglia. Glia **18**(1), 1-10.

Bettelli, E., M. P. Das, et al. (1998). IL-10 is critical in the regulation of autoimmune encephalomyelitis as demonstrated by studies of IL-10- and IL-4-deficient and transgenic mice. J Immunol **161**(7), 3299-306.

Biewenga, J., M. B. van der Ende, et al. (1995). Macrophage depletion in the rat after intraperitoneal administration of liposome-encapsulated clodronate: depletion kinetics and accelerated repopulation of peritoneal and omental macrophages by administration of Freund's adjuvant. Cell Tissue Res **280**(1), 189-96.

Bird, A. C. (1995). Retinal photoreceptor dystrophies LI. Edward Jackson Memorial Lecture. Am J Ophthalmol **119**(5), 543-62.

Boillee, S., L. Viala, et al. (2001). Differential microglial response to progressive neurodegeneration in the murine mutant Wobbler. Glia **33**(4), 277-87.

Boje, K. M. and P. K. Arora (1992). Microglial-produced nitric oxide and reactive nitrogen oxides mediate neuronal cell death. Brain Res **587**(2), 250-6.

Broderick, C., L. Duncan, et al. (2000). IFN-gamma and LPS-mediated IL-10-dependent suppression of retinal microglial activation. Invest Ophthalmol Vis Sci **41**(9), 2613-22.

Broderick, C., R. M. Hoek, et al. (2002). Constitutive retinal CD200 expression regulates resident microglia and activation state of inflammatory cells during experimental autoimmune uveoretinitis. Am J Pathol **161**(5), 1669-77.

Brogden, R. N., T. M. Speight, et al. (1975). Minocycline: A review of its antibacterial and pharmacokinetic properties and therapeutic use. Drugs **9**(4), 251-91.

Bron, A. J., Tripathi, R.C., Tripathi, B.J. (1997). Wolff's Anatomy of the Eye and Orbit. London, Chapman and Hall.

Bronstein, D. M., I. Perez-Otano, et al. (1995). Glia-dependent neurotoxicity and neuroprotection in mesencephalic cultures. Brain Res **704**(1), 112-6.

Brown, D. R. (2001). Microglia and prion disease. Microsc Res Tech **54**(2), 71-80.

Brune, B., A. von Knethen, et al. (1999). Nitric oxide (NO): an effector of apoptosis. Cell Death Differ **6**(10), 969-75.

Budd, S. L. and S. A. Lipton (1998). Calcium tsunamis: do astrocytes transmit cell death messages via gap junctions during ischemia? Nat Neurosci **1**(6), 431-2.

Bunker, C. H., E. L. Berson, et al. (1984). Prevalence of retinitis pigmentosa in Maine. Am J Ophthalmol **97**(3), 357-65.

Caffe, A. R., A. K. Soderpalm, et al. (2001). A combination of CNTF and BDNF rescues rd photoreceptors but changes rod differentiation in the presence of RPE in retinal explants. Invest Ophthalmol Vis Sci **42**(1), 275-82.

Celis, J. E., P. Madsen, et al. (1987). Cyclin (PCNA, auxiliary protein of DNA polymerase delta) is a central component of the pathway(s) leading to DNA replication and cell division. FEBS Lett **220**(1), 1-7.

Chang, G. Q., Y. Hao, et al. (1993). Apoptosis: final common pathway of photoreceptor death in rd, rds, and rhodopsin mutant mice. Neuron **11**(4), 595-605.

Chao, C. C., S. Hu, et al. (1995). Interleukin-1 and tumor necrosis factor-alpha synergistically mediate neurotoxicity: involvement of nitric oxide and of N-methyl-D-aspartate receptors. Brain Behav Immun **9**(4), 355-65.

Chaudhary, P., F. Ahmed, et al. (1999). Caspase inhibitors block the retinal ganglion cell death following optic nerve transection. Brain Res Mol Brain Res **67**(1), 36-45.

Chen, M., V. O. Ona, et al. (2000). Minocycline inhibits caspase-1 and caspase-3 expression and delays mortality in a transgenic mouse model of Huntington disease. Nat Med **6**(7), 797-801.

Cheung, D. O., K. Halsey, et al. (2000). Role of pulmonary alveolar macrophages in defense of the lung against Pseudomonas aeruginosa. Infect Immun **68**(8), 4585-92.

Clarke, G., R. A. Collins, et al. (2000). A one-hit model of cell death in inherited neuronal degenerations. Nature **406**(6792), 195-9.

Clarke, G., A. F. Goldberg, et al. (2000). Rom-1 is required for rod photoreceptor viability and the regulation of disk morphogenesis. Nat Genet **25**(1), 67-73.

Colton, C. A., J. Yao, et al. (1992). Regulation of microglial function by interferons. J Neuroimmunol **40**(1), 89-98.

Connell, G., R. Bascom, et al. (1991). Photoreceptor peripherin is the normal product of the gene responsible for retinal degeneration in the rds mouse. Proc Natl Acad Sci U S A **88**(3), 723-6.

Crocker, P. R. and S. Gordon (1986). Properties and distribution of a lectin-like hemagglutinin differentially expressed by murine stromal tissue macrophages. J Exp Med **164**(6), 1862-75.

Crocker, P. R., M. Hill, et al. (1988). Regulation of a murine macrophage haemagglutinin (sheep erythrocyte receptor) by a species-restricted serum factor. Immunology **65**(4), 515-22.

Cua, D. J. and S. A. Stohlman (1997). In vivo effects of T helper cell type 2 cytokines on macrophage antigen-presenting cell induction of T helper subsets. J Immunol **159**(12), 5834-40.

Danciger, M., J. Blaney, et al. (1995). Mutations in the PDE6B gene in autosomal recessive retinitis pigmentosa. Genomics **30**(1), 1-7.

Danton, G. H. and W. D. Dietrich (2003). Inflammatory mechanisms after ischemia and stroke. J Neuropathol Exp Neurol **62**(2), 127-36.

De La Rosa, G., N. Longo, et al. (2003). Migration of human blood dendritic cells across endothelial cell monolayers: adhesion molecules and chemokines involved in subset-specific transmigration. J Leukoc Biol **73**(5), 639-49.

De Simone, R., A. Giampaolo, et al. (1995). The costimulatory molecule B7 is expressed on human microglia in culture and in multiple sclerosis acute lesions. J Neuropathol Exp Neurol **54**(2), 175-87.

Dehmer, T., J. Lindenau, et al. (2000). Deficiency of inducible nitric oxide synthase protects against MPTP toxicity in vivo. J Neurochem **74**(5), 2213-6.

Delemarre, F. G., N. Kors, et al. (1990). Repopulation of macrophages in popliteal lymph nodes of mice after liposome-mediated depletion. J Leukoc Biol **47**(3), 251-7.

Demant, P., D. Ivanyi, et al. (1979). The map position of the rds gene on the 17th chromosome of the mouse. Tissue Antigens **13**(1), 53-5.

Diamond, M. S., D. E. Staunton, et al. (1990). ICAM-1 (CD54): a counter-receptor for Mac-1 (CD11b/CD18). J Cell Biol **111**(6 Pt 2), 3129-39.

Dick, A. D. (1999). Immune regulation of uveoretinal inflammation. Dev Ophthalmol **30**, 187-202.

Dick, A. D., M. Pell, et al. (1997). Direct ex vivo flow cytometric analysis of human microglial cell CD4 expression: examination of central nervous system biopsy specimens from HIV-seropositive patients and patients with other neurological disease. Aids **11**(14), 1699-708.

Dryja, T. P., J. T. Finn, et al. (1995). Mutations in the gene encoding the alpha subunit of the rod cGMP-gated channel in autosomal recessive retinitis pigmentosa. Proc Natl Acad Sci U S A **92**(22), 10177-81.

Dryja, T. P., J. A. McEvoy, et al. (2000). Novel rhodopsin mutations Gly114Val and Gln184Pro in dominant retinitis pigmentosa. Invest Ophthalmol Vis Sci **41**(10), 3124-7.

Dryja, T. P., T. L. McGee, et al. (1990). A point mutation of the rhodopsin gene in one form of retinitis pigmentosa. Nature **343**(6256), 364-6.

Du, Y., Z. Ma, et al. (2001). Minocycline prevents nigrostriatal dopaminergic neurodegeneration in the MPTP model of Parkinson's disease. Proc Natl Acad Sci U S A **98**(25), 14669-74.

Essner, E. and G. Gorrin (1979). An electron microscopic study of macrophages in rats with inherited retinal dystrophy. Invest Ophthalmol Vis Sci **18**(1), 11-25.

Fadok, V. A., D. L. Bratton, et al. (2001). Phagocyte receptors for apoptotic cells: recognition, uptake, and consequences. J Clin Invest **108**(7), 957-62.

Fadok, V. A., D. L. Bratton, et al. (1998). Macrophages that have ingested apoptotic cells in vitro inhibit proinflammatory cytokine production through autocrine/paracrine mechanisms involving TGF-beta, PGE2, and PAF. J Clin Invest **101**(4), 890-8.

Fadok, V. A., J. S. Savill, et al. (1992). Different populations of macrophages use either the vitronectin receptor or the phosphatidylserine receptor to recognize and remove apoptotic cells. J Immunol **149**(12), 4029-35.

Fain, G. L. and J. E. Lisman (1993). Photoreceptor degeneration in vitamin A deprivation and retinitis pigmentosa: the equivalent light hypothesis. Exp Eye Res **57**(3), 335-40.

Farber, D. B. and R. N. Lolley (1974). Cyclic guanosine monophosphate: elevation in degenerating photoreceptor cells of the C3H mouse retina. Science **186**(4162), 449-51.

Farrar, G. J., P. Kenna, et al. (1991). A three-base-pair deletion in the peripherin-RDS gene in one form of retinitis pigmentosa. Nature **354**(6353), 478-80.

Fishman, G. A., J. Cunha-Vaz, et al. (1981). Vitreous fluorophotometry in patients with retinitis pigmentosa. Arch Ophthalmol **99**(7), 1202-7.

Ford, A. L., E. Foulcher, et al. (1996). Microglia induce CD4 T lymphocyte final effector function and death. J Exp Med **184**(5), 1737-45.

Forrester, J. V., I. Huitinga, et al. (1998). Marrow-derived activated macrophages are required during the effector phase of experimental autoimmune uveoretinitis in rats. Curr Eye Res **17**(4), 426-37.

Frasson, M., J. A. Sahel, et al. (1999). Retinitis pigmentosa: rod photoreceptor rescue by a calcium-channel blocker in the rd mouse. Nat Med **5**(10), 1183-7.

Frei, K., H. Lins, et al. (1994). Antigen presentation in the central nervous system. The inhibitory effect of IL-10 on MHC class II expression and production of cytokines depends on the inducing signals and the type of cell analyzed. J Immunol **152**(6), 2720-8.

Friedlander, R. M. (2003). Apoptosis and caspases in neurodegenerative diseases. N Engl J Med **348**(14), 1365-75.

Geijtenbeek, T. B., P. C. Groot, et al. (2002). Marginal zone macrophages express a murine homologue of DC-SIGN that captures blood-borne antigens in vivo. Blood **100**(8), 2908-16.

Gerritse, K., J. D. Laman, et al. (1996). CD40-CD40 ligand interactions in experimental allergic encephalomyelitis and multiple sclerosis. Proc Natl Acad Sci U S A **93**(6), 2499-504.

Giulian, D. (1999). Microglia and the immune pathology of Alzheimer disease. Am J Hum Genet **65**(1), 13-8.

Giulian, D., T. J. Baker, et al. (1986). Interleukin 1 of the central nervous system is produced by ameboid microglia. J Exp Med **164**(2), 594-604.

Giulian, D., J. Chen, et al. (1989). The role of mononuclear phagocytes in wound healing after traumatic injury to adult mammalian brain. J Neurosci **9**(12), 4416-29.

Giulian, D., L. J. Haverkamp, et al. (1995). Senile plaques stimulate microglia to release a neurotoxin found in Alzheimer brain. Neurochem Int **27**(1), 119-37.

Giulian, D., J. Woodward, et al. (1988). Interleukin-1 injected into mammalian brain stimulates astrogliosis and neovascularization. J Neurosci **8**(7), 2485-90.

Giulian, D., D. G. Young, et al. (1988). Interleukin-1 is an astroglial growth factor in the developing brain. J Neurosci **8**(2), 709-14.

Goerdt, S. and C. E. Orfanos (1999). Other functions, other genes: alternative activation of antigen-presenting cells. Immunity **10**(2), 137-42.

Gordon, S. (2002). Pattern recognition receptors: doubling up for the innate immune response. Cell **111**(7), 927-30.

Gordon, S. (2003). Alternative activation of macrophages. Nat Rev Immunol **3**(1), 23-35.

Goureau, O., F. Regnier-Ricard, et al. (1999). Requirement for nitric oxide in retinal neuronal cell death induced by activated Muller glial cells. J Neurochem **72**(6), 2506-15.

Graeber, M. B., W. J. Streit, et al. (1988). Axotomy of the rat facial nerve leads to increased CR3 complement receptor expression by activated microglial cells. J Neurosci Res **21**(1), 18-24.

Graeber, M. B., W. Tetzlaff, et al. (1988). Microglial cells but not astrocytes undergo mitosis following rat facial nerve axotomy. Neurosci Lett **85**(3), 317-21.

Gupta, N., K. E. Brown, et al. (2003). Activated microglia in human retinitis pigmentosa, late-onset retinal degeneration, and age-related macular degeneration. Exp Eye Res **76**(4), 463-71.

Hafezi, F., A. Marti, et al. (1997). Light-induced apoptosis: differential timing in the retina and pigment epithelium. Exp Eye Res **64**(6), 963-70.

Haim, M., N. V. Holm, et al. (1992). Prevalence of retinitis pigmentosa and allied disorders in Denmark. I Main results. Acta Ophthalmol (Copenh) **70**(2), 178-86.

Han, B. H., D. Xu, et al. (2002). Selective, reversible caspase-3 inhibitor is neuroprotective and reveals distinct pathways of cell death after neonatal hypoxic-ischemic brain injury. J Biol Chem **277**(33), 30128-36.

Harada, T., C. Harada, et al. (2002). Microglia-Muller glia cell interactions control neurotrophic factor production during light-induced retinal degeneration. J Neurosci **22**(21), 9228-36.

Harada, T., C. Harada, et al. (2000). Modification of glial-neuronal cell interactions prevents photoreceptor apoptosis during light-induced retinal degeneration. Neuron **26**(2), 533-41.

Harrison, J. K., Y. Jiang, et al. (1998). Role for neuronally derived fractalkine in mediating interactions between neurons and CX3CR1-expressing microglia. Proc Natl Acad Sci U S A **95**(18), 10896-901.

Hart, D. N. and J. W. Fabre (1981). Demonstration and characterization of Ia-positive dendritic cells in the interstitial connective tissues of rat heart and other tissues, but not brain. J Exp Med **154**(2), 347-61.

Hartnell, A., J. Steel, et al. (2001). Characterization of human sialoadhesin, a sialic acid binding receptor expressed by resident and inflammatory macrophage populations. Blood **97**(1), 288-96.

Hengartner, M. O. (2000). The biochemistry of apoptosis. Nature **407**(6805), 770-6.

Hickey, W. F., B. L. Hsu, et al. (1991). T-lymphocyte entry into the central nervous system. J Neurosci Res **28**(2), 254-60.

Hickey, W. F. and H. Kimura (1988). Perivascular microglial cells of the CNS are bone marrow-derived and present antigen in vivo. Science **239**(4837), 290-2.

Hickey, W. F., K. Vass, et al. (1992). Bone marrow-derived elements in the central nervous system: an immunohistochemical and ultrastructural survey of rat chimeras. J Neuropathol Exp Neurol **51**(3), 246-56.

Hisatomi, T., T. Sakamoto, et al. (2003). Clearance of Apoptotic Photoreceptors: Elimination of Apoptotic Debris into the Subretinal Space and Macrophage-Mediated Phagocytosis via Phosphatidylserine Receptor and Integrin alphavbeta3. Am J Pathol **162**(6), 1869-79.

Hoek, R. M., S. R. Ruuls, et al. (2000). Down-regulation of the macrophage lineage through interaction with OX2 (CD200). Science **290**(5497), 1768-71.

Hoek, R. M., S. R. Ruuls, et al. (2000). Down-regulation of the macrophage lineage through interaction with OX2 (CD200). Science **290**(5497), 1768-71.

Hoffmann, P. R., A. M. deCathelineau, et al. (2001). Phosphatidylserine (PS) induces PS receptor-mediated macropinocytosis and promotes clearance of apoptotic cells. J Cell Biol **155**(4), 649-59.

http://www.clodronateliposomes.com.

http://www.sph.uth.tmc.edu/retnet/.

Huang, P. C., A. E. Gaitan, et al. (1993). Cellular interactions implicated in the mechanism of photoreceptor degeneration in transgenic mice expressing a mutant rhodopsin gene. Proc Natl Acad Sci U S A **90**(18), 8484-8.

Huang, S. H., S. J. Pittler, et al. (1995). Autosomal recessive retinitis pigmentosa caused by mutations in the alpha subunit of rod cGMP phosphodiesterase. Nat Genet **11**(4), 468-71.

Hughes, E. H., F. C. Schlichtenbrede, et al. (2003). Generation of Activated Sialoadhesin-Positive Microglia during Retinal Degeneration. Invest Ophthalmol Vis Sci **44**(5), 2229-34.

Hume, D. A., V. H. Perry, et al. (1983). Immunohistochemical localization of a macrophage-specific antigen in developing mouse retina: phagocytosis of dying neurons and differentiation of microglial cells to form a regular array in the plexiform layers. J Cell Biol **97**(1), 253-7.

Hume, D. A., I. L. Ross, et al. (2002). The mononuclear phagocyte system revisited. J Leukoc Biol **72**(4), 621-7.

Huynh, M. L., V. A. Fadok, et al. (2002). Phosphatidylserine-dependent ingestion of apoptotic cells promotes TGF-beta1 secretion and the resolution of inflammation. J Clin Invest **109**(1), 41-50.

Ischiropoulos, H. (1998). Biological tyrosine nitration: a pathophysiological function of nitric oxide and reactive oxygen species. Arch Biochem Biophys **356**(1), 1-11.

Itzhak, Y., J. L. Martin, et al. (1999). Methamphetamine- and 1-methyl-4-phenyl-1,2,3, 6-tetrahydropyridine-induced dopaminergic neurotoxicity in inducible nitric oxide synthase-deficient mice. Synapse **34**(4), 305-12.

Janeway, C. A., Jr. and R. Medzhitov (2002). Innate immune recognition. Annu Rev Immunol **20**, 197-216.

Jansen, H. G. and S. Sanyal (1984). Development and degeneration of retina in rds mutant mice: electron microscopy. J Comp Neurol **224**(1), 71-84.

Jeohn, G. H., L. Y. Kong, et al. (1998). Synergistic neurotoxic effects of combined treatments with cytokines in murine primary mixed neuron/glia cultures. J Neuroimmunol **85**(1), 1-10.

Jeon, C. J., Strettoi, E., Masland, R.H. (1998). The major cell populations of the mouse retina. J Neurosci. **18**(21), 8936-46.

Jiang, W., W. J. Swiggard, et al. (1995). The receptor DEC-205 expressed by dendritic cells and thymic epithelial cells is involved in antigen processing. Nature **375**(6527), 151-5.

Jomary, C., M. J. Neal, et al. (2001). Characterization of cell death pathways in murine retinal neurodegeneration implicates cytochrome c release, caspase activation, and bid cleavage. Mol Cell Neurosci **18**(4), 335-46.

Jordan, S. A., G. J. Farrar, et al. (1992). Polymorphic variation within "conserved" sequences at the 3' end of the human RDS gene which results in amino acid substitutions. Hum Mutat **1**(3), 240-7.

Katai, N., T. Kikuchi, et al. (1999). Caspaselike proteases activated in apoptotic photoreceptors of Royal College of Surgeons rats. Invest Ophthalmol Vis Sci **40**(8), 1802-7.

Katai, N. and N. Yoshimura (1999). Apoptotic retinal neuronal death by ischemia-reperfusion is executed by two distinct caspase family proteases. Invest Ophthalmol Vis Sci **40**(11), 2697-705.

Kedzierski, W., D. Bok, et al. (1998). Non-cell-autonomous photoreceptor degeneration in rds mutant mice mosaic for expression of a rescue transgene. J Neurosci **18**(11), 4076-82.

Kim, D. H., J. A. Kim, et al. (2002). Activation of caspase-3 during degeneration of the outer nuclear layer in the rd mouse retina. Ophthalmic Res **34**(3), 150-7.

Kobayashi, M., T. Kuroiwa, et al. (2000). Nitric oxide synthase expression in ischemic rat retinas. Jpn J Ophthalmol **44**(3), 235-44.

Koennecke, L. A., M. A. Zito, et al. (1999). Depletion of systemic macrophages by liposome-encapsulated clodronate attenuates increases in brain quinolinic acid during CNS-localized and systemic immune activation. J Neurochem **73**(2), 770-9.

Kohutnicka, M., E. Lewandowska, et al. (1998). Microglial and astrocytic involvement in a murine model of Parkinson's disease induced by 1-methyl-4-phenyl-1,2,3,6-tetrahydropyridine (MPTP). Immunopharmacology **39**(3), 167-80.

Koike, M., M. Shibata, et al. (2003). Involvement of two different cell death pathways in retinal atrophy of cathepsin D-deficient mice. Mol Cell Neurosci **22**(2), 146-61.

Kuida, K., T. S. Zheng, et al. (1996). Decreased apoptosis in the brain and premature lethality in CPP32-deficient mice. Nature **384**(6607), 368-72.

Lam, T. T., A. S. Abler, et al. (1999). N-methyl-D-aspartate (NMDA)--induced apoptosis in rat retina. Invest Ophthalmol Vis Sci **40**(10), 2391-7.

Lam, T. T., A. S. Abler, et al. (1999). Apoptosis and caspases after ischemia-reperfusion injury in rat retina. Invest Ophthalmol Vis Sci **40**(5), 967-75.

Lassmann, H., F. Zimprich, et al. (1991). Microglial cells are a component of the perivascular glia limitans. J Neurosci Res **28**(2), 236-43.

LaVail, M. M., D. Yasumura, et al. (1998). Protection of mouse photoreceptors by survival factors in retinal degenerations. Invest Ophthalmol Vis Sci **39**(3), 592-602.

Law, A., S. Gauthier, et al. (2001). Say NO to Alzheimer's disease: the putative links between nitric oxide and dementia of the Alzheimer's type. Brain Res Brain Res Rev **35**(1), 73-96.

Lee, Y. B., A. Nagai, et al. (2002). Cytokines, chemokines, and cytokine receptors in human microglia. J Neurosci Res **69**(1), 94-103.

Li, M., V. O. Ona, et al. (2000). Functional role and therapeutic implications of neuronal caspase-1 and -3 in a mouse model of traumatic spinal cord injury. Neuroscience **99**(2), 333-42.

Li, M., V. O. Ona, et al. (2000). Functional role of caspase-1 and caspase-3 in an ALS transgenic mouse model. Science **288**(5464), 335-9.

Liang, F. Q., N. S. Dejneka, et al. (2001). AAV-mediated delivery of ciliary neurotrophic factor prolongs photoreceptor survival in the rhodopsin knockout mouse. Mol Ther **3**(2), 241-8.

Liberatore, G. T., V. Jackson-Lewis, et al. (1999). Inducible nitric oxide synthase stimulates dopaminergic neurodegeneration in the MPTP model of Parkinson disease. Nat Med **5**(12), 1403-9.

Lin, J. H. (1996). Bisphosphonates: a review of their pharmacokinetic properties. Bone **18**(2), 75-85.

Lin, J. H., H. Weigel, et al. (1998). Gap-junction-mediated propagation and amplification of cell injury. Nat Neurosci **1**(6), 494-500.

Linehan, S. A., L. Martinez-Pomares, et al. (1999). Mannose receptor and its putative ligands in normal murine lymphoid and nonlymphoid organs: In situ expression of mannose receptor by selected macrophages, endothelial cells, perivascular microglia, and mesangial cells, but not dendritic cells. J Exp Med **189**(12), 1961-72.

Ling, E. A. and S. K. Leong (1987). Effects of intraneural injection of Ricinus communis agglutinin-60 into rat vagus nerve. J Neurocytol **16**(3), 373-87.

Liu, C., Y. Li, et al. (1999). Activation of caspase-3 in the retina of transgenic rats with the rhodopsin mutation s334ter during photoreceptor degeneration. J Neurosci **19**(12), 4778-85.

Liversidge, J., A. Dick, et al. (2002). Nitric oxide mediates apoptosis through formation of peroxynitrite and Fas/Fas-ligand interactions in experimental autoimmune uveitis. Am J Pathol **160**(3), 905-16.

Lolley, R. N., D. B. Farber, et al. (1977). Cyclic GMP accumulation causes degeneration of photoreceptor cells: simulation of an inherited disease. Science **196**(4290), 664-6.

Ma, J., J. C. Norton, et al. (1995). Retinal degeneration slow (rds) in mouse results from simple insertion of a t haplotype-specific element into protein-coding exon II. Genomics **28**(2), 212-9.

Marmor, M. F. (1980). Visual loss in retinitis pigmentosa. Am J Ophthalmol **89**(5), 692-8.

Martin, D. and S. L. Near (1995). Protective effect of the interleukin-1 receptor antagonist (IL-1ra) on experimental allergic encephalomyelitis in rats. J Neuroimmunol **61**(2), 241-5.

Martinez-Mir, A., E. Paloma, et al. (1998). Retinitis pigmentosa caused by a homozygous mutation in the Stargardt disease gene ABCR. Nat Genet **18**(1), 11-2.

Martinez-Pomares, L., M. Kosco-Vilbois, et al. (1996). Fc chimeric protein containing the cysteine-rich domain of the murine mannose receptor binds to macrophages from splenic marginal zone and lymph node subcapsular sinus and to germinal centers. J Exp Med **184**(5), 1927-37.

Maw, M. A., B. Kennedy, et al. (1997). Mutation of the gene encoding cellular retinaldehyde-binding protein in autosomal recessive retinitis pigmentosa. Nat Genet **17**(2), 198-200.

McGeer, P. L., S. Itagaki, et al. (1988). Reactive microglia are positive for HLA-DR in the substantia nigra of Parkinson's and Alzheimer's disease brains. Neurology **38**(8), 1285-91.

McGeer, P. L., S. Itagaki, et al. (1987). Reactive microglia in patients with senile dementia of the Alzheimer type are positive for the histocompatibility glycoprotein HLA-DR. Neurosci Lett **79**(1-2), 195-200.

McKnight, A. J. and S. Gordon (1998). The EGF-TM7 family: unusual structures at the leukocyte surface. J Leukoc Biol **63**(3), 271-80.

McKnight, A. J., A. J. Macfarlane, et al. (1996). Molecular cloning of F4/80, a murine macrophage-restricted cell surface glycoprotein with homology to the G-protein-linked transmembrane 7 hormone receptor family. J Biol Chem **271**(1), 486-9.

McLaughlin, M. E., M. A. Sandberg, et al. (1993). Recessive mutations in the gene encoding the beta-subunit of rod phosphodiesterase in patients with retinitis pigmentosa. Nat Genet **4**(2), 130-4.

McMenamin, P. G. (1999). Distribution and phenotype of dendritic cells and resident tissue macrophages in the dura mater, leptomeninges, and choroid plexus of the rat brain as demonstrated in wholemount preparations. J Comp Neurol **405**(4), 553-62.

Mertsch, K., U. K. Hanisch, et al. (2001). Characterization of microglial cells and their response to stimulation in an organotypic retinal culture system. J Comp Neurol **431**(2), 217-27.

Mervin, K. and J. Stone (2002). Developmental death of photoreceptors in the C57BL/6J mouse: association with retinal function and self-protection. Exp Eye Res **75**(6), 703-13.

Mervin, K. and J. Stone (2002). Regulation by oxygen of photoreceptor death in the developing and adult C57BL/6J mouse. Exp Eye Res **75**(6), 715-22.

Mevorach, D., J. O. Mascarenhas, et al. (1998). Complement-dependent clearance of apoptotic cells by human macrophages. J Exp Med **188**(12), 2313-20.

Molday, R. S., D. Hicks, et al. (1987). Peripherin. A rim-specific membrane protein of rod outer segment discs. Invest Ophthalmol Vis Sci **28**(1), 50-61.

Morimura, H., G. A. Fishman, et al. (1998). Mutations in the RPE65 gene in patients with autosomal recessive retinitis pigmentosa or leber congenital amaurosis. Proc Natl Acad Sci U S A **95**(6), 3088-93.

Mosley, K. and M. L. Cuzner (1996). Receptor-mediated phagocytosis of myelin by macrophages and microglia: effect of opsonization and receptor blocking agents. Neurochem Res **21**(4), 481-7.

Mouw, G., J. L. Zechel, et al. (2002). Caspase-9 inhibition after focal cerebral ischemia improves outcome following reversible focal ischemia. Metab Brain Dis **17**(3), 143-51.

Muhl, H., K. Sandau, et al. (1996). Nitric oxide donors induce apoptosis in glomerular mesangial cells, epithelial cells and endothelial cells. Eur J Pharmacol **317**(1), 137-49.

Munday, J., H. Floyd, et al. (1999). Sialic acid binding receptors (siglecs) expressed by macrophages. J Leukoc Biol **66**(5), 705-11.

Munder, M., K. Eichmann, et al. (1998). Alternative metabolic states in murine macrophages reflected by the nitric oxide synthase/arginase balance:

competitive regulation by CD4+ T cells correlates with Th1/Th2 phenotype. J Immunol **160**(11), 5347-54.

Nakagawa, T., H. Zhu, et al. (2000). Caspase-12 mediates endoplasmic-reticulum-specific apoptosis and cytotoxicity by amyloid-beta. Nature **403**(6765), 98-103.

Nakanishi, H., J. Zhang, et al. (2001). Involvement of nitric oxide released from microglia-macrophages in pathological changes of cathepsin D-deficient mice. J Neurosci **21**(19), 7526-33.

Nakazawa, M., Y. Wada, et al. (1998). Arrestin gene mutations in autosomal recessive retinitis pigmentosa. Arch Ophthalmol **116**(4), 498-501.

Neufeld, A. H. (1999). Microglia in the optic nerve head and the region of parapapillary chorioretinal atrophy in glaucoma. Arch Ophthalmol **117**(8), 1050-6.

Neumann, H., T. Misgeld, et al. (1998). Neurotrophins inhibit major histocompatibility class II inducibility of microglia: involvement of the p75 neurotrophin receptor. Proc Natl Acad Sci U S A **95**(10), 5779-84.

Newman, E. and A. Reichenbach (1996). The Muller cell: a functional element of the retina. Trends Neurosci **19**(8), 307-12.

Ng, T. F. and J. W. Streilein (2001). Light-induced migration of retinal microglia into the subretinal space. Invest Ophthalmol Vis Sci **42**(13), 3301-10.

Niemeyer, G. and K. Gurewitsch (1982). [Variability of visual acuity, dark adaptation and electroretinogram in retinitis pigmentosa]. Klin Monatsbl Augenheilkd **180**(5), 401-4.

O'Doherty, U., M. Peng, et al. (1994). Human blood contains two subsets of dendritic cells, one immunologically mature and the other immature. Immunology **82**(3), 487-93.

Okoye, G., J. Zimmer, et al. (2003). Increased expression of brain-derived neurotrophic factor preserves retinal function and slows cell death from rhodopsin mutation or oxidative damage. J Neurosci **23**(10), 4164-72.

Ona, V. O., M. Li, et al. (1999). Inhibition of caspase-1 slows disease progression in a mouse model of Huntington's disease. Nature **399**(6733), 263-7.

Pacione, L. R., M. J. Szego, et al. (2003). Progress toward understanding the genetic and biochemical mechanisms of inherited photoreceptor degenerations. Annu Rev Neurosci **26**, 657-700.

Pagon, R. A. (1988). Retinitis pigmentosa. Surv Ophthalmol **33**(3), 137-77.

Pawlyk, B. S., T. Li, et al. (2002). Absence of photoreceptor rescue with D-cis-diltiazem in the rd mouse. Invest Ophthalmol Vis Sci **43**(6), 1912-5.

Pearce-Kelling, S. E., T. S. Aleman, et al. (2001). Calcium channel blocker D-cis-diltiazem does not slow retinal degeneration in the PDE6B mutant rcd1 canine model of retinitis pigmentosa. Mol Vis **7**, 42-7.

Penfold, P. L., J. M. Provis, et al. (1993). Human retinal microglia express phenotypic characteristics in common with dendritic antigen-presenting cells. J Neuroimmunol **45**(1-2), 183-91.

Perry, V. H. (1998). A revised view of the central nervous system microenvironment and major histocompatibility complex class II antigen presentation. J Neuroimmunol **90**(2), 113-21.

Perry, V. H., P. R. Crocker, et al. (1992). The blood-brain barrier regulates the expression of a macrophage sialic acid-binding receptor on microglia. J Cell Sci **101**(Pt 1), 201-7.

Perry, V. H. and S. Gordon (1991). Macrophages and the nervous system. Int Rev Cytol **125**, 203-44.

Perry, V. H., D. A. Hume, et al. (1985). Immunohistochemical localization of macrophages and microglia in the adult and developing mouse brain. Neuroscience **15**(2), 313-26.

Piani, D., M. Spranger, et al. (1992). Macrophage-induced cytotoxicity of N-methyl-D-aspartate receptor positive neurons involves excitatory amino acids rather than reactive oxygen intermediates and cytokines. Eur J Immunol **22**(9), 2429-36.

Platt, N., H. Suzuki, et al. (1996). Role for the class A macrophage scavenger receptor in the phagocytosis of apoptotic thymocytes in vitro. Proc Natl Acad Sci U S A **93**(22), 12456-60.

Polfliet, M. M., P. H. Goede, et al. (2001). A method for the selective depletion of perivascular and meningeal macrophages in the central nervous system. J Neuroimmunol **116**(2), 188-95.

Pomeroy, C. and G. A. Filice (1988). Effect of intravenous silica on the course of Nocardia asteroides pneumonia. Infect Immun **56**(9), 2507-11.

Portera-Cailliau, C., C. H. Sung, et al. (1994). Apoptotic photoreceptor cell death in mouse models of retinitis pigmentosa. Proc Natl Acad Sci U S A **91**(3), 974-8.

Possel, H., H. Noack, et al. (2000). Selective upregulation of inducible nitric oxide synthase (iNOS) by lipopolysaccharide (LPS) and cytokines in microglia: in vitro and in vivo studies. Glia **32**(1), 51-9.

Pouvreau, I., J. C. Zech, et al. (1998). Effect of macrophage depletion by liposomes containing dichloromethylene-diphosphonate on endotoxin-induced uveitis. J Neuroimmunol **86**(2), 171-81.

Provis, J. M., P. L. Penfold, et al. (1995). Human retinal microglia: expression of immune markers and relationship to the glia limitans. Glia **14**(4), 243-56.

Puro, D. G., J. P. Yuan, et al. (1996). Activation of NMDA receptor-channels in human retinal Muller glial cells inhibits inward-rectifying potassium currents. Vis Neurosci **13**(2), 319-26.

Reichelt, W., M. Hernandez, et al. (1996). GABAA receptor currents recorded from Mueller glial cells of the baboon (Papio cynocephalus) retina. Neurosci Lett **203**(3), 159-62.

Reichenbach, A., F. Faude, et al. (1997). The Muller (glial) cell in normal and diseased retina: a case for single-cell electrophysiology. Ophthalmic Res **29**(5), 326-40.

Reuter, J. H. and S. Sanyal (1984). Development and degeneration of retina in rds mutant mice: the electroretinogram. Neurosci Lett **48**(2), 231-7.

Rezzonico, R., R. Chicheportiche, et al. (2000). Engagement of CD11b and CD11c beta2 integrin by antibodies or soluble CD23 induces IL-1beta production on primary human monocytes through mitogen-activated protein kinase-dependent pathways. Blood **95**(12), 3868-77.

Rim, J. and D. D. Oprian (1995). Constitutive activation of opsin: interaction of mutants with rhodopsin kinase and arrestin. Biochemistry **34**(37), 11938-45.

Ripps, H. (2002). Cell death in retinitis pigmentosa: gap junctions and the 'bystander' effect. Exp Eye Res **74**(3), 327-36.

Rogers, J., J. Luber-Narod, et al. (1988). Expression of immune system-associated antigens by cells of the human central nervous system: relationship to the pathology of Alzheimer's disease. Neurobiol Aging **9**(4), 339-49.

Roque, R. S., C. J. Imperial, et al. (1996). Microglial cells invade the outer retina as photoreceptors degenerate in Royal College of Surgeons rats. Invest Ophthalmol Vis Sci **37**(1), 196-203.

Roque, R. S., A. A. Rosales, et al. (1999). Retina-derived microglial cells induce photoreceptor cell death in vitro. Brain Res **836**(1-2), 110-9.

Saleh, M., J. P. Vaillancourt, et al. (2004). Differential modulation of endotoxin responsiveness by human caspase-12 polymorphisms. Nature **429**(6987), 75-9.

Sanchez Mejia, R. O., V. O. Ona, et al. (2001). Minocycline reduces traumatic brain injury-mediated caspase-1 activation, tissue damage, and neurological dysfunction. Neurosurgery **48**(6), 1393-9; discussion 1399-401.

Santos, A., M. S. Humayun, et al. (1997). Preservation of the inner retina in retinitis pigmentosa. A morphometric analysis. Arch Ophthalmol **115**(4), 511-5.

Sanyal, S. (1972). Changes of lysosomal enzymes during hereditary degeneration and histogenesis of retina in mice. II. Localization of N-acetyl- -glucosaminidase in macrophages. Histochemie **29**(1), 28-36.

Sanyal, S., A. De Ruiter, et al. (1980). Development and degeneration of retina in rds mutant mice: light microscopy. J Comp Neurol **194**(1), 193-207.

Sanyal, S. and R. K. Hawkins (1986). Development and degeneration of retina in rds mutant mice: effects of light on the rate of degeneration in albino and pigmented homozygous and heterozygous mutant and normal mice. Vision Res **26**(8), 1177-85.

Sarra, G. M., C. Stephens, et al. (2001). Gene replacement therapy in the retinal degeneration slow (rds) mouse: the effect on retinal degeneration following partial transduction of the retina. Hum Mol Genet **10**(21), 2353-61.

Sasaki, T., J. Hamada, et al. (2001). Inhibition of nitric oxide production during global ischemia ameliorates ischemic damage of pyramidal neurons in the hippocampus. Keio J Med **50**(3), 182-7.

Savill, J. and V. Fadok (2000). Corpse clearance defines the meaning of cell death. Nature **407**(6805), 784-8.

Savill, J., V. Fadok, et al. (1993). Phagocyte recognition of cells undergoing apoptosis. Immunol Today **14**(3), 131-6.

Schalken, J. J., J. J. Janssen, et al. (1990). Development and degeneration of retina in rds mutant mice: immunoassay of the rod visual pigment rhodopsin. Biochim Biophys Acta **1033**(1), 103-9.

Schermer, C. and C. Humpel (2002). Granulocyte macrophage-colony stimulating factor activates microglia in rat cortex organotypic brain slices. Neurosci Lett **328**(2), 180-4.

Schroeter, M., S. Jander, et al. (2001). CD8+ phagocytes in focal ischemia of the rat brain: predominant origin from hematogenous macrophages and targeting to areas of pannecrosis. Acta Neuropathol (Berl) **101**(5), 440-8.

Schroeter, M., S. Jander, et al. (1997). Phagocytic response in photochemically induced infarction of rat cerebral cortex. The role of resident microglia. Stroke **28**(2), 382-6.

Sedgwick, J. D., A. L. Ford, et al. (1998). Central nervous system microglial cell activation and proliferation follows direct interaction with tissue-infiltrating T cell blasts. J Immunol **160**(11), 5320-30.

Seguin, R., K. Biernacki, et al. (2003). Differential effects of Th1 and Th2 lymphocyte supernatants on human microglia. Glia **42**(1), 36-45.

Smith, M. E., K. van der Maesen, et al. (1998). Macrophage and microglial responses to cytokines in vitro: phagocytic activity, proteolytic enzyme release, and free radical production. J Neurosci Res **54**(1), 68-78.

Stein, M., S. Keshav, et al. (1992). Interleukin 4 potently enhances murine macrophage mannose receptor activity: a marker of alternative immunologic macrophage activation. J Exp Med **176**(1), 287-92.

Steiniger, B., P. Barth, et al. (1997). The species-specific structure of microanatomical compartments in the human spleen: strongly sialoadhesin-positive macrophages occur in the perifollicular zone, but not in the marginal zone. Immunology **92**(2), 307-16.

Stevenson, P. H. and J. R. Stevenson (1986). Cytotoxic and migration inhibitory effects of bisphosphonates on macrophages. Calcif Tissue Int **38**(4), 227-33.

Streilein, J. W. (2003). Ocular immune privilege: the eye takes a dim but practical view of immunity and inflammation. J Leukoc Biol **74**(2), 179-85.

Streit, W. J., M. B. Graeber, et al. (1989). Peripheral nerve lesion produces increased levels of major histocompatibility complex antigens in the central nervous system. J Neuroimmunol **21**(2-3), 117-23.

Streit, W. J., S. D. Hurley, et al. (2000). Comparative evaluation of cytokine profiles and reactive gliosis supports a critical role for interleukin-6 in neuron-glia signaling during regeneration. J Neurosci Res **61**(1), 10-20.

Streit, W. J. and G. W. Kreutzberg (1988). Response of endogenous glial cells to motor neuron degeneration induced by toxic ricin. J Comp Neurol **268**(2), 248-63.

Suber, M. L., M. Y. Hurwitz, et al. (2001). Immune consequences of intraocular administration of modified adenoviral vectors. Hum Gene Ther **12**(7), 833-8.

Suber, M. L., S. J. Pittler, et al. (1993). Irish setter dogs affected with rod/cone dysplasia contain a nonsense mutation in the rod cGMP phosphodiesterase beta-subunit gene. Proc Natl Acad Sci U S A **90**(9), 3968-72.

Sung, C. H., C. M. Davenport, et al. (1993). Rhodopsin mutations responsible for autosomal dominant retinitis pigmentosa. Clustering of functional classes along the polypeptide chain. J Biol Chem **268**(35), 26645-9.

Tai, X. G., K. Toyo-oka, et al. (1997). Expression of an inducible type of nitric oxide (NO) synthase in the thymus and involvement of NO in deletion of TCR-stimulated double- positive thymocytes. J Immunol **158**(10), 4696-703.

Takahashi, J. L., F. Giuliani, et al. (2003). Interleukin-1beta promotes oligodendrocyte death through glutamate excitotoxicity. Ann Neurol **53**(5), 588-95.

Tezel, G. and M. B. Wax (1999). Inhibition of caspase activity in retinal cell apoptosis induced by various stimuli in vitro. Invest Ophthalmol Vis Sci **40**(11), 2660-7.

Thanos, S. (1992). Sick photoreceptors attract activated microglia from the ganglion cell layer: a model to study the inflammatory cascades in rats with inherited retinal dystrophy. Brain Res **588**(1), 21-8.

Thanos, S., J. Mey, et al. (1993). Treatment of the adult retina with microglia-suppressing factors retards axotomy-induced neuronal degradation and enhances axonal regeneration in vivo and in vitro. J Neurosci **13**(2), 455-66.

Thepen, T., N. Van Rooijen, et al. (1989). Alveolar macrophage elimination in vivo is associated with an increase in pulmonary immune response in mice. J Exp Med **170**(2), 499-509.

Thillaye-Goldenberg, B., O. Goureau, et al. (2000). Delayed onset and decreased severity of experimental autoimmune uveoretinitis in mice lacking nitric oxide synthase type 2. J Neuroimmunol **110**(1-2), 31-44.

Tikka, T., B. L. Fiebich, et al. (2001). Minocycline, a tetracycline derivative, is neuroprotective against excitotoxicity by inhibiting activation and proliferation of microglia. J Neurosci **21**(8), 2580-8.

Tikka, T. M. and J. E. Koistinaho (2001). Minocycline provides neuroprotection against N-methyl-D-aspartate neurotoxicity by inhibiting microglia. J Immunol **166**(12), 7527-33.

Togo, T., H. Akiyama, et al. (2000). Expression of CD40 in the brain of Alzheimer's disease and other neurological diseases. Brain Res **885**(1), 117-21.

Tran, E. H., K. Hoekstra, et al. (1998). Immune invasion of the central nervous system parenchyma and experimental allergic encephalomyelitis, but not leukocyte extravasation from blood, are prevented in macrophage-depleted mice. J Immunol **161**(7), 3767-75.

Travis, G. H. (1998). Mechanisms of cell death in the inherited retinal degenerations. Am J Hum Genet **62**(3), 503-8.

Tso, M. O., C. Zhang, et al. (1994). Apoptosis leads to photoreceptor degeneration in inherited retinal dystrophy of RCS rats. Invest Ophthalmol Vis Sci **35**(6), 2693-9.

Ugolini, G., F. Cremisi, et al. (1995). TrkA, TrkB and p75 mRNA expression is developmentally regulated in the rat retina. Brain Res **704**(1), 121-4.

Ulshafer, R. J., C. A. Garcia, et al. (1980). Sensitivity of photoreceptors to elevated levels of cGMP in the human retina. Invest Ophthalmol Vis Sci **19**(10), 1236-41.

Ulvestad, E., K. Williams, et al. (1994). Human microglial cells have phenotypic and functional characteristics in common with both macrophages and dendritic antigen-presenting cells. J Leukoc Biol **56**(6), 732-40.

Usukura, J. and D. Bok (1987). Changes in the localization and content of opsin during retinal development in the rds mutant mouse: immunocytochemistry and immunoassay. Exp Eye Res **45**(4), 501-15.

van den Berg, T. K., J. J. Breve, et al. (1992). Sialoadhesin on macrophages: its identification as a lymphocyte adhesion molecule. J Exp Med **176**(3), 647-55.

van den Berg, T. K., D. Nath, et al. (2001). Cutting edge: CD43 functions as a T cell counterreceptor for the macrophage adhesion receptor sialoadhesin (Siglec-1). J Immunol **166**(6), 3637-40.

van Nie, R., D. Ivanyi, et al. (1978). A new H-2-linked mutation, rds, causing retinal degeneration in the mouse. Tissue Antigens **12**(2), 106-8.

Van Rooijen, N. (1989). The liposome-mediated macrophage 'suicide' technique. J Immunol Methods **124**(1), 1-6.

van Rooijen, N. and N. Kors (1989). Effects of intracellular diphosphonates on cells of the mononuclear phagocyte system: in vivo effects of liposome-encapsulated diphosphonates on different macrophage subpopulations in the spleen. Calcif Tissue Int **45**(3), 153-6.

van Rooijen, N., N. Kors, et al. (1989). Macrophage subset repopulation in the spleen: differential kinetics after liposome-mediated elimination. J Leukoc Biol **45**(2), 97-104.

Van Rooijen, N., N. Kors, et al. (1990). Depletion and repopulation of macrophages in spleen and liver of rat after intravenous treatment with liposome-

encapsulated dichloromethylene diphosphonate. Cell Tissue Res **260**(2), 215-22.

Van Rooijen, N. and A. Sanders (1994). Liposome mediated depletion of macrophages: mechanism of action, preparation of liposomes and applications. J Immunol Methods **174**(1-2), 83-93.

van Rooijen, N., A. Sanders, et al. (1996). Apoptosis of macrophages induced by liposome-mediated intracellular delivery of clodronate and propamidine. J Immunol Methods **193**(1), 93-9.

van Rooijen, N. and R. van Nieuwmegen (1984). Elimination of phagocytic cells in the spleen after intravenous injection of liposome-encapsulated dichloromethylene diphosphonate. An enzyme-histochemical study. Cell Tissue Res **238**(2), 355-8.

Vass, K. and H. Lassmann (1990). Intrathecal application of interferon gamma. Progressive appearance of MHC antigens within the rat nervous system. Am J Pathol **137**(4), 789-800.

Wakakura, M. and N. Yamamoto (1994). Cytosolic calcium transient increase through the AMPA/kainate receptor in cultured Muller cells. Vision Res **34**(9), 1105-9.

Wang, X., S. S. Tay, et al. (2000). An immunohistochemical study of neuronal and glial cell reactions in retinae of rats with experimental glaucoma. Exp Brain Res **132**(4), 476-84.

Wekerle, H., Linington, C, Lassmann, H, Meyermann, R (1986). Cellular immune reactivity within the CNS. Trends in Neurosciences **9**, 271-278.

Wells, J., J. Wroblewski, et al. (1993). Mutations in the human retinal degeneration slow (RDS) gene can cause either retinitis pigmentosa or macular dystrophy. Nat Genet **3**(3), 213-8.

Wright, G. J., M. J. Puklavec, et al. (2000). Lymphoid/neuronal cell surface OX2 glycoprotein recognizes a novel receptor on macrophages implicated in the control of their function. Immunity **13**(2), 233-42.

Wu, D. C., V. Jackson-Lewis, et al. (2002). Blockade of microglial activation is neuroprotective in the 1-methyl-4- phenyl-1,2,3,6-tetrahydropyridine mouse model of Parkinson disease. J Neurosci **22**(5), 1763-71.

Yoshizawa, K., K. Kiuchi, et al. (2002). Caspase-3 inhibitor transiently delays inherited retinal degeneration in C3H mice carrying the rd gene. Graefes Arch Clin Exp Ophthalmol **240**(3), 214-9.

Yoshizawa, K., J. Yang, et al. (2000). Caspase-3 inhibitor rescues N -methyl- N -nitrosourea-induced retinal degeneration in Sprague-Dawley rats. Exp Eye Res **71**(6), 629-35.

Yrjanheikki, J., T. Tikka, et al. (1999). A tetracycline derivative, minocycline, reduces inflammation and protects against focal cerebral ischemia with a wide therapeutic window. Proc Natl Acad Sci U S A **96**(23), 13496-500.

Yuan, J. and B. A. Yankner (2000). Apoptosis in the nervous system. Nature **407**(6805), 802-9.

Yuan, L. and A. H. Neufeld (2001). Activated microglia in the human glaucomatous optic nerve head. J Neurosci Res **64**(5), 523-32.

Zhang, C., Chiang, S, Yang, F, Shen, J, Sinha, D, Lam,T, Tso, M (2003). Retinal Microglial Activation and Migration Following Photic Injury. Association for Research in Vision and Ophthalmology, Florida.

Zhu, S., I. G. Stavrovskaya, et al. (2002). Minocycline inhibits cytochrome c release and delays progression of amyotrophic lateral sclerosis in mice. Nature **417**(6884), 74-8.

GLOSSARY OF ABBREVIATIONS

ALS	Amyotrophic Lateral Sclerosis
CNS	Central Nervous System
DAB	Diaminobenzidine
DAPI	4'6 diamidino-2-phenylindole
EAE	Experimental allergic encephalomyelitis
EAU	Experimental autoimmune uveitis
FITC	Fluorescein-5-isothiocyanate
iNOS	Inducible nitric oxide synthase
IL1β	Interleukin 1 β (beta)
LPS	Lipopolysaccharide
MHC	Major Histocompatibility Complex
NO	Nitric oxide
ONL	Outer nuclear layer
PBS	Phosphate buffered saline
PBSA	Phosphate buffered bovine serum albumin
PCNA	Proliferating cell nuclear antigen
PDE	Phosphodiesterase
PLP	Periodate Lysine Paraformaldehyde
RCS	Royal College of Surgeons (rat)
rd	Retinal degeneration (mouse)
rds	Retinal degeneration slow (mouse)
RPE	Retinal Pigment Epithelium
RP	Retinitis Pigmentosa
SEM	Standard Error of the Mean
TGFβ	Transforming Growth Factor β (beta)
TMR	Tetramethylrhodamine
TNFα	Tumour necrosis factor α (alpha)
TRITC	Tetramethylrhodamine isothiocyanate
TUNEL	Terminal deoxylnucleotidyl transferase (TdT) – mediated dUTP nick end-labelling

PUBLICATIONS BASED ON THIS THESIS

Original articles

Hughes E.H., Schlichtenbrede F.C., Murphy C.C., Sarra G-M, Luthert P, Ali R.R., Dick A.D. (2003). Generation Of Sialoadhesin Positive Activated Microglia During Retinal Degeneration. *Invest Ophthalmol Vis Sci* **44**:2229-2234.

Hughes E.H., Schlichtenbrede F.C., Murphy C.C., Broderick C., van Rooijen N., Ali R.R., Dick A.D. (2004). Minocycline Delays Photoreceptor Death in the rds Mouse Through a Microglia-Independent Mechanism. *Exp Eye Res* Jun;**78(6)**:1077-84.

Published abstracts

Hughes E.H., Schlichtenbrede F.C., Ali R.R., Dick A.D. (2002). Generation Of Sialoadhesin Positive Activated Microglia During Retinal Degeneration. *Ophthal Res* **34**:152

Hughes E.H., Schlichtenbrede F.C., Murphy C.C., Ali R.R., Dick A.D. (2003) Minocycline Suppresses Photoreceptor Apoptosis in the rds Mouse Through a Mechanism Unrelated to Microglial Inhibition. *ARVO* supplement of *IOVS* May 2003